

Techno-Economic Study of CO₂ Capture from Natural Gas Based Hydrogen Plants

by

Cynthia B. Tarun

A thesis
presented to the University of Waterloo
in fulfilment of the
thesis requirement for the degree of
Master of Applied Science
in
Chemical Engineering

Waterloo, Ontario, Canada, 2006

© Cynthia B. Tarun 2006

I hereby declare that I am the sole author of this thesis. This is a true copy of the thesis, including any required final revisions, as accepted by my examiners.

I understand that my thesis may be made electronically available to the public.

Abstract

As reserves of conventional crude oil are depleted, there is a growing need to develop unconventional oils such as heavy oil and bitumen from oil sands. In terms of recoverable oil, Canadian oil sands are considered to be the second largest oil reserves in the world. However, the upgrading of bitumen from oil sands to synthetic crude oil (SCO) requires nearly ten times more hydrogen (H_2) than the conventional crude oils. The current H_2 demand for oil sands operations is met mostly by steam reforming of natural gas. With the future expansion of oil sands operations, the demand of H_2 for oil sand operations is likely to quadruple in the next decade. As natural gas reforming involves significant carbon dioxide (CO_2) emissions, this sector is likely to be one of the largest emitters of CO_2 in Canada.

In the current H_2 plants, CO_2 emissions originate from two sources, the combustion flue gases from the steam reformer furnace and the off-gas from the process (steam reforming and water-gas shift) reactions. The objective of this study is to develop a process that captures CO_2 at minimum energy penalty in typical H_2 plants.

The approach is to look at the best operating conditions when considering the H_2 and steam production, CO_2 production and external fuel requirements. The simulation in this study incorporates the kinetics of the steam methane reforming (SMR) and the water gas shift (WGS) reactions. It also includes the integration of CO_2 capture technologies to typical H_2 plants using pressure swing adsorption (PSA) to purify the H_2 product. These typical H_2 plants are the world standard of producing H_2 and are then considered as the base case for

this study. The base case is modified to account for the implementation of CO₂ capture technologies. Two capture schemes are tested in this study. The first process scheme is the integration of a monoethanolamine (MEA) CO₂ scrubbing process. The other scheme is the introduction of a cardo polyimide hollow fibre membrane capture process. Both schemes are designed to capture 80% of the CO₂ from the H₂ process at a purity of 98%.

The simulation results show that the H₂ plant with the integration of CO₂ capture has to be operated at the lowest steam to carbon (S/C) ratio, highest inlet temperature of the SMR and lowest inlet temperatures for the WGS converters to attain lowest energy penalty. H₂ plant with membrane separation technology requires higher electricity requirement. However, it produces better quality of steam than the H₂ plant with MEA-CO₂ capture process which is used to supply the electricity requirement of the process. Fuel (highvale coal) is burned to supply the additional electricity requirement. The membrane based H₂ plant requires higher additional electricity requirement for most of the operating conditions tested. However, it requires comparable energy penalty than the H₂ plant with MEA-CO₂ capture process when operated at the lowest energy operating conditions at 80% CO₂ recovery.

This thesis also investigates the sensitivity of the energy penalty as function of the percent CO₂ recovery. The break-even point is determined at a certain amount of CO₂ recovery where the amount of energy produced is equal to the amount of energy required. This point, where no additional energy is required, is approximately 73% CO₂ recovery for the MEA based capture plant and 57% CO₂ recovery for the membrane based capture plant.

The amount of CO₂ emissions at various CO₂ recoveries using the best operating conditions is also presented. The results show that MEA plant has comparable CO₂ emissions to that of the membrane plant at 80% CO₂ recovery. MEA plant is more attractive than membrane plant at lower CO₂ recoveries.

Acknowledgements

I thank GOD for all the gifts He has bestowed on me and also in directing my path to the following persons who have been instrumental in the completion of my thesis.

Dr. Peter Douglas and Dr. Eric Croiset, my supervisors, for the opportunity to have worked with them and for their energetic assistance and untiring support in the conduct of my research.

Dr. Kelly Thambimuthu, Mr. Murlidhar Gupta and the whole CANMET Energy Resources, for their valuable insights and financial assistance.

To my friends in Waterloo especially the COMPASS Catholic Fellowship group for the friendship and spiritual insights and the Khankhet family for their kindness.

To my Papa and Mama and to the rest of my family, for their unceasing love, unwavering support and constant prayers that guided me through all my endeavors.

For this achievement, I give back all the glory and praises to the omnipotent Father Almighty.

Table of Contents

CHAPTER 1: INTRODUCTION.....	1
1.1 BACKGROUND	1
1.2 MOTIVATION	3
1.3 RESEARCH OBJECTIVES	4
1.4 OUTLINE OF THESIS	5
CHAPTER 2: LITERATURE REVIEW.....	7
2.1 OIL SANDS TECHNOLOGY	9
2.2 HYDROGEN PRODUCTION TECHNOLOGY	12
2.3 CO ₂ CAPTURE TECHNOLOGY	30
2.4 CO ₂ CAPTURE WITH AMINE ABSORPTION	31
2.5 CO ₂ CAPTURE WITH MEMBRANE SEPARATION PROCESS.....	33
2.6 CO ₂ STORAGE AND UTILIZATION	37
CHAPTER 3: MODEL DEVELOPMENT	39
3.1 H ₂ PRODUCTION PLANT WITHOUT CO ₂ CAPTURE.....	39
3.2 H ₂ PRODUCTION PLANT WITH MEA-CO ₂ CAPTURE	62
3.3 H ₂ PRODUCTION PLANT WITH MEMBRANE CAPTURE	71
CHAPTER 4: RESULTS AND DISCUSSION	76
4.1 MODEL VALIDATION	76
4.2 SIMULATION RESULTS	77
4.3 COMPARISON OF THE H ₂ PLANT WITH CO ₂ CAPTURE.....	90
4.4 SENSITIVITY OF ENERGY PENALTY TO CO ₂ RECOVERY	92
CHAPTER 5: CONCLUSIONS	97
CHAPTER 6: RECOMMENDATIONS.....	99
NOMENCLATURE.....	101
ACRONYMS AND ABBREVIATIONS.....	103
REFERENCES.....	104
APPENDIX A: KINETIC PARAMETERS FOR SMR (XU AND FROMENT, 1989)	109
APPENDIX B: KINETIC PARAMETERS FOR WGS (RASE, 1977)	111
APPENDIX C: SIMULATION STREAM RESULTS (H₂ PLANT – BASE CASE)....	113

**APPENDIX D: STREAM RESULTS IN APPROXIMATING ELECTRICITY
REQUIREMENT FOR THE BASE CASE CONDITION (MEA CAPTURE PLANT)
..... 120**

**APPENDIX E: STREAM RESULTS IN APPROXIMATING ELECTRICITY
REQUIREMENT FOR THE BASE CASE CONDITION (MEMBRANE CAPTURE
PLANT)..... 122**

List of Tables

TABLE 2.1: GAS PERMEABILITY AND SELECTIVITY OF RUBBERY AND GLASSY POLYMERS	34
TABLE 3.1: PARAMETERS FOR THE SMR IN ASPEN PLUS	45
TABLE 3.2: EQUIVALENT KINETIC FACTOR PARAMETER VALUES OF SMR IN ASPEN PLUS	48
TABLE 3.3: EQUIVALENT DRIVING FORCE CONSTANT PARAMETER VALUES FOR K ₂ IN ASPEN PLUS	48
TABLE 3.4: EQUIVALENT ADSORPTION CONSTANT PARAMETER VALUES IN ASPEN PLUS	48
TABLE 3.5: SMR DATA FOR HEAT TRANSFER COEFFICIENT IN ASPEN PLUS	49
TABLE 3.6: ASPEN SIMULATION SPECIFICATIONS AND CONFIGURATIONS FOR SMR	52
TABLE 3.7: PARAMETERS FOR THE WGS CONVERTERS	52
TABLE 3.8: EQUIVALENT KINETIC FACTOR PARAMETER VALUES FOR WGS CONVERTERS IN ASPEN PLUS	55
TABLE 3.9: EQUIVALENT DRIVING FORCE PARAMETER VALUES FOR WGS CONVERTERS IN ASPEN PLUS	55
TABLE 3.10: ASPEN SIMULATION SPECIFICATIONS AND CONFIGURATIONS FOR HTS AND LTS	56
TABLE 3.11: ASPEN SIMULATION SPECIFICATIONS AND CONFIGURATIONS FOR PSA	58
TABLE 3.12: ASPEN SIMULATION SPECIFICATIONS AND CONFIGURATIONS FOR BLOCK SMR SYNGAS HEAT EXCHANGE	59
TABLE 3.13: ASPEN SIMULATION SPECIFICATIONS AND CONFIGURATIONS FOR HTS AND LTS HEAT EXCHANGE OPERATION	60
TABLE 3.14: ASPEN SIMULATION SPECIFICATIONS AND CONFIGURATIONS FOR SMR FURNACE FLUE GAS HEAT EXCHANGE OPERATION	62
TABLE 3.15: PROPERTIES OF HIGHVALE COAL	67
TABLE 3.16: ASPEN SIMULATION SPECIFICATIONS AND CONFIGURATIONS FOR HX OPERATION WITHIN THE H ₂ PLANT WITH MEA BASED CAPTURE	69
TABLE 3.17: ASPEN SIMULATION SPECIFICATIONS AND CONFIGURATIONS FOR APPROXIMATING POWER NEED OF THE MEA CAPTURE PLANT	71
TABLE 3.18: PARAMETERS OF THE MEMBRANE USED IN THE SIMULATION	73
TABLE 3.19: SPECIFICATIONS AND PARAMETERS FOR UNITS USED FOR H ₂ PLANT WITH MEMBRANE SEPARATION TECHNOLOGY	75
TABLE 4.1: COMPARISON BETWEEN SIMULATION RESULTS AND REFERENCE DATA	77
TABLE 4.2: SIMULATION RESULTS FOR THE 3 H ₂ PLANT CASES USING THE BASE CASE PARAMETERS	79
TABLE 4.3: OPERATING VARIABLES USED IN THE SIMULATION	81
TABLE 4.4: SENSITIVITY OF OPERATING PARAMETERS	82
TABLE 4.5 COMPARISON OF CO ₂ AVOIDED	92

List of Figures

FIGURE 1.1: REFERENCE TYPICAL H ₂ PLANT	3
FIGURE 2.1: PROJECTED H ₂ DEMAND FOR UPGRADING OF BITUMEN	8
FIGURE 2.2: CONVENTIONAL H ₂ PLANT - MEA (1960s – MID 1970s)	19
FIGURE 2.3: TYPICAL H ₂ PLANT – PSA (1970s – MID 1980s)	20
FIGURE 2.4: LATEST H ₂ PLANT – MEA + PSA (1980s - PRESENT)	21
FIGURE 2.5: BASIC PROCESS FLOW DIAGRAM FOR MEA-CO ₂ CAPTURE PROCESS	32
FIGURE 2.6: PROCESS FLOW OF MEMBRANE SEPARATION	35
FIGURE 3.1: H ₂ PLANT WITHOUT CO ₂ CAPTURE	40
FIGURE 3.2: ASPEN FLOWSHEET FOR H ₂ PLANT WITHOUT CO ₂ CAPTURE	43
FIGURE 3.3: TUBE WALL TEMPERATURE PROFILE OF SMR	50
FIGURE 3.4: BLOCK #1 - SMR	51
FIGURE 3.5: BLOCK # 2 – HTS	55
FIGURE 3.6: BLOCK # 3 – LTS	56
FIGURE 3.7: BLOCK # 4 - PSA	57
FIGURE 3.8: BLOCK #5 - SMR SYNGAS HEAT EXCHANGE SYSTEM	58
FIGURE 3.9: BLOCK # 6 - HTS HEAT EXCHANGE SYSTEM	59
FIGURE 3.10: BLOCK # 7 - LTS HEAT EXCHANGE SYSTEM	60
FIGURE 3.11: BLOCK # 8 - SMR FURNACE FLUE GAS HEAT EXCHANGE SYSTEM	61
FIGURE 3.12: PROCESS FLOW DIAGRAM FOR THE H ₂ PLANT WITH MEA-CO ₂ CAPTURE	63
FIGURE 3.13: H ₂ PLANT WITH SIMULATION IN APPROXIMATING THE AMOUNT OF ELECTRICITY NEEDED BY THE MEA CAPTURE PLANT	40
FIGURE 3.14: SIMULATION FLOWSHEET TO APPROXIMATE THE POWER NEEDED FOR THE MEA CAPTURE PLANT	70
FIGURE 3.15: ONE-STAGE MEMBRANE SEPARATION PROCESS	72
FIGURE 3.16: H ₂ PLANT WITH MEMBRANE SEPARATION TECHNOLOGY	75
FIGURE 4.1: SENSITIVITY OF ELECTRICITY REQUIREMENT OF CO ₂ CAPTURE PROCESS TO CO ₂ PRODUCTION (CASE OF 80% CO ₂ CAPTURE FROM THE FURNACE OF THE SMR)	85
FIGURE 4.2: SENSITIVITY OF ADDITIONAL ELECTRICITY REQUIREMENT AND CO ₂ PRODUCTION TO H ₂ PRODUCTION (MEA)	87
FIGURE 4.3: SENSITIVITY OF ADDITIONAL ELECTRICITY REQUIREMENT AND CO ₂ PRODUCTION TO H ₂ PRODUCTION (MEMBRANE)	88
FIGURE 4.4: COMPARISON OF CO ₂ EMISSIONS TO THE ATMOSPHERE: T _{SMRIN} = 900 K, T _{HTSIN} = 570 K T _{LTSIN} = 490 K	90
FIGURE 4.5: SENSITIVITY OF ADDITIONAL ELECTRICITY REQUIREMENT OF CO ₂ CAPTURE PROCESS TO CO ₂ PRODUCTION	91
FIGURE 4.6: SENSITIVITY OF ADDITIONAL ELECTRICITY REQUIREMENT TO PERCENT CO ₂ RECOVERY (MEA)	93
FIGURE 4.7: SENSITIVITY OF ADDITIONAL ELECTRICITY REQUIREMENT TO PERCENT CO ₂ RECOVERY (MEMBRANE)	94

FIGURE 4.8: COMPARISON OF CO₂ EMISSIONS TO THE ATMOSPHERE AT VARIOUS CO₂
RECOVERIES 95

Chapter 1

Introduction

1.1 Background

The demand for hydrogen gas (H_2) is rapidly increasing, especially because of the growing interest in producing unconventional oils from oil sands. The upgrading of raw bitumen from oil sands to produce synthetic crude oil (SCO) requires much larger quantities of H_2 than for conventional oil. It is estimated that this will contribute to an increase of greater than 400% of the current H_2 production in Western Canada in the next decade [Thumbimuthu, K., 2004]. The increase in the demand of H_2 for oil sands operations will then contribute subsequently to a major increase in CO_2 emissions, which is the major concern among all greenhouse gases. The Kyoto Accord or Protocol has been instituted to reduce the global greenhouse gas (GHG) emissions by the year 2008-2012. Thus, it is now important to look at the most efficient way of producing H_2 at lower CO_2 productions.

There are a number of ways to reduce greenhouse gases emitted from fossil-fuel based plants. One of these is by capturing the CO_2 emitted. The principal technologies include absorption, adsorption, membrane separation, cryogenic separation and CO_2/O_2 combustion. The present study will consider membrane and absorption technologies for CO_2 capture.

Hydrogen production using steam methane reforming (SMR) is currently the most economical, efficient and widely used process [Yurum, 1995]. This method is currently used

to supply the H₂ demand for oil sands operations. There are three process schemes for the production of H₂ from natural gas; they are so-called “conventional”, “typical” and “latest” schemes [Newman, 1985]. Figure 1.1 shows the “typical H₂ process” flowsheet used in this study as the reference. The other two schemes are shown in the next Chapter. The “conventional plant” uses amine absorption followed by methanation while the “latest plant” uses the combination of the amine absorption and the PSA in purifying the H₂ product. The “typical H₂ plant” uses PSA for purifying the H₂ product and is used by most current H₂ production plants. In the so-called “typical plant”, CO₂ is produced from two sources: from SMR and WGS reactions and from the natural gas burnt in the furnace of the SMR. Also, as can be seen in Figure 1.1, there are a number of heat integration opportunities (denoted by HX). Extra steam is the main by-product of the H₂ plant and is typically used for the process and for export. In this study, part of this steam is converted to electricity to supply the power needed for the H₂ and CO₂ capture processes (especially when using the membrane), as well as for CO₂ compression. Most of this steam is used to supply the heat needed by the reboiler of the stripper when amine scrubbing is used to capture CO₂.

Flue Gas (N_2 , H_2O , CO_2 , O_2 , CO)

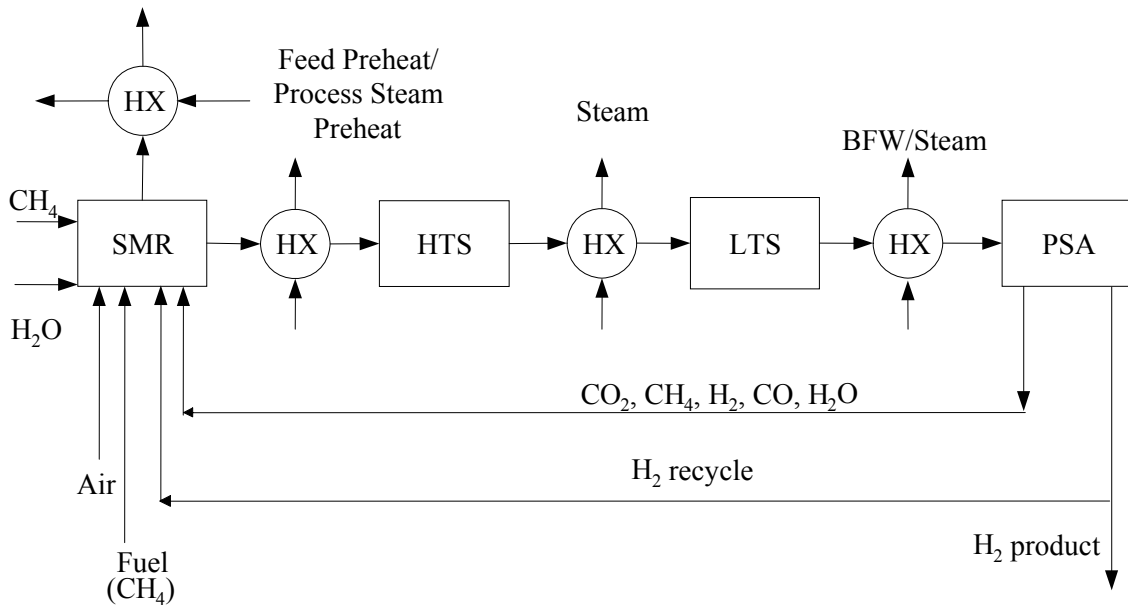


Figure1.1: Reference typical H₂ plant

1.2 Motivation

The increasing need for H₂ by chemical and petrochemical industries and in particular the projected expansion of Western Canadian oil sands operations which requires huge amounts of H₂ raises concern about CO₂ emission from its production. This study therefore looks at integrating CO₂ capture processes in a “typical H₂ plant”. In particular, there are two capture processes considered; chemical absorption and membrane separation. These two CO₂ capture processes require large amounts of energy. The steam produced from the H₂ plant is used to supply as much energy as possible needed by the CO₂ capture plant. Thus, finding optimum operating conditions for the H₂ plant with CO₂ capture in terms of energy penalty

by considering H₂, steam and CO₂ production and external combustion fuel used will greatly help balance energy usage.

1.3 Research Objectives

The objective of the study is to develop a CO₂ capture process at minimum energy penalty for the so-called “typical H₂ plant”. This is accomplished by investigating combinations of key operating parameters that minimize energy penalty. This minimum energy penalty is a function of H₂, steam and CO₂ production and external combustion fuel used. Two methods for capturing CO₂ are considered; 1) chemical absorption using amine solvent and 2) membrane technology. These two processes require different types of energy: the amine process requires considerable amounts of heat (usually provided in the form of steam) whereas the membrane process requires only energy for compression prior to feeding to a membrane which is supplied in the form of electricity. In addition to this, these two processes require electricity for compressing captured CO₂ for sequestration. The selection of the capture process thus influence the quality of steam and therefore the operation of the whole hydrogen plant. Performance comparison between the two capture processes considered is also presented as well.

As will be shown in this thesis, the steam produced cannot provide the entire energy requirement when high level of CO₂ is to be captured. In this situation energy (mostly electrical energy) must be provided externally. This study therefore also present for each

capture process considered the maximum amount of CO₂ that can be captured without the need to buy extra power to supply the need of the H₂ plant with CO₂ capture.

1.4 Outline of Thesis

The outline in attaining the objectives of this study is documented in the thesis as follows:

- Chapter 1 provides the background of the study and states the objectives of the study.
- Chapter 2 includes a literature review on oil sands operations, hydrogen production and CO₂ capture processes. A brief description of each process is provided, with focus on the processes used in the simulation, which is H₂ production using SMR, MEA-CO₂ capture process and membrane CO₂ separation technology.
- Chapter 3 provides details of the model developed for H₂ production with CO₂ capture process.
- Chapter 4 presents model validation, simulation results for all cases and comparison of MEA and membrane capture processes. This chapter also evaluates the sensitivity of energy penalty to the amount of CO₂ recovery.
- Chapter 5 presents the conclusions of the study.

- Chapter 6 presents some recommendations for future research.

Chapter 2

Literature Review

The production of hydrocarbon from oil sands has long been known and its initial production begun in the year 1967. Oil sands in Canada are one of the largest hydrocarbon resources. It ranked second to Saudi Arabia in terms of oil reserves. Most of these resources are located within the province of Alberta. The technological advancements and the higher energy prices have made the oil sands operation increasingly more economic to develop [National Energy Board, 2004]. It has been foreseen that the production of hydrocarbon from oil sands is expected to more than double in the next decade to that of the 2004 production. However, concerns have been raised on the impact of producing hydrocarbons from oil sands. The Government of Canada included oil sands producers as one of the Largest Industrial Emitters in the Climate Change Plan for Canada on November 21, 2002. This sector is expected to produce about half of Canada's total GHG emissions by 2010. [National Energy Board, 2004]

Some significant environmental concerns are GHG emissions and associated climate change, boreal forest disturbance and water conservation. [National Energy Board, 2004]. The major concern among these air emissions that cause global climate change are the large amounts of CO₂ produced, some methane (CH₄) and nitrous oxide (N₂O). CO₂ accounts to 85-95% of the total effect and thus is the GHG that requires the most attention to look at considering the international commitment of Canada in reducing its greenhouse gas (GHG) emissions by 6% in the year 2012.

Figure 2.1 shows the projected H₂ demand for upgrading raw bitumen [Ordorica-Garcia et al., 2004]. In addition to this, H₂ is also needed in refining synthetic crude oil (SCO). There are a number of technologies that mitigates CO₂ emissions. Future oil sand operations can integrate these technologies to support the Kyoto protocol. These technologies include the use of renewable energy sources, fuel switching and optimized energy efficiency. For deep CO₂ reduction in the medium term, CO₂ capture and storage has been proposed as a promising measure to reduce CO₂ emission produced from fossil fuels. However, CO₂ capture technology requires a vast amount of energy.

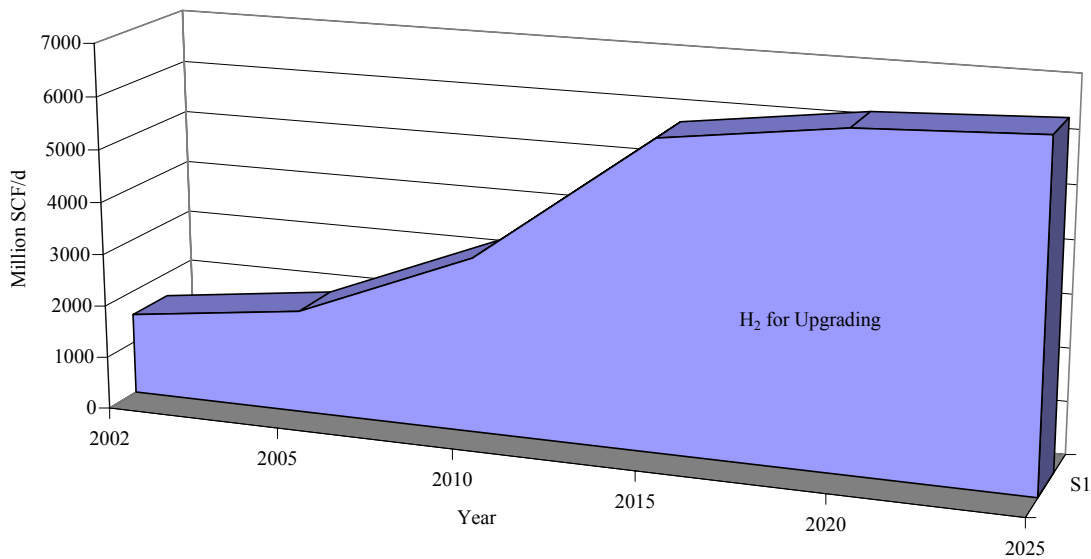


Figure 2.1: Projected H₂ demand for upgrading of bitumen

The following sections present a literature review on oil sands industry, hydrogen production and CO₂ capture processes. Special focus is given on H₂ production using SMR. Two CO₂ capture processes considered in this work are also presented in more details.

2.1 Oil Sands Technology

Oil sand is defined as sand and other rock material which contain bitumen. Each particle of oil sand is coated with a layer of water and a thin film of bitumen [Syncrude Canada Ltd., 2006]. Its composition is typically 75-80 % inorganic material, 3-5 % water and 10-12 % bitumen. Bitumen is characterized by its high densities, high metal concentrations and a high ratio of carbon-to-hydrogen molecules. Its properties are typically: density - 970 - 1015 kg/m³ and viscosity – 50000 centipoise (room temperature) [National Energy Board, 2004]. Due to these properties, these bitumen deposits cannot be transported via pipeline. The bitumen in the oil sands is then upgraded into SCO, which will in turn be suitable for pipeline transport.

There are several technologies for extracting oil sands. These are thru mining and in-situ technologies. Mining is used when oil sands are close enough to the surface while in-situ technologies are used for other deeper deposits. The bitumen from the oil sands is then extracted and upgraded into SCO. Mining involves gigantic draglines that are connected to a processing plant by a system of conveyor belts. However, recent innovations have switched to much cheaper shovel-and-truck operations using the biggest power shovels and dump trucks in the world. Some in-situ technologies are quite new and some innovative processes

are expected to come out in the future. To name a few, there are the steam assisted gravity drainage (SAGD), vapor extraction process (VAPEX), toe-to-heel air injection (THAI) and nexen/OPTI long lake project. [National Energy Board, 2004; Alberta Chamber of Resources, 2004]

The extraction of the bitumen from oil sands includes conditioning, separation, secondary separation and froth treatment. The extracted bitumen is then sent to an upgrader for conversion into SCO. [Canadian Institute of Mining, Metallurgy and Petroleum, 2006]

Bitumen is upgraded to produce SCO and other petroleum products. Bitumen has a very high ratio of carbon-to-hydrogen molecules when compared to conventional crude oils. Upgrading can be done by addition of hydrogen or removal of carbon or changing of molecular structures. Prior to upgrading, the naphtha left over from froth treatment is removed by distillation. There are four main steps for upgrading which are thermal conversion, catalytic conversion, distillation and hydrotreating. [Canadian Institute of Mining, Metallurgy and Petroleum, 2006]

Thermal conversion involves breaking heavy hydrocarbon molecules into smaller hydrocarbon molecules through heating. Cracking is the term used for this reaction. An intense thermal cracking is termed as coking. There are two types of coking process used by the oil sands industry which are the delayed coking and the fluid coking. The by-product of the coking process is the called coke. In the delayed coking, bitumen is heated to 500°C where it cracks into solid coke and gas vapour. This process uses a double-sided coker where one side of the coker is filled up first and then followed by the other side of the coker.

The fluid coking process uses only one coking drum. The process involves heating up the bitumen up to 500°C and then spray it in a fine mist in the coker where the bitumen cracks into gas vapour and coke. The coke formed is then drained from the bottom. The coke produced is used as a fuel for coke furnaces and hydrocracking. The next step is the catalytic conversion where refinement into even smaller molecules is done. High-pressure H₂ is added to help produce lighter H₂-rich molecules. This process is termed as hydroprocessing. Another alternative in upgrading is to remove carbon. The following step is the distillation of the semi-refined bitumen. This is carried out in a distillation or a fractionating tower where successive vaporization and condensation of various compounds occurs. The separation is based on the difference in the boiling points of each compound. Higher boiling point compounds are collected in the lower part of the tower while the lighter gas condenses into heavy and light gas oils, kerosene and naphtha. The last step is the hydrotreating process. This is considered as the major process in upgrading. This involves stabilizing the hydrocarbon produced from the distillation process (gas oils, kerosene, naphtha) by adding hydrogen to the unsaturated molecules. Hydrotreating also reduces or removes chemical impurities such as nitrogen, sulfur, and trace metals from hydrocarbon molecules. [Canadian Institute of Mining, Metallurgy and Petroleum, 2006]

The upgrading of bitumen consumes about 5-10 times more H₂ than conventional crude oil refining. Figure 2.1 shows the projected H₂ demands for upgrading. The annual demand growth is around 17%. With the inclusion of the H₂ demand for refining of SCO, it is then expected that there will be a huge increase in H₂ production which will make oil sands

operation the largest user of H₂ in the world. Since H₂ production releases CO₂, it is then expected that oil sands operations will be tagged as the largest CO₂ emitter in Canada.

2.2 Hydrogen Production Technology

Different technologies can be used in producing H₂ depending on the capacity needed. Production by electrolysis is preferable for small quantities of very high purity H₂ (below 100 Nm³/h or 90 Mscfd). H₂ production from methanol or ammonia cracking/reforming is suitable for small, constant or intermittent requirements. Such small quantities of H₂ are typically used in the food, electronics and pharmaceutical industries. Steam reforming and/or high temperature reforming processes using oxygen (O₂) is used for the production of larger quantities of H₂ (above 500 Nm³/h or 450 Mscfd) [Dybkjaer and Madsen, 1997/98].

H₂ can be produced from both renewable and non-renewable energy sources. This is described in the following sections.

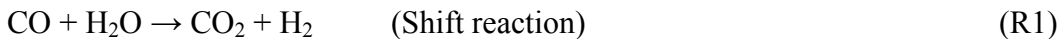
2.2.1 H₂ Production from Non- renewable Energy Source

Methods for H₂ production from non-renewable source such as fossil fuels include gasification of coal, steam reforming of natural gas and autothermal reforming of oil and natural gas. The majority of these processes are based on heating up hydrocarbons, steam and in some instances air or oxygen, which are then combined in a reactor. Under this process, the water molecule and the raw material are split, and the result is H₂, carbon

monoxide (CO) and CO₂. Another method is to heat up hydrocarbons without air until they split into H₂ and carbon (C). A brief description of each process is given below.

Gasification of coal

This is the oldest method of producing H₂. The gas contains 60% H₂ but also large amounts of CO₂. The process typically converts coal into a gaseous form by heating it up to 900°C. This gas is then mixed with steam and passed over a catalyst, usually nickel-based. There are also other complex methods of gasifying coal. The common factor is that they turn coal, treated with steam and oxygen at high temperatures, into H₂, CO and CO₂. These gases are then reacted with steam in CO-shift converters where the CO is converted into H₂, as shown in the following reaction:



Two types of CO-shift converters operated at different temperatures are used in the process to maximize the conversion of CO. The high temperature shift (HTS) converter is usually operated at 300-500°C while the low temperature shift (LTS) converter is operated at 200°C, with different catalysts in the two converters. The CO₂ produced is then separated from H₂. The CO₂ separated from the H₂ can be sequestered to avoid release in the atmosphere. Possible depositories include empty oil and gas reservoirs, or underground water reservoirs, called aquifers [Buch et al., 2002].

Steam methane reforming (SMR)

This method is currently the most economical to produce H₂, and accounts for about 76% of all H₂ produced. It is thus the leading technology for production of hydrogen-rich gases [Dybkjaer and Madsen, 1997/98]. This process involves the heating of steam with CH₄ gas in a reactor filled with a nickel catalyst at a temperature of 700-1000°C and a pressure of 1.7-2.8 MPa [Van Weenan, 1983]. In addition to the natural gas being part of the reaction process, an extra 1/3 of the natural gas fed is needed to power the reaction [Buch et. al., 2002]. Gases from the reformer are then sent to shift-converters to produce more H₂. CO₂ separation and depositing follow next.

Autothermal reforming of oil and natural gas

This method involves reacting hydrocarbons with a mixture of O₂ and in a “thermo reactor” with a catalyst. The process is a combination of partial oxidation and steam reforming. The name implies heat exchange between endothermic steam reforming and exothermic partial oxidation [Buch et al., 2002]. This is a cost-effective option when O₂ is readily available [Dybkjaer and Madsen, 1997/98].

This method is used for heavy hydrocarbons with low fluidity and high sulphur concentrations. These hydrocarbons are subjected to partial oxidation, or are autothermally converted in a flame reaction by adding steam and O₂ at 1300-1500°C. The relative ratio of O₂ to steam is controlled so that the gasification process requires no external energy. The reformer outlet gas is then passed to two shift-converters successively in order to increase the

production of H₂. This can then be followed by separation and sequestration of CO₂ [Buch et al., 2002].

Thermal dissociation

Thermal dissociation is done by heating hydrocarbon compounds without O₂ at very high temperatures to separate the hydrocarbon compounds into H₂ and C. To produce hydrogen without emitting any greenhouse gases, this process assumes permanent deposition of the carbon. The following reaction occurs with the use of CH₄ [Buch et al., 2002]. The overall reaction is shown in equation (R2).



An example of this is the carbon black and hydrogen process. A plasma burner is used in this process to supply the adequate amount of heat needed to split H₂ compounds in a high temperature reactor. Recycled H₂ from the process is used as plasma gas. This was first commercialized in June, 1999 by Kvaerner and was referred to as the Kvaerner Carbon Black and Hydrogen Process. Kvaerner states that there are no emissions from this process, which makes it suitable for H₂ production. Its feed ranges from light gases to heavy oil fractions [Palm et al., 1999].

2.2.2 Hydrogen Production Using Renewable Energy Source

H₂ is found in large amounts on earth, bound in organic material and in H₂O. H₂O is composed of 11% H₂ by weight and covers 70% of the earth. There is definitely an abundant

supply of H_2 . H_2 is totally renewable since it binds itself to the O_2 in the air and its combustion product is pure H_2O .

H_2O can be separated into its components, H_2 and O_2 , with the use of energy such as heat, light, electricity or chemical energy. Examples of H_2 production from renewable energy sources are described below.

Electrolysis of water

This process involves passing an electric current through H_2O to separate it into H_2 and O_2 [Buch et al., 2002].

Photoelectrolysis

This process uses sunlight to split H_2O into its components via a semi-conducting material sandwich. This method is still in the experimental stage and has not yet evolved beyond the laboratory [Rocky Mountain Institute, 2003].

Thermal decomposition of water

This process involves breaking H_2O into its components, H_2 and O_2 , by heating it to over $2000^\circ C$. This is considered to be an innovative and inexpensive method of producing H_2 directly from solar energy. Research is also being done on the use of catalysts to reduce the temperature for dissociation. One central problem is the separation of gases at high temperatures to avoid recombination [Buch et al., 2002].

Gasification of biomass

H₂ can be extracted from biomass thru thermal gasification. Examples of biomass are forestry by-products, straw, municipal solid waste and sewage. Biomass contains about 6-6.5 weight percent of H₂ compared to almost 25% for natural gas. The process involves the breaking of biomass into H₂, CO and CH₄ at high temperatures. This gas then undergoes steam reforming and shift conversion. The by-product in this process is CO₂, but CO₂ from biomass is considered “neutral” with respect to greenhouse gas. It does not increase the net CO₂ concentration in the atmosphere [Buch et al., 2002].

Biological Production

In 1896, it was discovered that certain species of blue-green algae (*Anabaena*) produces H₂ in the presence of sunlight. Algae produce H₂ with an efficiency of up to 25%. However, O₂ is also produced during the process which inhibits the H₂-producing enzyme hydrogenase, so only small amounts of H₂ are actually produced. Current research is being conducted on this method [Buch et al., 2002].

2.2.3 H₂ Production Using SMR

Steam reforming of hydrocarbons has been the principal process for the generation of H₂ and synthesis gas in the chemical industry. In addition to being the cheapest method of producing H₂, it is also the most efficient. Natural gas is the feedstock to the process. About 76% of all H₂ produced comes from steam reforming (primary and secondary) of natural gas [Adris and Pruden, 1996]. The need for hydrogen is expected to increase, considering the deteriorating quality of crude oils, stringent petroleum product specifications, and strict

environmental regulations. Although H_2 is regarded as the cleanest energy carrier, its CO_2 emission may become a major barrier in satisfying environmental regulations. There are two emission sources of GHG in the process. One is the flue gas exiting the SMR and the other, the gases from the process reactions (SMR and water-gas shift (WGS) reactions). The reformer products are CO_2 , CO , N_2 (if air is used in the feedstock), O_2 and unconvertible CH_4 .

The process essentially consists of 4 main steps: desulphurization, synthesis gas generation, water-gas shift reaction and purification. There are different purification methods used which are classified depending on the chronological order of their implementation. The conventional method involves purification with the use of an amine solvent and methanation to remove CO_2 and to eliminate carbon oxides (CO , CO_2), respectively. This was prevalent in the early 1960s until the mid 1970s. In the 1970s, pressure swing adsorption (PSA) was introduced. Most new hydrogen plants use PSA technology since the mid 1980's. A recent purification method is the combination of both amine scrubbing and PSA [Barba et al., 1998]. These purification methods are implemented to capture CO_2 and other impurities produced from both the steam reformer reactions and water-gas shift reactions. These three processes are shown in Figure 2.2 to Figure 2.4 [Newman, 1985].

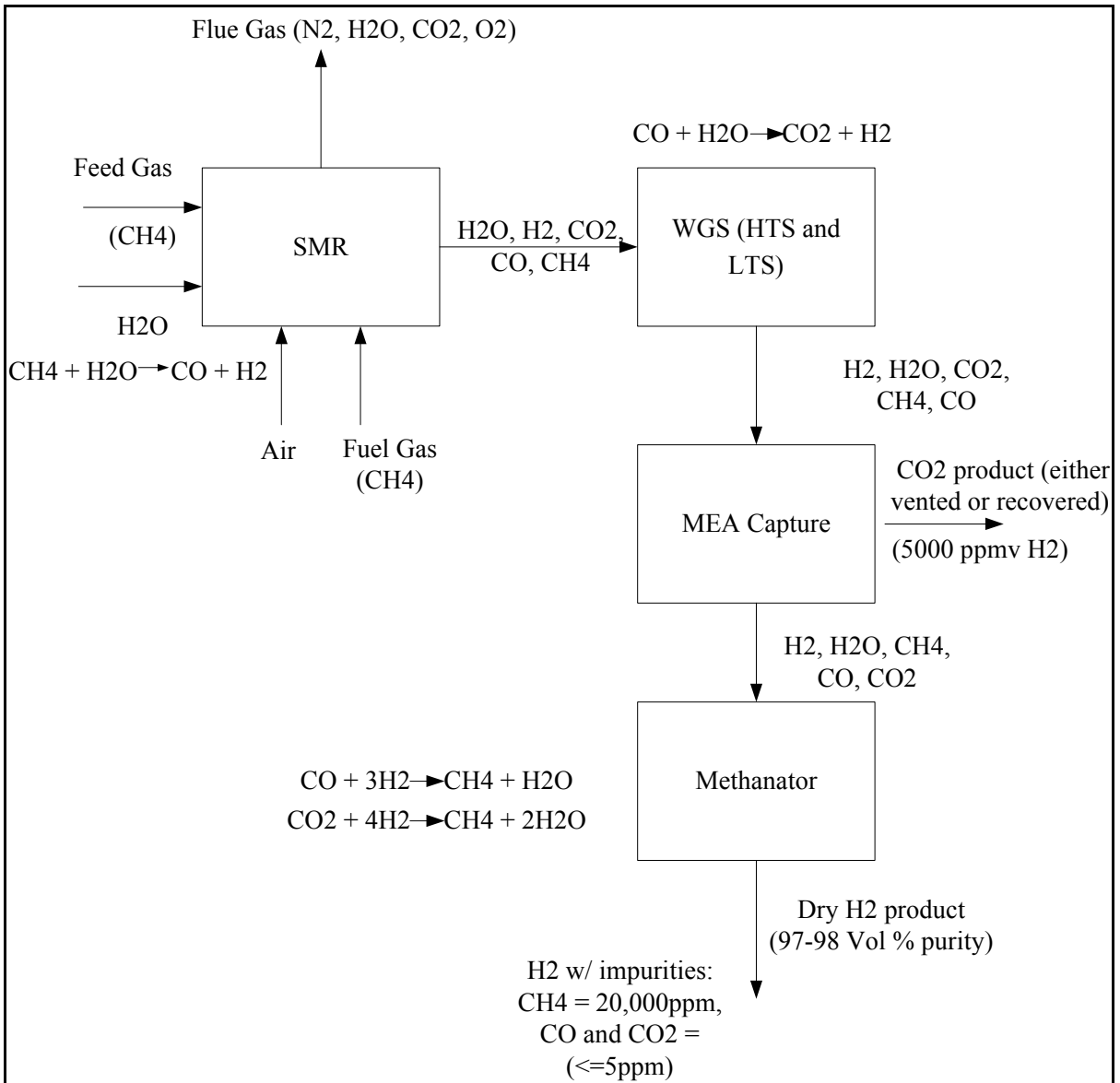


Figure 2.2: Conventional H₂ plant - MEA (1960s – mid 1970s)

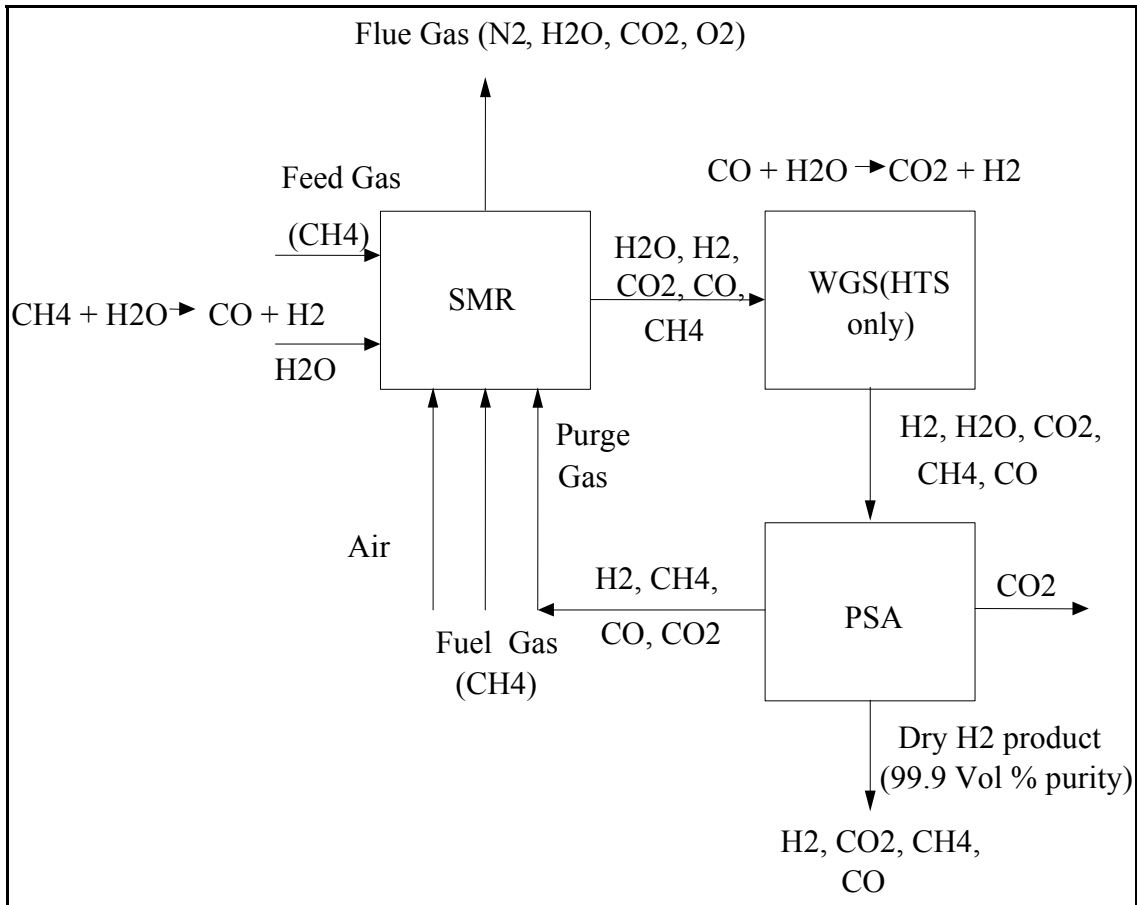


Figure 2.3: Typical H₂ plant – PSA (1970s – mid 1980s)

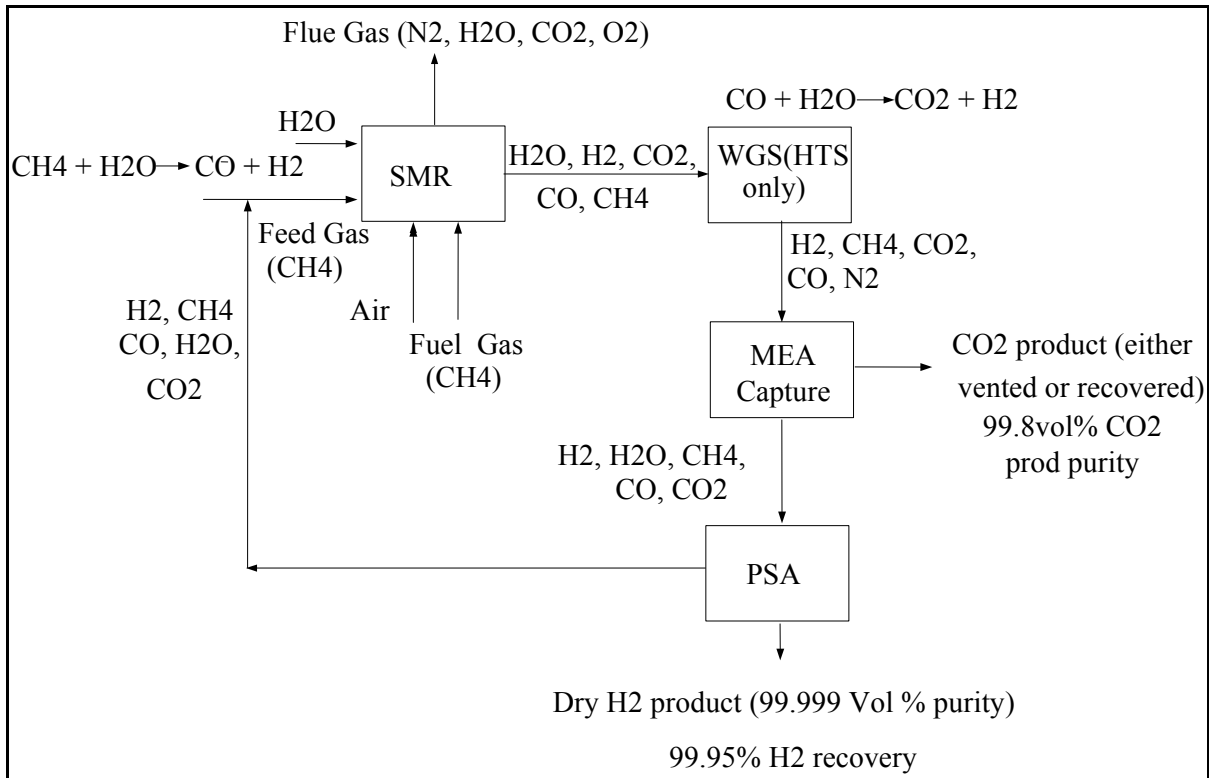


Figure 2.4: Latest H₂ plant – MEA + PSA (1980s - present)

The above figures are variations of the different purification methods in hydrogen production. The difference among the processes is the method of purifying hydrogen. The description of each method is given in the following sections.

Conventional H₂ Plant

Figure 2.2 shows the conventional H₂ plant. This method uses a methanator and amine scrubbing to purify the product H₂. The process uses some of the product H₂ to react with carbon oxides to produce CH₄ in the methanator. Oxides of carbon usually exit with a concentration in the order of 5 ppm which is acceptable for downstream users of H₂. Reactions (R3) and (R4) show the methanation reaction.



This method produces an H₂ product purity of 95-97 vol%. The impurities include CH₄ and possibly N₂ (if air is present in the feedstock). More CH₄ is generated by this method. It comes from the unconverted CH₄ in the SMR and the CH₄ formed in the methanator. Thus, the steam to carbon ratio (S/C) used (5:1 to 7:1) is critical to obtain high levels of CH₄ conversion. The use of some H₂ to generate more CH₄ reduces the purity of H₂.

The use of a low-temperature shift (LTS) converter helps in reducing the residual CO in order to get higher purity of product H₂. Product CO₂ is either vented or recovered from MEA. This method is typically used when a large amount of CO₂ by-product relative to the H₂ production rate is required [Newman, 1985].

Typical H₂ Plant (PSA)

The typical method uses one shift converter (HTS) and a PSA to purify the H₂ product. Some literature shows typical plant as consisting of two shift converters (HTS and LTS) [Rajesh et al, 2000]. This method generates a high purity H₂ (99.9 vol %), which is its advantage over the conventional method. The process is operated at a lower S/C ratio of 3:1. Thus, there is a high level of impurities produced in the synthesis gas (syngas) due to a lower S/C ratio. These impurities are recycled as fuel to the furnace from the PSA, and therefore it is not as important to get a high purity syngas.

This method is typically used by modern plants due to its high reliability and high purity. It is now the world standard for H₂ production. This study uses this method using two shift converters (HTS and LTS shift converters) instead of only one. An additional shift converter is used to avoid large volumes of CO in the flue gas.

The 4 main steps of this process, desulphurization, synthesis gas generation, water-gas shift and purification, are described in the following sections. In this study, the feed gas is assumed free of sulfur and hence the desulphurization unit is not simulated.

Desulphurization

The feed gas typically contains sulphur compounds which are removed by the desulphurization unit of the plant. The removal of these sulfur compounds is required to maximize the life of the catalysts used in downstream steam reforming and elsewhere. Sulphur is the major poison in catalysts used in steam reforming plants. Concentrations as low as 0.1 ppm produce a deactivating layer on the catalyst surface [Yurum, 1995]. Permanent deactivation of the catalyst may occur together with the mechanical problems caused by carbon deposits if high pulses of sulfur concentration occur in the feedstock. Chlorine and other halogen compounds as well as lead, arsenic and vanadium are the other poisons [Yurum, 1995]. Chlorine compounds are less common and metal compounds are typically found in some heavier LPG and naphtha feedstocks [Phillipson, 1970].

In the desulphurization unit, the feed gas is first preheated to about 371°C by heat exchange with the reformer product. In practice, the reaction temperature is not higher than

400°C in order to minimize cracking of the feedstock. Zinc oxide (ZnO) alone is used both as a catalyst and an adsorbent preferably at a temperature range of 350-400°C for cases where the natural gas contains only hydrogen sulfide (H₂S) and mercaptans. Activated charcoal or molecular sieves are mainly used as adsorbents but their efficiency is low in adsorbing low-boiling point sulfur compounds. Furthermore, the presence of condensable hydrocarbons can rapidly saturate the adsorbent. A combination of cobalt molybdate (CoMo) and ZnO is used when the natural gas contains higher boiling point feedstocks that may include thiophenic compounds. CoMo removes organo-sulfur compounds by a reaction with H₂ to convert the sulfur to H₂S. This H₂S is then adsorbed by the ZnO. [Phillipson, 1970] Organo-chlorides are similarly converted to yield chlorine as HCl. CoMo is the most common type of hydrodesulphurization catalyst in service. Nickel molybdate is preferred under certain conditions such as high CO or olefin content in the feed [Johnson Matthey Catalysts, 2003].

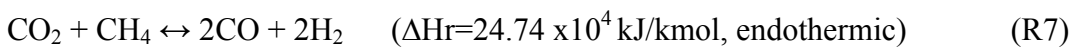
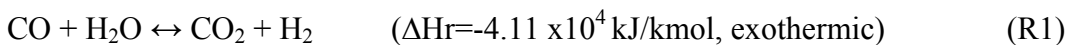
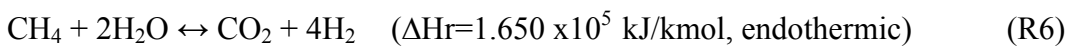
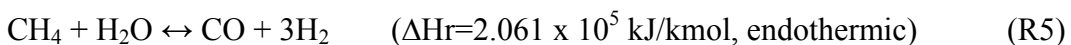
Steam-Methane Reformer Unit

After desulphurization, the feed gas is mixed with steam. This mixture of gases is preheated in the convection section of the reformer to a temperature of 482°C before entering the reformer. Subsequently, the preheated gas-stream mixture is then passed through the reformer which contains a number of vertical catalyst-filled tubes. The reaction takes place inside the reformer with the help of a nickel oxide catalyst. The reformer operates at an outlet pressure of 1.7-2.8 MPa and an outlet temperature of 816-871°C. The overall SMR reaction is an endothermic reaction and the heat needed for the reaction to occur is supplied

by firing burners on the outside of the tubes. The fuel used to supply heat in the reformer tubes is typically part of the feed gas.

The fired duty in an SMR amounts to 50% of the heat content in the process natural gas. About one-half of the fired duty is transferred through the reformer tubes and adsorbed by the process (60% for reaction, 40% for temperature increase) [Rostrup-Nielsen, 1984]. The rest leaves the reformer as hot flue gas. The heat from the hot flue gas is recovered by cooling it in a series of heat-exchange operations. Some of these heat-exchange operations are carried out by preheating the steam reformer feed, heating boiler feedwater to produce superheated steam, and preheating combustion air. The burner exhaust gas leaves the heat-recovery units at 150°C for release to the atmosphere.

The different types of reformer burners that may be used are side-wall fired, terrace wall fired, down-fired and top-fired [Van Weenan, (1983)]. Any pair of the following four reversible reactions will account for the stoichiometry in SMR [Hyman, 1968].



The net heat of reaction can be accounted for with the proper application of any pair. Any pair among these is adequate for representing equilibrium compositions. Reactions (R5)

and (R1) are commonly used. These two reactions apply when the ratio of steam to methane is high enough to prevent the presence of carbon at equilibrium [Rase, 1977]. A great deal of research has been done on the kinetics of the reactions. Akers and Camp, (1955) contended that reactions (R5) and (R6) must be the actual kinetic mechanism. Their result showed that both CO and CO₂ are the primary products of the methane-steam reforming reaction. They were the first ones to study the kinetics behind SMR. They showed that reaction (R1) does not contribute to the formation of CO₂. Van Weenan (1983) and Grover (1970) used equations (R5) and (R1) in their research. Other researchers contended that reactions (R6) and (R7) must be the actual kinetic mechanism [Hyman, 1968]. Van Hook (1980) presents a complete review of the kinetics of the SMR at that time. The intrinsic kinetics for the SMR, WGS and methanation has also been dealt by Xu and Froment, 1989. Their model predicted that (R5), (R6) and (R1) describe the reaction mechanism of the SMR process. The summary of their works are included in the Appendix A. This is implemented in this study.

Reaction (R1) is commonly referred to as the WGS. Its conversion is favored by low temperatures. The WGS reaction in the SMR unit is found to be at thermodynamic equilibrium at 50% or greater methane conversion [Akers and Camp, 1955; Van Hook, 1980].

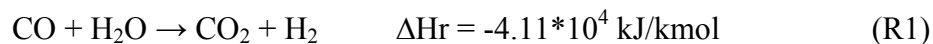
Bridger (1970) reported that the steam methane reforming reaction does not approach equilibrium. Its deviation from equilibrium is characterized by an ‘approach to equilibrium’ which is related to the catalyst activity. This defines the extent of the methane steam reaction. The approach increases as the catalyst deteriorates. This ‘approach to equilibrium’

is estimated as 10-15°C for temperatures up to 800°C and pressures up to 3.10 MPa using nickel oxide (raschig rings) catalyst [Bridger, 1970].

The reformer product stream is then cooled to a temperature of about 350°C by passing through a waste heat boiler and by heat exchange with the reformer feed gas. The reformer serves as an energy converter as seen in the process above. The heat of the reformer product is used to preheat the reformer feed and the boiler feed water. The convection section of the reformer is also used to preheat boiler feed water and the feed gas.

Water-Gas Shift Converter

After the outlet gas exits the cooler, it is fed to a high-temperature shift (HTS) converter where CO is reacted with steam to form CO₂ plus additional H₂. This is termed as the CO shift reaction. The reaction is exothermic and is described by:



The HTS converter product leaves at a temperature of 400-423°C and is cooled by the preheating boiler feedwater and deaerator feedwater.

The exit gases from the HTS converter enter the LTS converter to convert residual CO to H₂. The LTS converter operates at a temperature of 190-210°C. Final cooling may be done by water cooling or a combination of air and water cooling. The condensate is then separated from the product gas [Van Weenan, 1983].

Rase (1977) presented a case study on the design of a shift converter. The reaction kinetics that occurs on the shift converter is reaction (R1) with no side reactions. Complete list of the rate expressions is presented in Appendix B and is used in this study.

Gas Purification

The gas exiting from the condenser enters a PSA where H₂ product is purified. PSA is designed to adsorb impurities from an H₂-rich feed gas onto a fixed bed of adsorbents at high pressure. The impurities are desorbed and an extremely pure H₂ product is produced. The impurities or the off-gas from the PSA is used as fuel to the furnace of the SMR.

Purification of hydrogen can also be accomplished by absorption, adsorption, membrane processes, cryogenic processes and CO₂/O₂ combustion cycles. These processes can also be used to purify flue gas exiting from the steam reformer.

Latest H₂ Plant

Figure 2.4 describes the latest H₂ plant. It also has a desulphurization unit, an SMR and a WGS (with only one HTS). Its difference from the other two methods lies in the use of both an MEA and a PSA to purify H₂. This method generates a dry H₂ product purity of 99.999 vol% at 99.95% recovery. H₂ product purity obtained by this method is independent of the reformer process conditions. Larger reductions in reformer S/C ratios can be undertaken since the increasing unconverted CH₄ slippage is caught by the PSA unit and recycled without affecting final H₂ product purity. This leads to major energy savings. Reductions to as low as 3:1 S/C ratio can be used. Purge gases (CH₄, CO, H₂O, H₂ and trace amounts of

CO₂) are fed to the reformer either as feed or fuel. 100% recovery of H₂ product is essentially attained when these purge gases are fed as feed to the reformer. Of these recycled purge gas constituents, the CH₄ is reformed, the CO is shifted, the CO₂ removed and the H₂ is recovered, thereby achieving maximum conversion and recovery of the reformer CH₄ to H₂ product. A small slipstream of the purge gas is sent to the reformer fuel to prevent an N₂ buildup in the loop for cases where N₂ is present in the reformer feed gas. The methanator vessel is eliminated in this process since residual CO and CO₂ are removed from the syngas in the PSA unit for recycle. Without the methanator, H₂ consumption and CH₄ generation into the H₂ product via methanation are negated. The LTS converter is optional since unshifted CO from the HTS effluent is recycled by the PSA unit to the reformer feed. This method is typically used by new plants today.

2.2.4 Modelling, Simulation and Optimization of Hydrogen Production

Plants

A number of researchers have dealt with modeling, simulating and optimizing H₂ plants [Hyman, 1968; Grover, 1970; Van Weenan et al, 1983; Karasiuk, 1985; Rajesh et al, 2000; Rajesh et al, 2001]. Hyman [Hyman, 1968] modeled an SMR using numerical integration that determines the process stream conditions at the outlet of an SMR tube. The work of Grover [Grover, 1970] formulated a theoretical model that predicts CH₄ conversion, product distribution and temperature profile along the length of the reactor. The model can be used to test the optimum process variables needed to come-up with optimum results. Van Weenan et al. [Van Weenan et al, 1983] determined the best process flow scheme for an H₂ plant. Their research compared the efficiency of seven different H₂ production process flow

schemes. The differences among the process flow diagrams are the heat integration within the H₂ plant, the amount of feed and fuel used and the use of steam. Karasiuk [1985] designed a control strategy that determines the best way to operate an H₂ plant depending on the amount of H₂ desired or the maximum H₂ product. Multi-objective optimizations of an SMR and of the whole H₂ plant were presented by Rajesh et al [Rajesh et al, 2000; 2001]. His works output a set of operating conditions for an SMR unit for a desired H₂ production rate [Rajesh et al, 2000]. His other work also dealt with the whole H₂ plant by maximizing the H₂ and steam productions subject to operational constraints and decision variables.

The present study uses the constraints and the bounds on the decision variables given by Rajesh et al. [Rajesh et al, 2001].

2.3 CO₂ Capture Technology

Several processes for capturing CO₂ are available. The principal technologies include chemical and physical absorption, adsorption, membrane separation, cryogenic separation and CO₂/O₂ combustion.

The present study investigates and compares an absorption process and membrane separation process in capturing the CO₂ from the flue gas of the furnace of the SMR. The absorption process uses monoethanolamine as the solvent absorber and the membrane separation process uses a cardo-polyimide membrane.

The absorption process using monoethanolamine (MEA) as the CO₂ gas absorbent is considered because of the wealth of literature available and also because of the existence of industrial applications. Membrane gas separation was considered because, compared to MEA scrubbing, it presents potential advantages such as simplicity of process design, compactness, light weight, low maintenance, ease of installation, avoids corrosion of equipment and high process flexibility (modular design permitting easy scale up or operation at reduced capacity as necessary). Membrane technology has seen significant advances in the past decade. This includes investigating new materials that could lead to better energy consumption and cost-effective process. These two processes are tested and compared when integrated to the H₂ plant in capturing CO₂ emissions.

2.4 CO₂ Capture with Amine Absorption

The present study uses MEA as the CO₂ gas absorbent. Other solvents are discussed elsewhere [Khol and Riesenfeld, 1985]. Singh et al. (2003) and Alie et al (2005) presented simulation of the CO₂ capture plant in Aspen Plus. Their works used MEA as the acid absorbent since extensive literature abounds. It is also being used by most industries and has been in the world market for many years [IEA GHG, 2003].

The basic process flow for amine absorption of acid gases is shown in Figure 2.5.

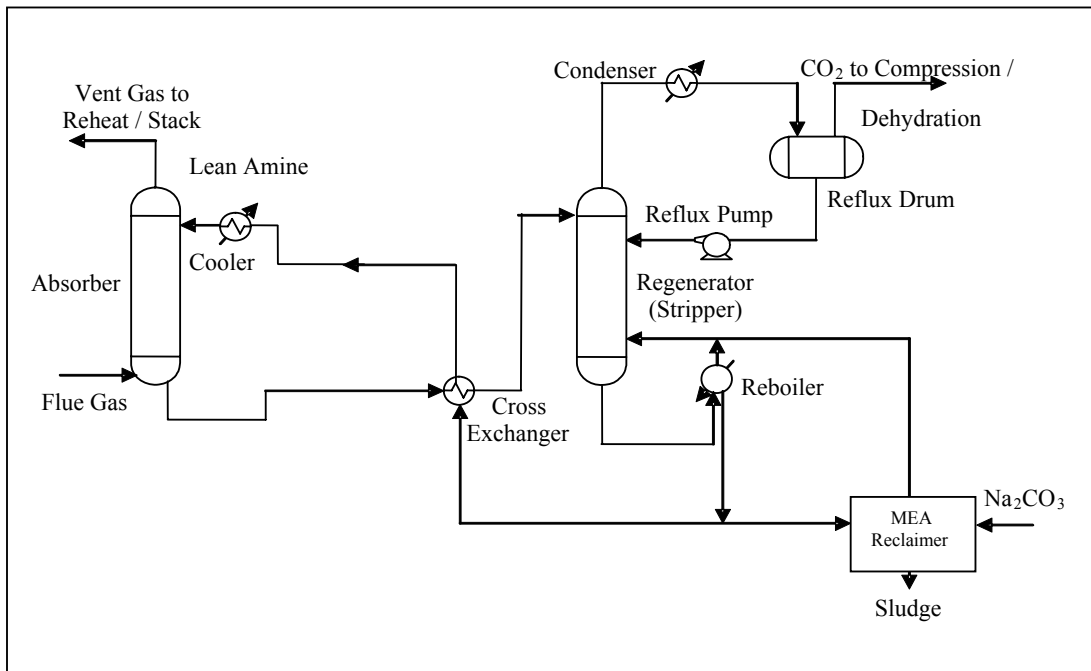


Figure 2.5: Basic process flow diagram for MEA-CO₂ capture process

The gas to be purified enters the bottom of an absorption column and flows upward countercurrently with a stream of extracting solution injected at the top of the absorber. The extracting MEA solution contains 30% MEA (by wt) and 70% H₂O (by wt). The ratio of the number of moles of CO₂ to the number of moles of MEA is called the loading. The extracting solution entering at the top of the absorption column is called the lean loading since it contains less CO₂. Conversely, the solution leaving the absorption column is called rich loading. Typically, the lean solution has a CO₂ loading of 0.1-0.2 mol/mol while the rich solution typically has a CO₂ loading of 0.4-0.5 mol/mol MEA [Freguia and Rochelle, 2002]. The rich solvent is then sent to a stripper at some point near the top where the CO₂ and water vapour are stripped from the amine solvent by the steam from the reboiler column. The CO₂ with water vapour is cooled to condense a major portion of the water vapour. The

condensed vapour returns to the stripping column and is brought into intimate contact with the vapours leaving the stripper. This prevents the amine solution from being progressively more concentrated and also to force back the amine vapours carried by the acid-gas stream. A heat-exchange operation is done by heating the rich solution from the bottom of the absorber with the hot lean solution exiting from the bottom of the stripper. This lean solution is further cooled by exchange with water or air before it is returned to the top of the absorber [Khol and Riesenfeld, 1985].

A correlation of 1.7 kg steam/kg of CO₂ is found by Singh et al. (2003). This is used in this study.

2.5 CO₂ Capture with Membrane Separation Process

There are a number of membrane processes or unit operations which differ primarily on the basis of the driving force for mass transfer through the membrane, the predominant transport mechanism and the phases that are present. Section 2.5.1 presents the different types of membrane materials for CO₂ separation. Section 2.5.2 describes the membrane gas separation process as well as the theory behind the separation.

2.5.1 Membrane Materials for CO₂ Separation

A number of researchers are developing new membrane materials characterized by excellent permeability and permselectivity. This enhanced technology could lead to a better energy consumption and cost-effective method in capturing CO₂. One of the recent membrane

material developed is the cardo polyimide hollow fibre membranes [Kazama, et al, 2004]. An asymmetric hollow fibre membrane of a bromated cardo polyimide showed excellent CO₂ separation properties: CO₂ permeation rate – $1e^{-3} \text{ cm}^3 \text{ (STP)}/(\text{cm}^3 \text{ sec cmHg})$; CO₂/N₂ selectivity – 40 [Kazama, et al, 2004]. Achieving a CO₂ permeation rate of around $10^{-3} \text{ cm}^3 \text{ (STP)}/(\text{cm}^3 \text{ sec cmHg})$ is the first accomplishment in polymeric membranes. This study then uses this membrane material in capturing the CO₂ from the furnace of the SMR. This has recently been tested for the flue gas of a coal fired power plant [Kazama et al, 2004]. Other materials investigated for CO₂ separation are listed in Table 2.1 [Du, 2005; Kazama et al, 2004]]. P_{CO₂} stands for the permeability of CO₂ and $\alpha_{\text{CO}_2/\text{N}_2}$ is the selectivity of CO₂ to N₂.

Table 2.1: Gas Permeability and selectivity of rubbery and glassy polymers

Polymer	T(°C)	P_{CO₂}(cm³(STP)/(cm² sec cmHg)	$\alpha_{\text{CO}_2/\text{N}_2}$
Poly (methyl methacrylate)	35	6.20E-11	31
Polysulfone	35	4.60E-10	25.6
Cellulose Acetate	35	5.50E-10	23.9
Polycarbonate	35	6.50E-10	25
Polystyrene	35	1.24E-09	23.8
6FDA-TAPA Polyimide	35	6.50E-09	30
Poly [1-(trimethylsilyl)-1-propyne	35	2.80E-06	5.6
Natural Rubber	25	1.34E-08	15.4
Poly (cis-isoprene)	35	1.91E-08	13.2
Silicone-nitrile copolymer	25	6.70E-08	20.3
Polydimethylsiloxane	35	4.55E-07	3.37
Cardo Polyimide	25	1.00E-03	40

2.5.2 Membrane Separation Process and Theory

Membrane processes are primarily used for separations. Their major attributes include well-defined mass transfer area independent of the operating conditions, selectivity property

between two phases, built as modules, provide high surface area per unit volume, easy to operate and scale at different loads.

Selective solubility and differential diffusion rates are the mechanism for transport thru the membrane phase. Figure 2.6 shows the process which is integrated to the H₂ plant to capture CO₂. The feed enters the separator and flows through the gap formed between the fibres and exits the module at its right end. Gases are being absorbed at different rates due to the different permselectivities of the membrane material. The primary transmembrane driving force is the chemical activity mainly promoted by partial pressure gradient (5×10^4 N/m²- 8×10^5 N/m²).

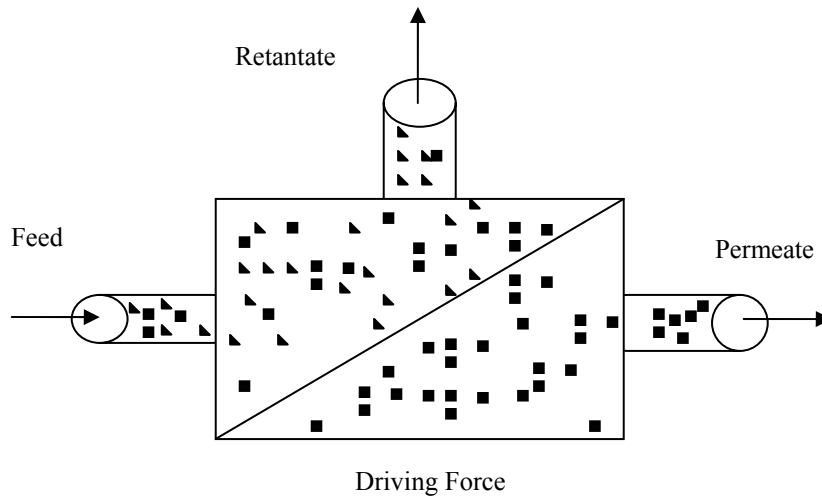


Figure 2.6: Process flow of membrane separation

Asymmetric membranes are commercially available. They consist of one porous layer and another nonporous layer. There are a number of models that describe the method

of transport in the membrane. One of these is a macroscopic model, which is used in this study.

Gas separation occurs in a nonporous or dense layer for all asymmetric membranes. Solution-diffusion model best describes mass transport through the dense layer where the difference in the partial pressure is the driving force for the permeation through the membrane.

Equation (2-1) describes the permeation rate where P (cm^3 (STP) cm/cm^2 s cmHg) is a measure of the ability of the membrane to permeate gas, D is the diffusion coefficient (cm^2/s) and S (cm^3 (STP)/ cm^3 cmHg) is the sorption coefficient.

$$P = D * S \quad (2-1)$$

Selectivity or separation factor describes the ability of a membrane to achieve separation. This is mathematically described as

$$\alpha_{i/j} = \frac{P_i}{P_j} = \frac{D_i}{D_j} * \frac{S_i}{S_j} \quad (2-2)$$

where $\frac{D_i}{D_j}$ = ratio of the diffusion coefficient or diffusivity selectivity

$\frac{S_i}{S_j}$ = ratio of solubility coefficient or solubility selectivity

Equation (2-2) is an example of binary systems consisting of gases “i” and “j” with gas “i” as the fast permeating gas. The ideal separation factor is equal to the ratio of permeability coefficients for components i vs. j [Koros, 2002].

Mathematical and Calculation Methods

There are a number of mathematical models and calculation methods for predicting the performance of gas separation in the literature. The work of Pan [Pan, 1986] is widely accepted as the most practical representation of multicomponent gas separation in hollow fiber asymmetric membranes. Chowdhury et al. (2005) presented a different solution approach of the Pan’s model. One of the advantages of the solution method of Chowdhury et al. (2005) is the possibility of incorporating the model into commercial process simulators such as Aspen Plus [Chowdhury et al, 2005]. The present study uses Pan’s model with the solution method of Chowdhury for integration of the membrane separation process within the H₂ plant using Aspen Plus.

2.6 CO₂ Storage and Utilization

Captured CO₂ can either be utilized or stored. It can be used to enhance oil recovery, to enhance production of coal bed methane and as a raw material for the production of chemicals and food. The possible options for storing CO₂ are in depleted oil and gas fields, deep saline reservoirs and deep ocean. Storing in depleted oil and gas fields is an attractive option due to its geological seal, which promises long term storage. However, this method has not been implemented yet. CO₂ can also be stored in deep saline reservoirs where the

CO₂ is injected in a porous permeable reservoir covered with a cap rock at least 800 m beneath the earth's surface where CO₂ can be stored under supercritical conditions. This also ensures long term storage from 100 to several thousand years depending on the size, properties and location of the reservoir [Ahmed et al., 2003]. Deep ocean is also the other option of storing CO₂. In this method, the CO₂ is pumped to a depth of 1000 m or more where it might be dispersed or induced to form a sinking plume. Another way of storing in deep ocean is by injecting CO₂ as a liquid at a 3000 m depth, where it is deposited on a seabed [Freund, 1999].

Chapter 3

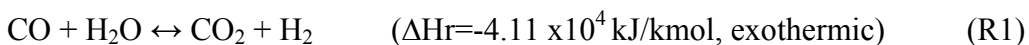
Model Development

This chapter presents the model development for the H₂ plant without CO₂ capture, H₂ plant with MEA based capture and H₂ plant with membrane based capture.

3.1 H₂ Production Plant without CO₂ Capture

3.1.1 Process Description

A diagram of the H₂ production process is shown in Figure 3.1. Feed, which is predominantly CH₄, is fed to the SMR with the process steam. Reactions (R1), (R6) and (R5) occur inside the SMR. The overall reaction is endothermic and the heat needed for the reaction is supplied by burning the off-gas from the PSA plus additional fuel gas with air.



The outlet of the SMR exits at 1047 K and is cooled to 623 K before it enters the HTS. In this reactor, CO is converted to H₂ as shown in (R1). The reaction is exothermic and thus is more favourable at lower temperature. The syngas exits the HTS at 675 K and is again cooled to 466.7 K. The LTS reactor is mainly used to convert the residual CO to H₂. The same reaction as in HTS occurs inside the LTS. The outlet of the LTS is again cooled to

ambient temperature (313.15 K) and is condensed to remove H₂O from the product gas before entering the PSA. The PSA is designed to absorb impurities from a H₂-rich feed gas into a fixed bed of adsorbents at high pressure. An extremely pure H₂ product is produced by desorbing the impurities into an off-gas stream. H₂ product of 99.95% purity at 90% recovery is obtained at the outlet of the PSA. The off-gas is then used as part of the total fuel to the furnace of the SMR. Part of the H₂ produced (around 10%) is recycled to keep the catalyst active in the early part of the reformer tubes. The flue gas, which comes from the combustion of the external fuel and the off-gas, is vented to the atmosphere. This serves as the base case of this study, i.e. the case without CO₂ capture.

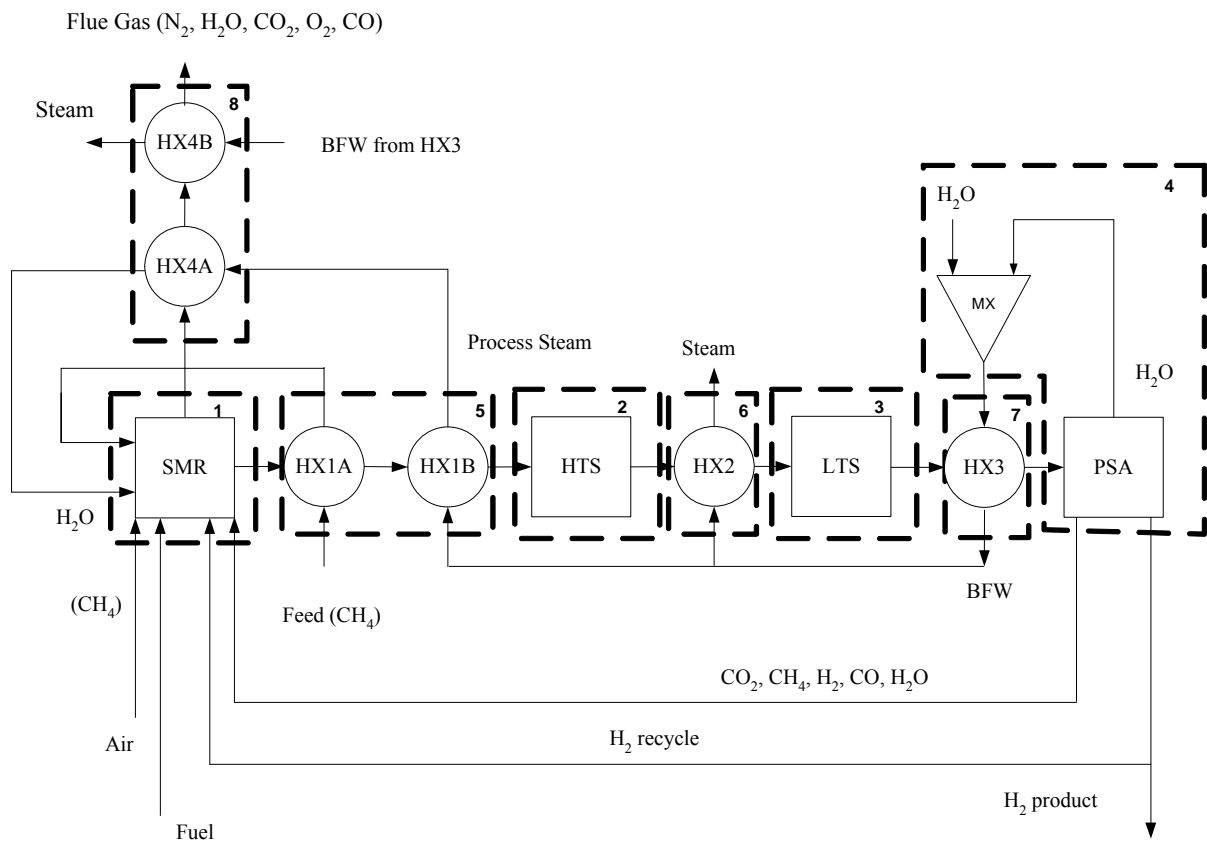


Figure 3.1: H₂ plant without CO₂ capture

As shown in Figure 3.1, there are several heat exchange (HX) opportunities. For this case, HX3 is used to produce boiler feed water (BFW) at a temperature of 430 K. This BFW is split into three streams which are sent to HX1B, HX2 and HX4B. Superheated steam at 573 K is generated from HX2 and HX4B at medium pressure of 2.45×10^6 N/m² and exported as a commodity. The numbered blocks indicated in figure 3.1 (i.e. 1 to 8) are used to show the corresponding equivalent units in the more complex Aspen Plus flowsheet. This is explained in the following section.

3.1.2 Process Simulation Basis

The H₂ plant without CO₂ capture shown in Figure 3.1 is simulated in Aspen Plus. The following are considered in developing the H₂ plant flowsheet in Aspen Plus [Aspen Technology, Inc., 2003] as presented in Figure 3.2.

1. The feed is natural gas and is constant flowrate.
2. The feed is considered free of sulphur assuming that a desulphurization unit is located upstream of the flowsheet developed here.
3. The off-gas from the PSA is used as part of the fuel to the furnace of the reformer.
4. Extra fuel gas (CH₄) is supplied to the furnace of the reformer.
5. The plant produces superheated steam at a temperature of 573 K and at a medium pressure 2.452×10^6 N/m².
6. The steam produced is exported.
7. The electricity needed by the H₂ production plant is supplied by outside sources.
8. The flue gas is vented to the atmosphere.

Each numbered block in Figure 3.1 refers to the block of the same number in Figure 3.2. Block number 1, which is SMR block in Figure 3.1, is simulated containing one reactor (SMR), two mixers (MIXER-1 and MIXER-3) and one furnace (FURNCE-4). The second and third blocks are simulated as reactors (HTS and LTS, respectively). Block number 4 in Figure 3.1 corresponds to PUMP3, MIXER-4, VALVE, HTER-3, COND and PSA units in Figure 3.2. The same rule applies to other block numbers (i.e. 5 to 8).

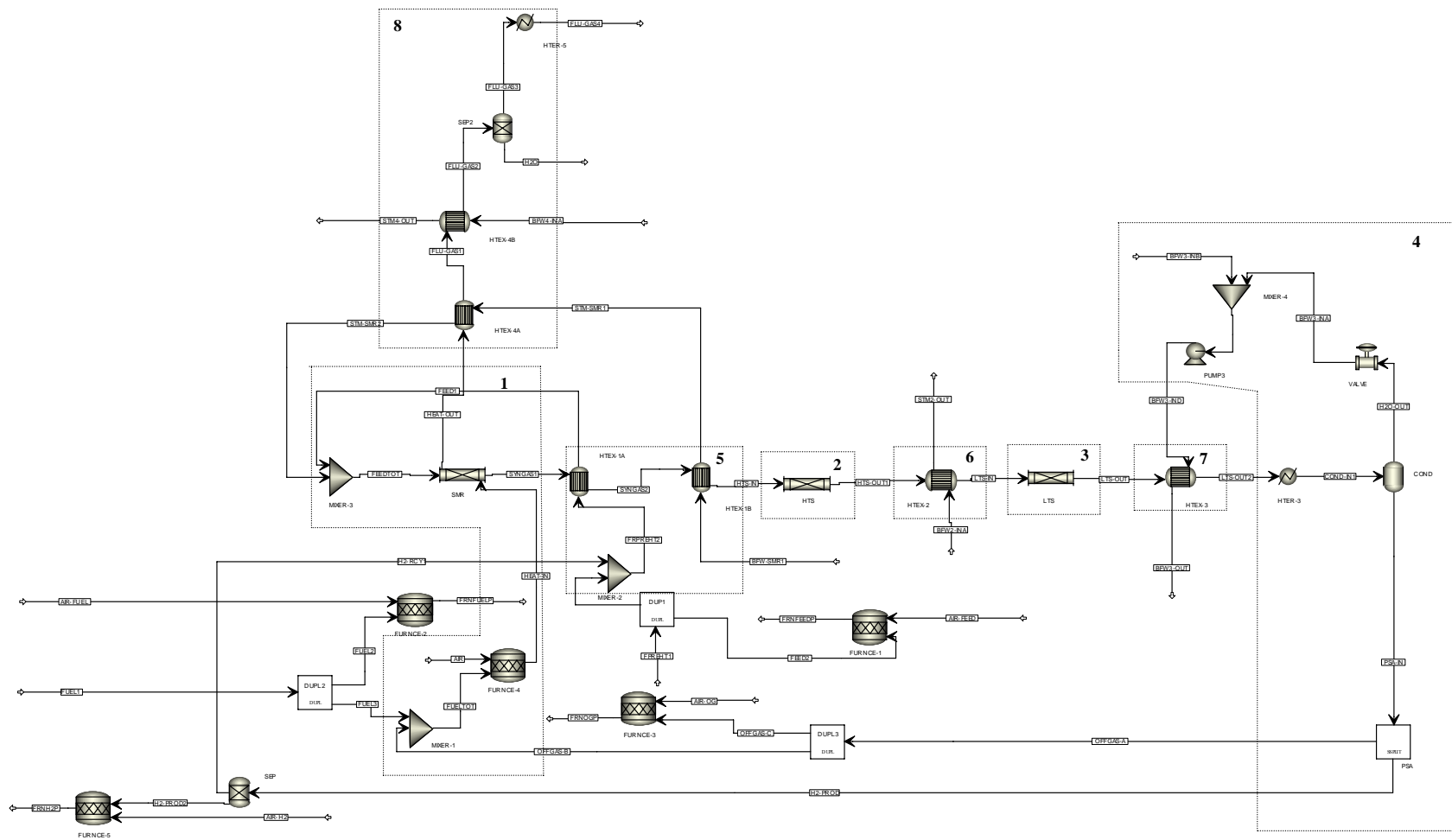


Figure 3.2: Aspen flowsheet for H₂ plant without CO₂ capture

3.1.3 Process Parameters and Aspen Plus Models

The reactors (SMR, WGS-HTS and WGS-LTS) and the PSA unit are first modeled individually. These units are integrated with other auxiliary units to come up with the whole flowsheet shown in Figure 3.2.

Steam Methane Reformer

Data from Elnashaie and Elishishini (1989) are used as the reference case. The SMR is considered as side-fired and its construction and operating conditions are shown in Table 3.1.

Table 3.1: Parameters for the SMR in Aspen Plus

Parameter	Values/Specification
Reformer Tubes	
Heated length, m	11.95
Inside diameter, m	0.0795
Outside diameter, m	0.102
Number of tubes	176
Catalysts Pellet	
Shape	Rashig rings
Dimensions, m	0.016 x 0.006 x 0.016
Bulk density, kg/m ³	1362
Solid catalyst density, kg/m ³	2355.2
Fuel	
Temperature, K	319.1
Inlet feed conditions	
Process gas flow rate (methane equivalent), kmol/s	0.20
Temperature, K	733
Pressure, N/m ²	2.45x10 ⁶
S/C	4.6
H ₂ /CH ₄	0.25
CO ₂ /CH ₄	0.091
N ₂ /CH ₄	0.02

Other parameters such as heat transfer coefficient (U) and extra fuel to the SMR are calculated using Aspen Plus' design specification (DS) where a specification is met by varying certain variable that has an either implicit or explicit affect on the required specification.

The works of Xu and Froment (1989) are considered in this study using the Langmuir-Hinshelwood Hougen-Watson (LHHW) approach. There are three reactions inside the SMR. These are reactions (R5), (R6) and (R1). The kinetic equations are available in Appendix A. The equilibrium constants for (R5), (R6) and (R1) are calculated using an equilibrium block representing an SMR in Aspen Plus. A correlation is obtained by running the SMR block at various temperatures. The output correlation is fit to its equivalent value in Aspen Plus. Other parameters such as adsorption constants and rate constants are also converted to their equivalent values to be used in the built-in LHHW expression in Aspen Plus. Equation (3.1) shows the rate of reaction formula used in Aspen Plus [Aspen Plus 12.1, 2003].

$$r = \left(\frac{\textit{kinetic factor} * \textit{driving force expression}}{\textit{adsorption term}} \right) \quad (3.1)$$

Where:

$$\textit{Kinetic factor} = A \left(\frac{T}{T_0} \right)^n e^{-\left(\frac{E}{R} \right) \left[\frac{1}{T} - \frac{1}{T_0} \right]} \quad (3.2)$$

$$\textit{Driving force expression} = k_1 \prod_{i=1}^N C_i^{\alpha_i} - k_2 \prod_{j=1}^N C_j^{\beta_j} \quad (3.3)$$

$$\textit{Adsorption term} = \left[\sum_{i=1}^M K_{adi} \left(\prod_{j=1}^N C_j^{nu_{ij}} \right) \right]^m \quad (3.4)$$

The meaning of the characters in the equations above is included in the nomenclature of this report. From the driving force expression (3.3), k_1 is equivalent to 1 for (R5), (R6) and (R1) and k_2 represents the reciprocal of the equilibrium constants for each of the reaction. These parameters (k_1 and k_2) are termed as the driving force constants. The driving force constants (k_1 and k_2) and the adsorption constants (K_{ad}), are temperature dependent and are mathematically expressed in Aspen Plus as in equation (3.5).

$$\ln(k_1, k_2, K_{ad}) = A + \frac{B}{T} + C * \ln(T) + D * T \quad (3.5)$$

Each equation as shown in the Appendix (A.1, A.2 and A.3) is converted to equation (3.1) to follow the built-in expression for LHHW model in Aspen Plus. Table 3.2 to 3.4 show the derived values used in Aspen Plus simulation. The coefficients (i.e. A, B, C and D) for the driving force constants for k_2 and the adsorption constants for all compounds involved are shown in Table 3.3 and Table 3.4, respectively. The coefficients for k_1 are all equal to 0 since k_1 is equivalent to 1. The units are expressed in SI units as per requirement in Aspen Plus [Aspen Plus 12.1, 2003].

Table 3.2: Equivalent kinetic factor parameter values of SMR in Aspen Plus

Parameter	Reaction		
	(R5)	(R6)	(R1)
Pre-exponential factor k,	3.63E-05	4.33E-06	4.72E-08
Exponent, n	0	0	0
Activation Energy E, MJ/kmol	240.1	243.9	67.13
Reference Temperature T ₀ , K	648	648	648

Table 3.3: Equivalent driving force constant parameter values for k₂ in Aspen Plus

Constants	Reaction		
	(R5)	(R6)	(R1)
A	177.94	145.96	-31.98
B	0.00	0.00	0.00
C	-29.56	-24.99	4.58
D	0.00	0.00	0.00

Table 3.4: Equivalent adsorption constant parameter values in Aspen Plus

Constants	Process Gas			
	K _{CO}	K _{H2}	K _{CH4}	K _{H2O}
A	-20.92	-30.42	-18.83	0.57
B	8497.71	9971.13	4604.28	-10666
C	0	0	0	0
D	0	0	0	0

The heat transfer coefficient (U) for the SMR is obtained by fitting the tube wall temperature of the SMR to the reference data [Elanashaie and Elshishini, 1993]. Prior to finding U, two assumptions are considered. The first one is that the fired duty of the SMR represents 50% of the heat content of the process natural gas [Rostrup-Nielsen, 1984]. The other assumption is for the furnace not to exceed an outlet temperature of 2200 K [Rajesh et al., 2000]. The following steps are taken in finding the U value.

1. Calculate the external fuel to the SMR using a design specification (DS) in Aspen Plus. This is done by first creating a furnace block that burns the off-gas from the PSA and the external fuel.
2. Using the design specification (DS), vary the external fuel that corresponds to the equivalent 50% of the heat content of the process natural gas. This value is used as the initial external combustion fuel for the furnace of the SMR.
3. Find U by minimizing the square of the difference between the reactor outlet temperature of the reference SMR and the simulation data. An optimization feature in Aspen Plus is used. The optimum error, which is equivalent to the minimum error, is achieved by varying values for both U and the furnace outlet temperature. The U that corresponds to the minimum error is the optimum U value.

Table 3.5 presents the values used in the simulation as well as the optimum U value. Figure 3.3 shows the best fit for the tube wall temperature of the SMR. The simulation data does not present a good fit for the first half of the reactor. The effect of this is the difference in the conversion along the reactor; however, it results in similar final conversion due to perfect fit at the reactor outlet temperature.

Table 3.5: SMR data for heat transfer coefficient in Aspen Plus

Parameters	Values
High heating value (HHV) of CH ₄ feed, MJ/s	174.26
Furnace heat duty, MJ/s	87.13
Furnace outlet temperature, K	1880.66
SMR heat transfer coefficient, U, J/(s m ² K)	156.76

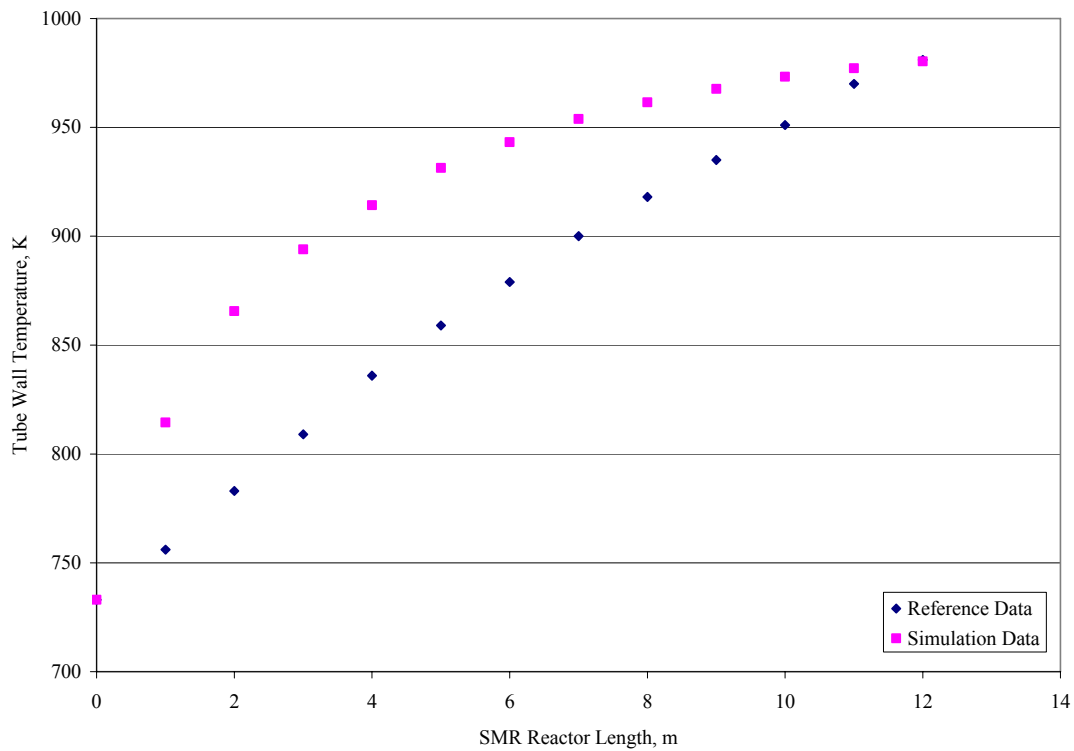


Figure 3.3: Tube wall temperature profile of SMR

The SMR block (block number 1 in Figure 3.1) is simulated in Aspen Plus by using several Aspen unit models, as shown in Figure 3.4. The description of the models used is presented in Table 3.6.

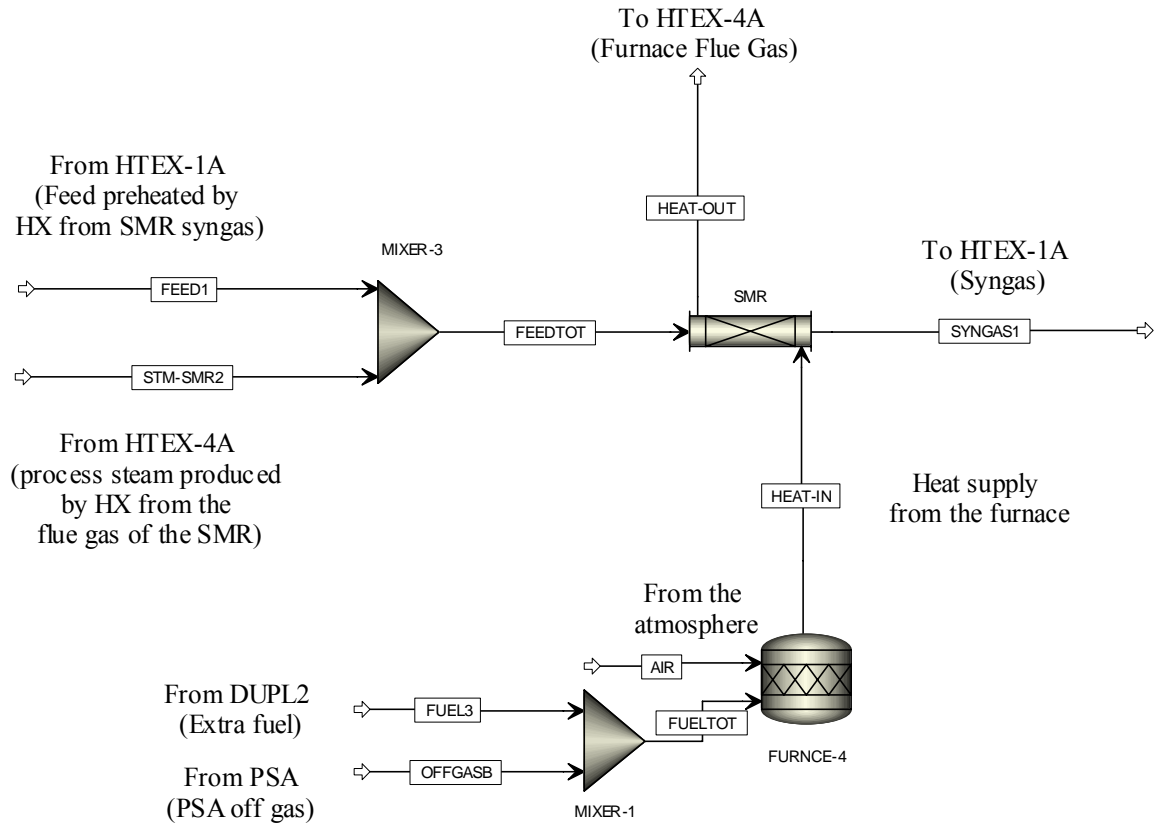


Figure 3.4: Block #1 - SMR

Table 3.6: Aspen simulation specifications and configurations for SMR

Block Number	Equipment	Aspen Block Model	Specifications/Configuration
1	SMR	Rplug	Reactor with co-current coolant, $U = 156.76 \text{ J/sec m}^2 \text{ K}$, Multitube reactor, Number of tubes = 176, Tube Length = 11.95 m, Tube diameter = 0.0795 m, Pressure drop = $3.65 \times 10^5 \text{ N/m}^2$, Catalyst loading = 3617.59 kg, Bed voidage = 0.605
	MIXER-3	Mixer	Pressure = $2.45 \times 10^6 \text{ N/m}^2$
	FURNCE-4	Rstoic	Outlet temperature = 1880.66 K, Define combustion reaction for CH_4 and H_2
	MIXER-1	Mixer	Use default in Aspen Plus

HTS and LTS Converters

The kinetic equations used for the WGS are included in Appendix B. The parameters used for the shift converters are shown in Table 3.7 [Elnashaie and Elishihini, 1989; Rase, 1977].

Table 3.7: Parameters for the WGS converters

Parameter	Values	
	HTS	LTS
Bed length, m	5.48	5.48
Bed diameter, m	3.89	3.89
Feed temperature, K	623	466.7
Feed pressure, N/m^2	2087300	2087300

Reaction (R1) is the reaction that occurs inside the HTS and the LTS converters. The HTS converter uses an iron based catalysts while the LTS converter uses a copper based catalyst.

For the HTS converter, equations (B.1), (B.2) and (B.5) as presented in Appendix B are used. These equations are first converted to their equivalent formulas in SI units and then derived to their equivalent LHHW kinetic expressions in Aspen Plus. The SI equivalents of the equations are shown in equations (3.6), (3.7) and (3.8).

$$(-r_{CO}) = 7.33e^{-7} \psi k \left(y_{CO} y_{H_2O} - \frac{y_{CO_2} y_{H_2}}{K} \right), \frac{\text{kmole CO reacted}}{\text{kgcat s}} \quad (3.6)$$

$$k = \exp\left(15.95 - \frac{4900}{T}\right), T \text{ in K} \quad (3.7)$$

$$K = \exp\left(-4.33 + \frac{4578}{T}\right), T \text{ in K} \quad (3.8)$$

Equation (B8) is used to calculate the activity factor, ψ , since the HTS converter is carried at a pressure greater than 20 atm. The activity factor, ψ , is equivalent to the product of the total pressure in atmospheres and the ratio of the first-order constant at the operating pressure to that at atmospheric pressure [Rase,1977]. From Rase (1977), this ratio is equivalent to 4 for pressures greater than 20 atm. This gives an activity factor of 89.02 atm.

Equation (3.6) is used in determining the rate of CO conversion in the LTS converter. The LTS uses a copper-zinc oxide catalyst and its corresponding rate constant is calculated using equation (B.3). Equation (B.4) is used to calculate the equilibrium constant. The equivalent formulas in SI units for the LTS converters are shown in (3.9) and (3.10).

$$k = \exp\left(12.88 - \frac{1855.56}{T}\right), T \text{ in } K \quad (3.9)$$

$$K = \exp\left(-4.72 + \frac{4800}{T}\right), T \text{ in } K \quad (3.10)$$

The ratio used in calculating the activity factor, ψ , is obtained from equation (B.9) which is used for operating pressure lower than 24.8 atm.

Equation (3.6) is converted to the LHHW kinetic expression in Aspen Plus. Tables 3.8 and 3.9 provide the values of the parameters used in Aspen Plus for both the HTS and the LTS. The constants for the adsorption term in the LHHW equation in Aspen Plus are equal to 0 since the adsorption expression does not exist in equation (3.6).

Table 3.8: Equivalent kinetic factor parameter values for WGS converters in Aspen

Plus

Parameter	Unit Operation	
	HTS	LTS
Pre-exponential factor k,	8237.01	8213.46
Exponent, n	0	0
Activation Energy E, MJ/kmol	43.56	33.57
Reference Temperature T _o , K	637.1	457.6

Table 3.9: Equivalent driving force parameter values for WGS converters in Aspen

Plus

Constants	Unit Operation	
	HTS	LTS
A	4.33	4.72
B	4578	-4800
C	0	0
D	0	0

The above data are incorporated in Aspen Plus simulation. Figure 3.5 and Figure 3.6 shows the Aspen Plus flowsheets for the HTS and LTS, respectively. Table 3.10 presents the model and the parameter used in the simulation.

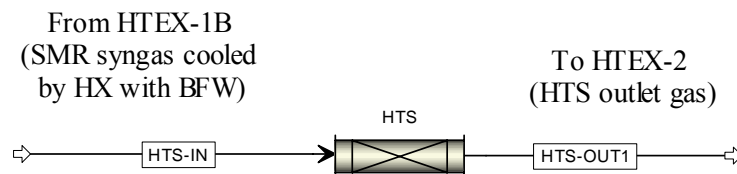


Figure 3.5: Block # 2 – HTS

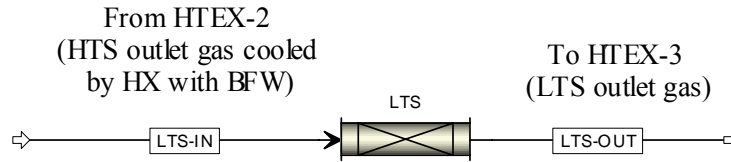


Figure 3.6: Block # 3 – LTS

Table 3.10: Aspen simulation specifications and configurations for HTS and LTS

Block Number	Equipment	Aspen Block Model	Specifications/Configuration
2	HTS	Rplug	Adiabatic reactor, Reactor length = 5.48 m, Reactor diameter = 3.89 m, Pressure drop = 0, Catalyst loading = 74389.24 kg, Particle density = 1250 kg/m ³
3	LTS	Rplug	Adiabatic reactor, Reactor length = 5.48 m, Reactor diameter = 3.89 m, Pressure drop = 0, Catalyst loading = 74389.24 kg, Particle density = 1250 kg/m ³

PSA

The PSA unit is modeled as a separator block on the basis that PSA recovery and purity are not sensitive to the changes in composition and pressure of the feed [Chlendi et al, 1995].

Equations (3.11) to (3.12) are used in predicting the outlet gas composition of the PSA unit.

The separator block is designed to recover 90% of the H₂ in the feed at 99.95% purity.

$$\gamma_i = (1 - 99.95) \frac{x_i}{\sum x_i} \quad (3.11)$$

$$F_{H_2, out} = \frac{0.9 x_{H_2, in} F_{PSA, in}}{0.9995} \quad (3.12)$$

The PSA block in Figure 3.1 is simulated in Aspen Plus as containing other auxiliary equipments. The simulation flowsheet is shown in Figure 3.7 and the parameters for the blocks used are presented in Table 3.11.

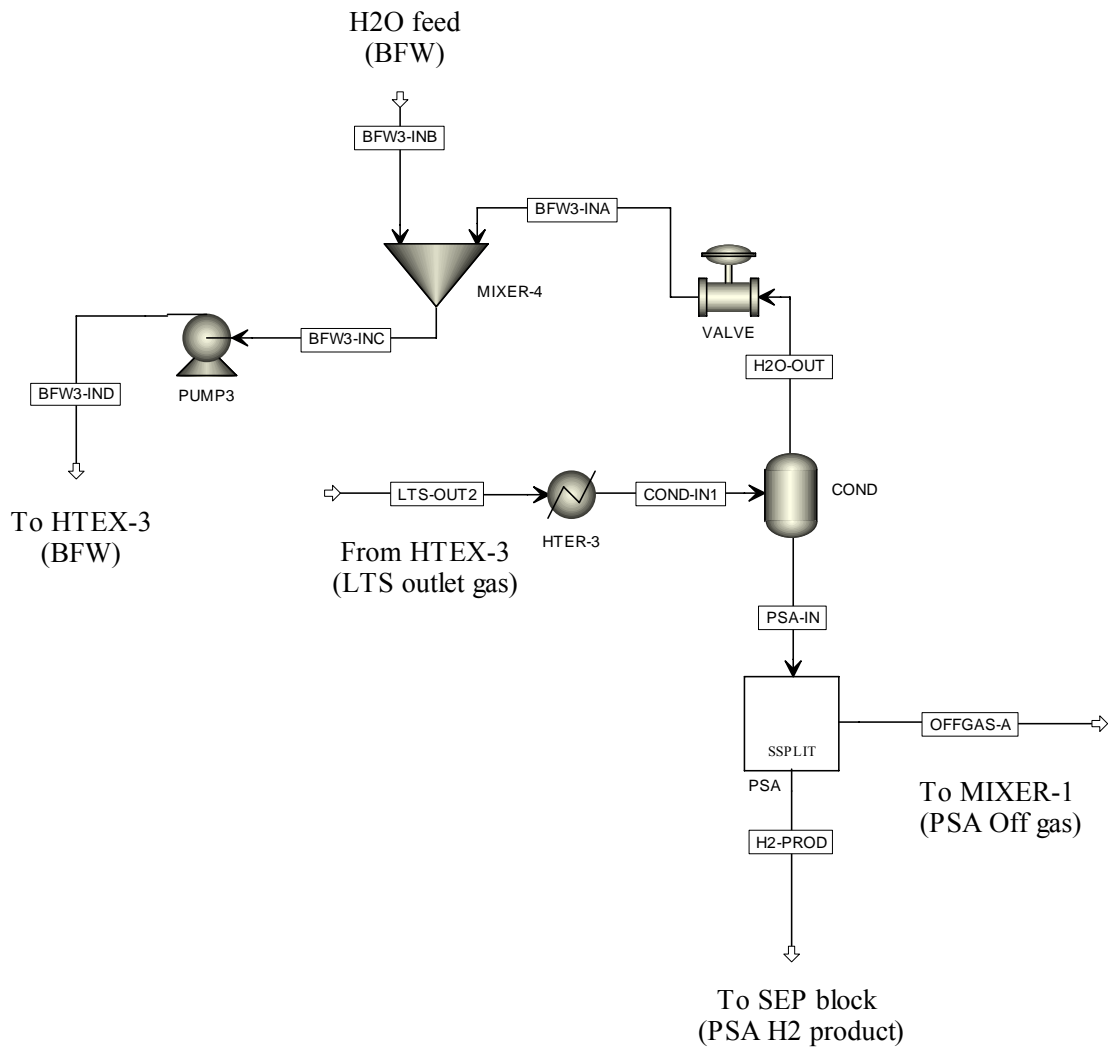


Figure 3.7: Block # 4 - PSA

Table 3.11: Aspen simulation specifications and configurations for PSA

Block Number	Equipment	Aspen Block Model	Specifications/Configuration
4	PSA	Ssplit	Set to recover 90% H ₂ at 99.95 % purity using internal calculations
	HTE-3	Heater	Outlet temperature = 313.15 K, Pressure drop = 0 N/m ²
	COND	Flash2	Outlet temperature = 298.15 K
	VALVE	Valve	Outlet pressure = 101325 N/m ²
	MIXER-4	Mixer	Use default in Aspen Plus
	PUMP3	Pump	Discharge pressure = 2.45x10 ⁶ N/m ² , Efficiency = 0.6

Heat-exchange Operation

The outlet of the SMR contains significant heat and is cooled before it enters the HTS reactor. These are used to preheat feed and BFW for process steam generation. Figure 3.8 and Table 3.12 present the Aspen Plus flowsheet and the specifications configurations of the models used in the simulation, respectively.

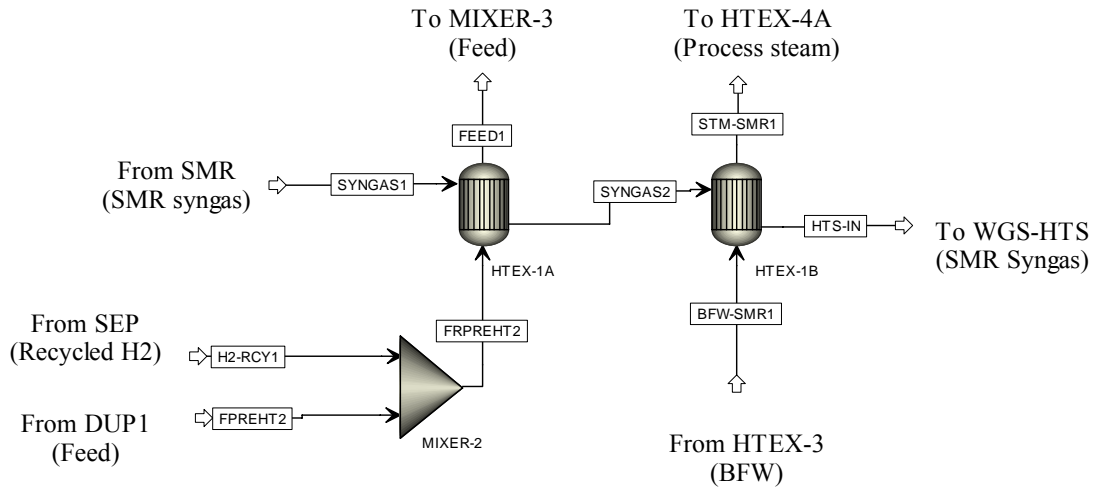


Figure 3.8: Block #5 - SMR syngas heat exchange system

Table 3.12: Aspen simulation specifications and configurations for block SMR syngas heat exchange

Block Number	Equipment	Aspen Block Model	Specifications/Configuration
5	MIXER-2	Mixer	Outlet pressure = $2.45 \times 10^6 \text{ N/m}^2$
	HTEX-1A	HeatX	Cold stream outlet temperature = 733 K, Minimum temperature approach = 10 K
	HTEX-1B	HeatX	Hot stream outlet temperature = 623 K, Minimum temperature approach = 10 K

The outlet of the HTS is cooled before it enters the LTS. Before separation of the product H_2 is performed, the LTS outlet gas is first condensed and cooled at ambient temperature. The heat-exchange operation is shown as follows (Figure 3.9 and Figure 3.10).

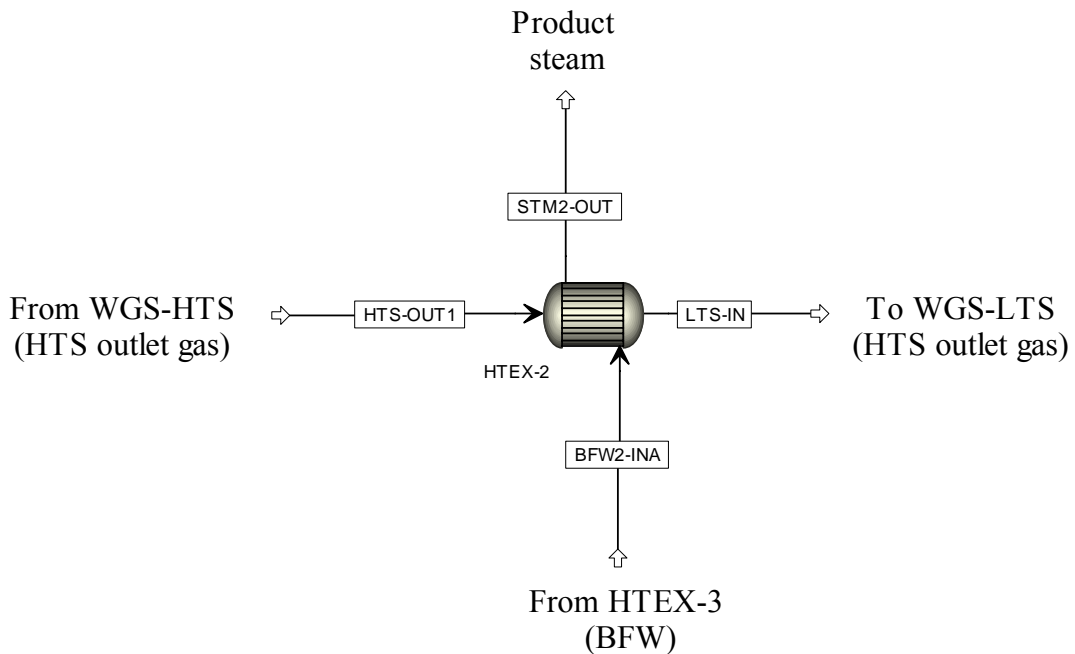


Figure 3.9: Block # 6 - HTS heat exchange system

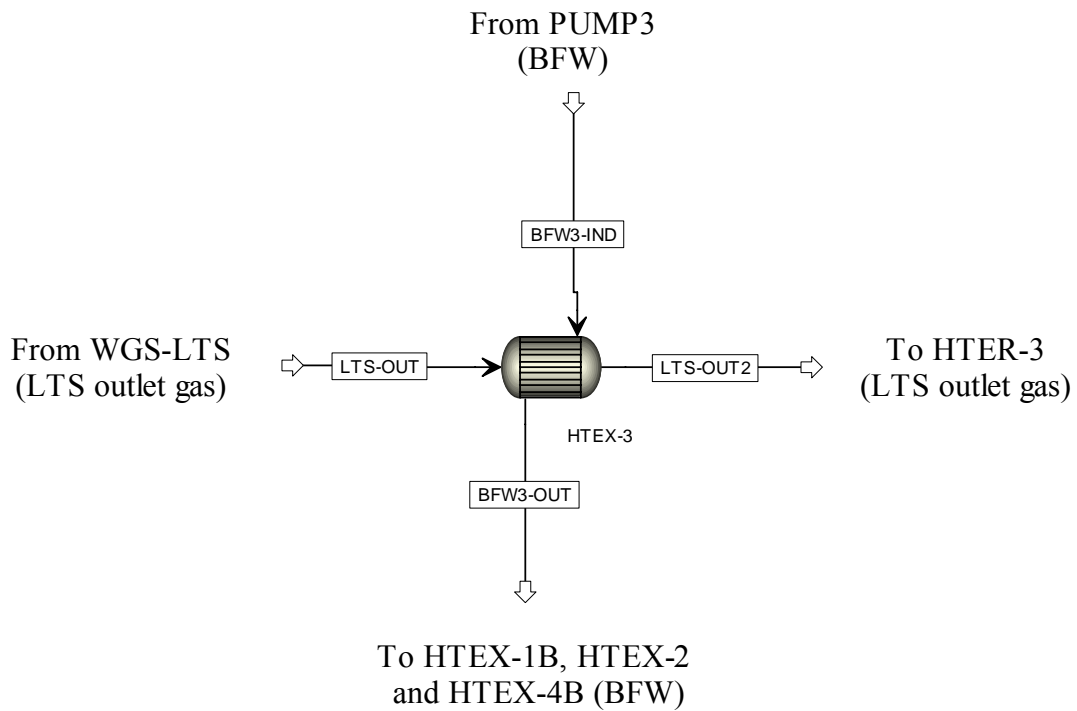


Figure 3.10: Block # 7 - LTS heat exchange system

Table 3.13 presents the specifications and configurations of the models used in Aspen Plus

Table 3.13: Aspen simulation specifications and configurations for HTS and LTS heat exchange operation

Block Number	Equipment	Aspen Block Model	Specifications/Configuration
6	HTEX-2	HeatX	Hot stream outlet temperature = 466.7 K, Minimum temperature approach = 10 K, DS is configured to produce steam at 573 K and 2.45×10^6 N/m ² by varying inlet BFW flow
7	HTEX-3	HeatX	Hot stream outlet temperature = 313 K, Minimum temperature approach = 10 K

The convection section of the SMR provides another opportunity for heat exchange operation. This is used to produce process steam and steam for export (Figure 3.11) The Aspen Plus model parameters are presented in Table 3.14.

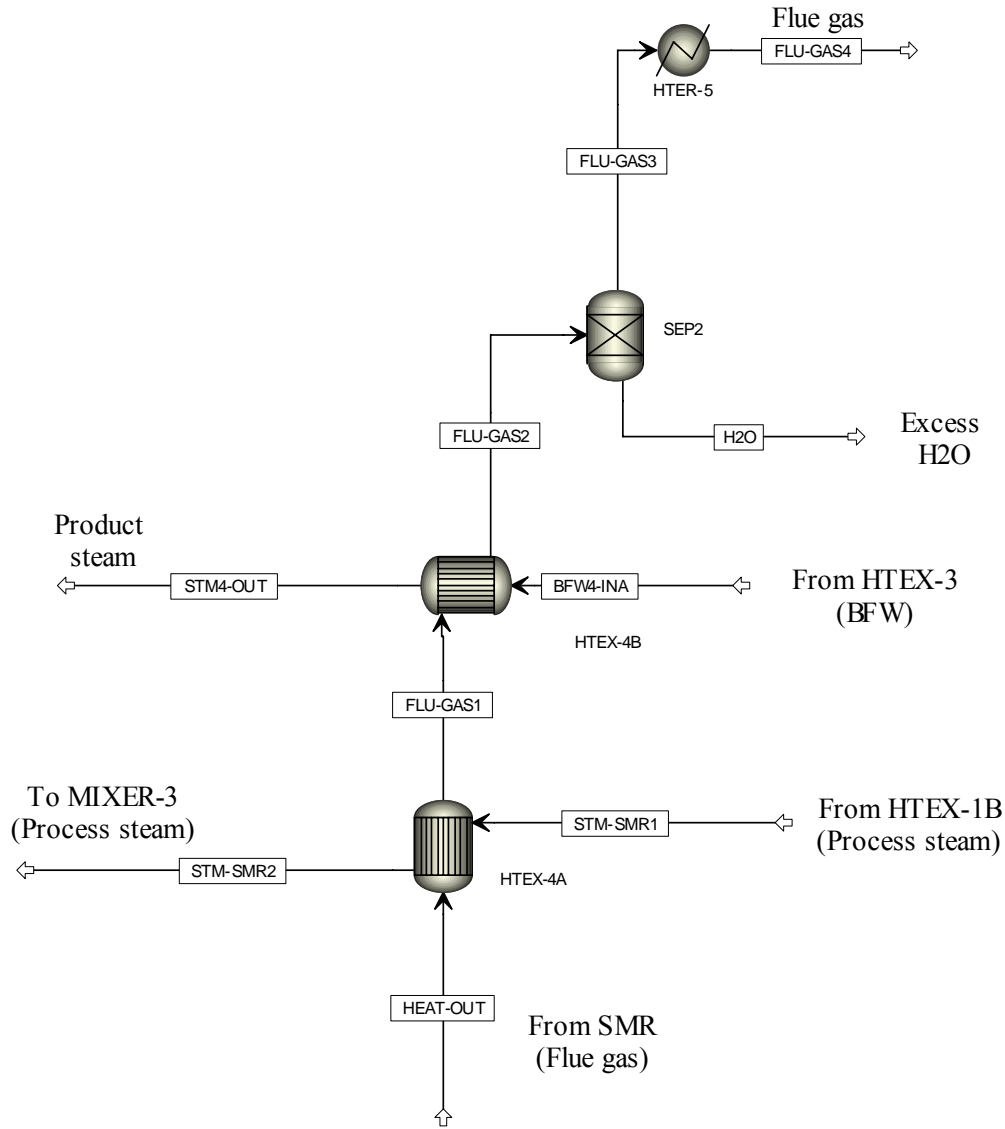


Figure 3.11: Block # 8 - SMR furnace flue gas heat exchange system

Table 3.14: Aspen simulation specifications and configurations for SMR furnace flue gas heat exchange operation

Block Number	Equipment	Aspen Block Model	Specifications/Configuration
8	HTEX-4A	HeatX	Cold stream outlet temperature = 733 K, Minimum temperature approach = 10 K
	HTEX-4B	HeatX	Hot stream outlet temperature = 440 K, Minimum temperature approach = 10 K, DS is configured to produce steam at 573 K and 24.52×10^6 N/m ² by varying inlet BFW flow
	SEP2	Sep	Outlet stream H ₂ O split fraction = 1
	HTE-5	Heater	Outlet temperature = 313.15, Pressure drop = 0

As can be seen in Figure 3.2, there are other Aspen blocks used in the simulation. These are not included herewith since these are not considered as major part of the H₂ plant simulation. These are used only for internal calculations. Furnace blocks (i.e. FURNCE-1, FURNCE-2, FURNCE-3 and FURNCE-5) are used only to calculate HHV of the H₂, feed, off gas and external fuel while duplication blocks (i.e. DUPL1, DUPL2, DUPL3) are used only to pass the same value to other blocks.

3.2 H₂ Production Plant with MEA-CO₂ Capture

3.2.1 Process Description

The process flow diagram for the H₂ plant with the MEA-CO₂ capture plant is the same as shown in Figure 3.1 except for the modification of the heat exchange operation due to the

different types of steam produced. The modified process flow diagram is shown in Figure 3.12.

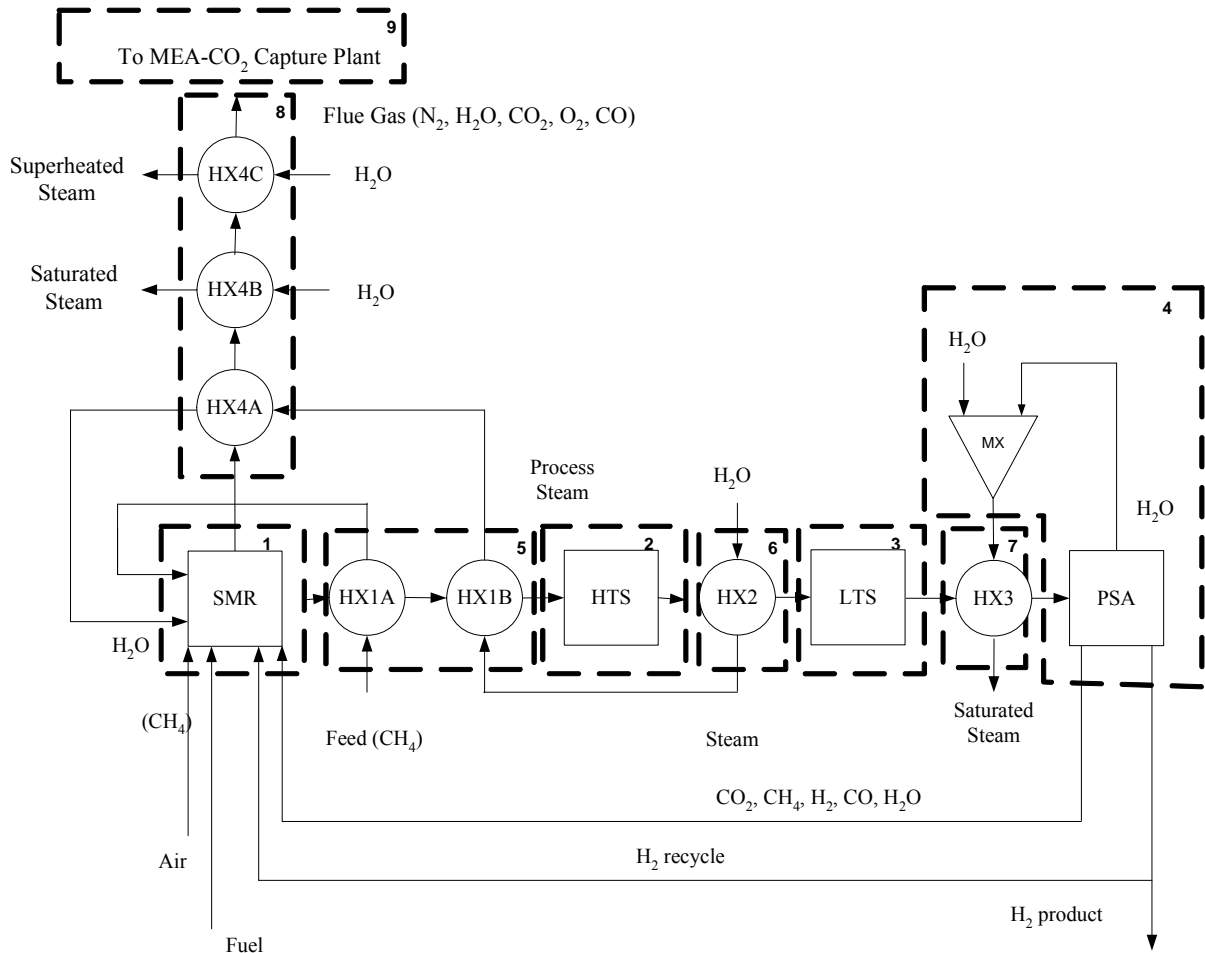


Figure 3.12: Process flow diagram for the H₂ Plant with MEA-CO₂ capture

In this case, HX3 and HX4B generate saturated steam. Since the reboiler temperature is limited to 398 K to avoid MEA degradation, using 10°C approach temperature, the steam used in the reboiler is saturated at 409 K. The flue gas leaving HX4B still contains significant heat. This steam is utilized to generate superheated steam at low pressure. This

steam is converted into electricity to supply the need of the MEA plant. The process steam is produced by passing through HX2, HX1B and HX4A.

The flue gas is cooled to a temperature not lower than 343.15 K before it is sent to a MEA-CO₂ capture plant. There is a limitation on the cooling of the flue gas since the possibility of condensation can occur below 343.15 K. The simulation of the MEA-CO₂ capture plant is not performed in this study. This has already been simulated by Alie et al. (2005) and Singh et al. (2003). A correlation is used in this study derived from the work of Singh et al. (2003) to calculate the amount of steam needed by the stripper of the reboiler as a function of the amount of CO₂ to be captured. This correlation gives 1.7 kg steam/kg of CO₂ captured. An approximation of the electricity requirement of the MEA-CO₂ capture plant is calculated by passing 80% of the CO₂ captured from the H₂ plant at 98% purity through a compressor (2% impurity is assumed to be H₂O). The CO₂ product enters the compressor at a temperature of 301.15 K and at a pressure of 2×10^5 N/m² and exits at 313 K and 1.5×10^7 N/m².

The units in Figure 3.12 are grouped in block numbers to help in presenting its equivalent units in Aspen Plus simulation as discussed in the following this section.

3.2.2 Process Simulation Basis

The assumptions for this case are the same as the base case described in section 3.1.2 except the following modifications and additional assumptions.

1. The plant produces different types of steam. In this case, low pressure steam at two different temperatures is produced. One type of steam is produced at saturation temperature of 409 K for solvent regeneration in the stripper and the other at superheated temperature (423 K) for power generation.
2. The superheated steam produced is converted into electricity to supply the need of the MEA-CO₂ capture plant instead of exporting it as assumed in the base case.
3. The flue gas is cooled at a minimum of 343.15 K to avoid condensation of the flue gas.
4. Additional electricity is supplied by burning coal.
5. The CO₂ captured is compressed to 1.5×10^7 N/m².
6. CO₂ recovery and purity is set at 80% and 98% (by mole), respectively.

Figure 3.13 presents the Aspen Plus flowsheet developed using the assumptions given above.

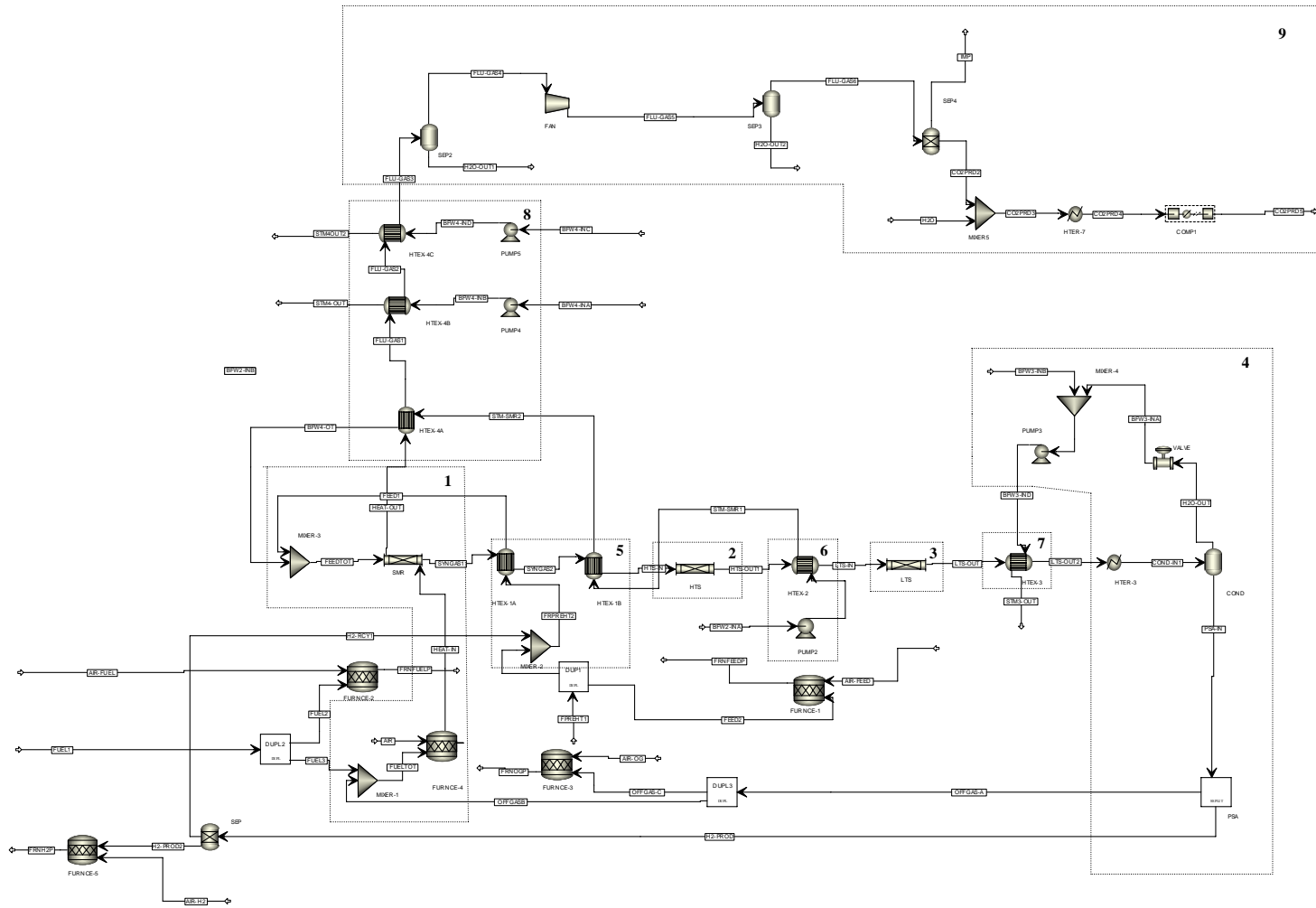


Figure 3.13: H₂ Plant with simulation in approximating the amount of electricity needed by the MEA capture plant

3.2.2 Process Parameters and Aspen Plus Models

The unit parameters for the H₂ plant are the same as described in Section 3.1.3. Other parameters used are described as follows. A simple correlation is used to determine the amount of steam needed by the reboiler of the stripper. This is equivalent to 1.7 kg of steam/kg of CO₂ captured [Singh et al, 2003] as mentioned previously.

The electricity needed by the H₂ plant with the MEA-CO₂ capture process is supplied by the power generated from the superheated low pressure steam produced by the H₂ plant. The equivalent electricity of the steam produced is calculated using 30% efficiency [Rao et al, 2002]. Additional electricity is generated on-site to power MEA-CO₂ capture plant. Sub-bituminous coal (Highvale), at which composition is given in Table 3.15, is assumed as the fuel burned in producing electricity. The conversion efficiency of the coal plant is 42% [Zanganeh et al, 2004] and its equivalent CO₂ emission is calculated based on the high heating value (HHV) of the Highvale coal.

Table 3.15: Properties of Highvale coal

Moisture, as received (wt%)	11.9
Ultimate analysis (wt %, dry)	
Carbon	63.01
Hydrogen	3.87
Nitrogen	0.86
Sulphur	0.24
Ash	17.25
Oxygen (by difference)	14.77
Heating value (MJ/kg, dry)	24.05

The unit operation for the H₂ plant with MEA CO₂ capture is modeled in a similar way as the H₂ plant of the base case. However, since the heat exchange operations are modified because of the different steam characteristics produced, the operating parameters for each HX are different from the base case. Modifications are as follows: the inlet feed for the HTEX-1B in Figure 3.8 comes from the outlet of HTEX-2 instead of from the HTEX-3; the inlet of HTEX-2 in Figure 3.9 is H₂O at ambient temperature instead of BFW from HTEX-3; the inlet of HTEX-4B in Figure 3.11 is H₂O at ambient temperature instead of BFW and is used to produce the remaining steam needed by the reboiler of the MEA capture plant; the outlets of HTEX-3 and HTEX-4B in Figure 3.10 and 3.11, respectively are saturated steam at 409 K for the reboiler of the MEA capture plant instead of 573 K; an additional HX operation is added (HTEX-4C) to produce steam for power generation. Table 3.16 provides the simulation parameters for the HX operation of this case.

Table 3.16: Aspen simulation specifications and configurations for HX operation within the H₂ plant with MEA based capture

Block Number	Equipment	Aspen Block Model	Specifications/Configuration
5	MIXER-2	Mixer	Outlet pressure = 2.45×10^6 N/m ²
	HTEX-1A	HeatX	Cold stream outlet temperature = 733 K, Minimum temperature approach = 10 K
	HTEX-1B	HeatX	Hot stream outlet temperature = 623 K, Minimum temperature approach = 10 K
6	HTEX-2	HeatX	Hot stream outlet temperature = 466.7 K, Minimum temperature approach = 10 K
	PUMP2	Pump	Discharge pressure = 2.45×10^6 N/m ² , Efficiency = 0.6
7	HTEX-3	HeatX	Hot stream outlet temperature = 313 K, Minimum temperature approach = 10 K, DS is configured to produce saturated steam at 409 K by varying inlet BFW flow
8	HTEX-4A	HeatX	Cold stream outlet temperature = 733 K, Minimum temperature approach = 10 K
	HTEX-4B	HeatX	Hot stream outlet temperature = 440 K, Minimum temperature approach = 10 K, DS is configured to produce steam at 423 K and 3.13×10^5 N/m ² by varying inlet BFW flow
	HTEX-4C	HeatX	Hot stream outlet temperature = 370 K, Minimum temperature approach = 10 K, DS is configured to produce saturated steam at 423 K and 3.13×10^5 N/m ² by varying inlet BFW flow
	PUMP 4	Pump	Discharge pressure = 3.13×10^5 N/m ² , Efficiency = 0.6
	PUMP 5	Pump	Discharge pressure = 3.13×10^5 N/m ² , Efficiency = 0.6

The next figure (Figure 3.14) shows the simulation flowsheet to approximate the electricity needed by the MEA capture plant. Table 3.17 shows the specifications of the blocks used in the simulation.

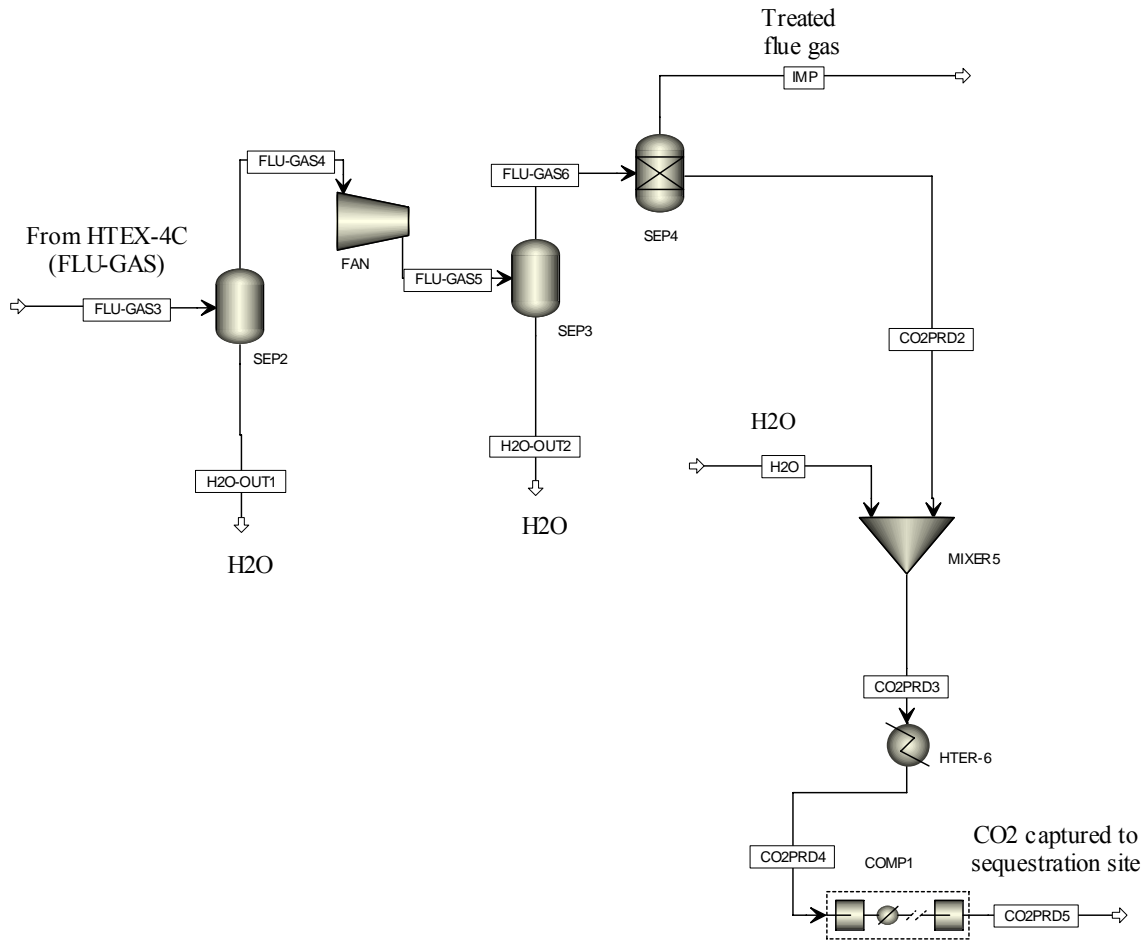


Figure 3.14: Simulation flowsheet to approximate the power needed for the MEA capture plant

Table 3.17: Aspen simulation specifications and configurations for approximating power need of the MEA capture plant

Block Number	Equipment	Aspen Block Model	Specifications/Configuration
9	SEP2	Flash2	Outlet temperature = 313.15 K, Pressure drop = 0 N/m ²
	FAN	Compr	Compressor type = isentropic, Discharge pressure = 120000 N/m ² , Efficiency = 0.75
	SEP3	Flash2	Outlet temperature = 313.15 K, Pressure drop = 0 N/m ²
	SEP4	Sep	Outlet stream CO2PRD split fraction component CO ₂ = 0.8
	MIXER-5	Mixer	Outlet pressure = 2x10 ⁵ N/m ²
	HTER-6	Heater	Outlet temperature = 301.15 K, Pressure drop = 0 N/m ²
	COMP1	Mcompr	Number of stages = 5, Compressor model = isentropic, Discharge pressure from last stage = 1.5x10 ⁷ N/m ² , Efficiency = 0.75, Cooler outlet temperature = 313.15 K, Pressure drop = 0 N/m ²

3.3 H₂ Production Plant with Membrane Capture

3.3.3 Process Description

Figure 3.1 shows the process description for the H₂ plant without membrane capture process. The flue gas from the furnace of the SMR is sent to a membrane separation process where the CO₂ is captured. The impure CO₂ rich off-gas from the H₂ plant is sent to a four-stage membrane separation process which is set to recover 80% CO₂ with 98% purity. This is achieved by introducing the CO₂ rich gas mixture at the shell side of the membrane module at atmospheric pressure and by recovering it at a reduced pressure from the bore side of the

hollow fibres. A simple one stage membrane separation process is shown in Figure 3.15 where MEM1 represents the membrane and VAC the vacuum pump.

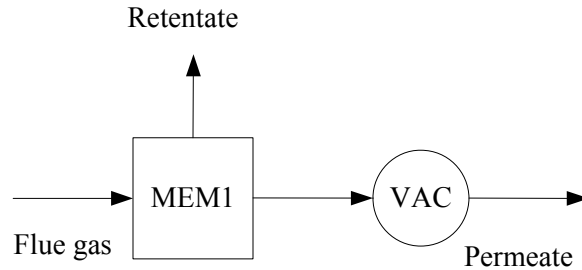


Figure 3.15: One-stage membrane separation process

The permeate side pressure is maintained at $1 \times 10^4 \text{ N/m}^2$ by using a vacuum pump which is the major energy consumer of the process. The membrane properties used in the simulation are available in Kazama et al. (2004) except for the CO permeability. The permeability of CO is assumed close to the permeability of N_2 [Alentiev et al, 1998]. The CO_2 produced is compressed to $1.5 \times 10^7 \text{ N/m}^2$ to be delivered to sequestration site.

3.3.1 Process Simulation Basis

The basis of the simulation of the H_2 plant is similar to the base case. The difference in this case is that the flue gas is sent to a membrane separation technology to capture CO_2 . Due to the integration of this capture process to the H_2 plant, the following modification and additional assumptions are considered.

1. The superheated steam produced by the H₂ plant is converted into electricity to supply the power needed by the membrane separation process instead of exporting steam.
2. The flue gas is cooled at a minimum of 343.15 K to avoid condensation of the gas.
3. Additional electricity, when needed, is supplied by burning coal.
4. The CO₂ captured is compressed to 1.5x10⁷ N/m².
5. CO₂ recovery and purity is set at 80% and 98% (by mole), respectively.

3.3.2 Process Parameters and Aspen Plus Models

The parameters for the H₂ plant for this case are the same as the base case. For the membrane plant, the model uses cardo polyimide hollow fibre membrane. Table 3.18 shows the properties of the membrane used in the simulation.

Table 3.18: Parameters of the membrane used in the simulation

Parameter	Value
Fibre Inside diameter, m	0.0003
Fibre outside diameter, m	0.0005
Fibre length, m	0.5
Permeate pressure, N/m ²	10000
CO ₂ permeation rate, mol/(m ² sec Pa)	3.35E-07
N ₂ permeation rate, Nm ³ /(m ² sec Pa)	8.37E-09
O ₂ permeation rate, Nm ³ /(m ² sec Pa)	4.78E-08
AR permeation rate, Nm ³ /(m ² sec Pa)	1.91E-08
CO permeation rate, Nm ³ /(m ² sec a)	8.37E-09

A four-stage membrane is used to recover 80% of the CO₂ from the flue gas at 98% purity. The number of fibres used is dependent on the CO₂ recovery for each stage of the membrane. This is determined by using the DS feature of Aspen Plus.

Electricity is supplied by generating power from the superheated medium pressure steam produced by the H₂ plant. Highvale coal is used for additional electricity requirement of the membrane plant. The equivalent CO₂ emissions are calculated based on the HHV of the Highvale coal. The conversion efficiencies used from steam to electricity and from coal to electricity are the same as the efficiency used for the MEA capture plant case.

The simulation model used for the H₂ plant is the same as the base case. Figure 3.16 shows the four-stage membrane separation flowsheet in Aspen Plus. Table 3.19 gives the specifications and the parameters used by each unit operations.

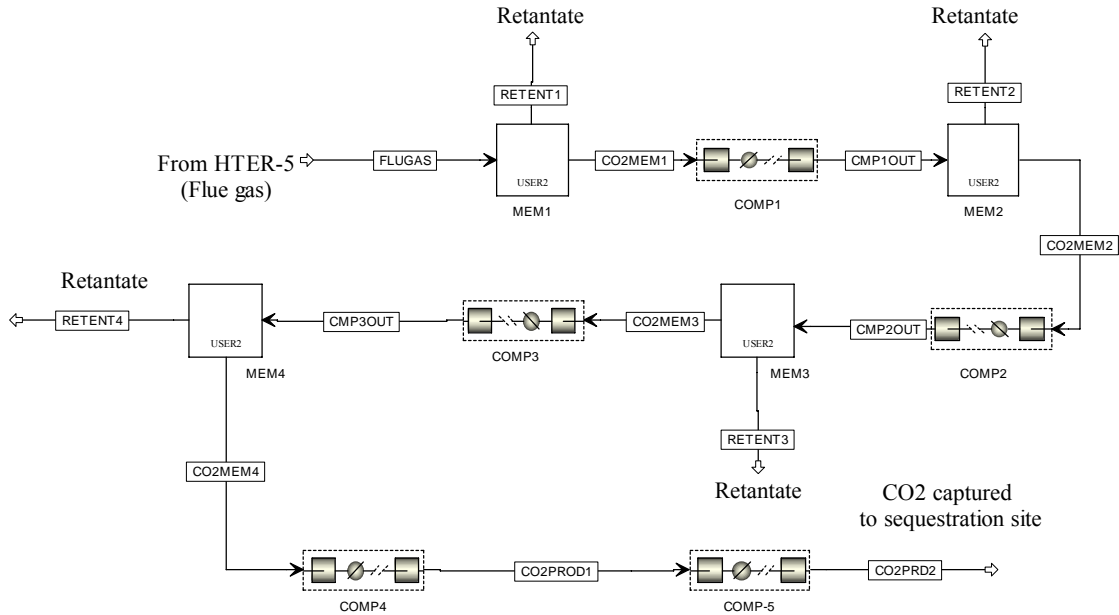


Figure 3.16: H₂ plant with membrane separation technology

Table 3.19: Specifications and parameters for units used for H₂ plant with membrane separation technology

Equipment	Aspen Block Model	Specifications/Configuration
MEM1, MEM2, MEM3, MEM4	User2	Configured in the block the parameters given in Table 3.10, DS is configured to determine the number of fibres dependent on the CO ₂ recovery
COMP1, COMP2, COMP3, COMP4	Mcompr	Number of stages = 5, Compressor model = isentropic, Discharge pressure from last stage = $1.01 \times 10^5 \text{ N/m}^2$, Efficiency = 0.75, Cooler outlet temperature = 313.15 K, Pressure drop = 0 N/m ²
COMP5	Mcompr	Number of stages = 5, Compressor model = isentropic, Discharge pressure from last stage = $1.5 \times 10^7 \text{ N/m}^2$, Efficiency = 0.75, Cooler outlet temperature = 313.15 K, Pressure drop = 0 N/m ²

Chapter 4

Results and Discussion

This chapter presents the results of the simulations. Section 4.1 provides the validation of the models used in the simulation. The next section presents the results and section 4.3 presents the comparison between the two capture processes. Finally, the last section (Section 4.4) presents the sensitivity of the energy penalty to the CO₂ recovery in the capture process.

4.1 Model Validation

The results of the simulation are validated using SMR and HTS data from Elnashaie and Elishishini (1993). The simulation model results show good agreement with the literature as shown in Table 4.1. This implies that the heat transfer coefficient and the kinetic parameters implemented in Aspen Plus are valid. The result for LTS is only validated based on the typical range of CO outlet after shift conversion [Johnson Matthey Catalysts, 2003] which is from 0.1% to 0.2% (dry gas basis).

Table 4.1: Comparison between simulation results and reference data

	Current Simulation	Elnashaie et al. (1993)	% Difference
SMR			
Process gas temp (K)	980.69	981.10	0.04
CH ₄ Conversion	0.56	0.57	2.10
CH ₄ Equilibrium conversion	0.58	0.59	1.07
HTS			
CO Conversion (%)	76.5	74.5	2.68
Exit Temperature (K)	687.4672	687.3	0.02
LTS			
Exit CO (mole %, dry basis)	0.1	Johnson Matthey Catalysts (2003) 0.1 - 0.2	

4.2 Simulation Results

4.2.1 Results for the Three Cases

Table 4.2 presents the base case results and the results for cases of CO₂ capture with MEA capture process and membrane separation process

For the base case (i.e. no CO₂ capture), the steam produced and the electricity needed are assumed to be exported to and supplied by outside sources, respectively. Thus, there is no additional CO₂ produced from the coal-fired power plant for electricity generation. The electricity consumed of (~ 0.09 MW) is mainly for the large pump used in the H₂ plant. The efficiency, η , is calculated as shown in equation (4.1).

$$\eta = 100 \left(\frac{\text{Heat output}}{\text{Heat input}} \right) \quad (4.1)$$

The heat input is equivalent to the heat of combustion of the feed and fuel. This fuel includes CH₄ for the furnace of the SMR and coal burned for additional electricity requirement. The heat output is taken as the sum of the heats of combustion of H₂ and the enthalpy of the extra steam produced. Higher heating values (HHV) are used in the calculation. The H₂ plant without CO₂ capture shows an efficiency of 77.15%.

Table 4.2: Simulation results for the 3 H₂ plant cases using the base case parameters

	No CO₂ capture	Membrane based CO₂ capture	MEA based CO₂ capture
H ₂ production, kg/s	0.89	0.89	0.89
CO ₂ production from the H ₂ plant , kg/s	10.18	10.18	10.18
Steam for the reboiler, kg/s	-	-	13.85
Steam for electricity generation, kg/s		12.12	3.77
Steam for Export, kg/s	12.12	-	-
Electricity required, MW			
H ₂ plant	0.09	0.09	0.05
CO ₂ plant	-	13.37	3.59
Total	0.09	13.46	3.63
Electricity generated by the H ₂ plant, MW	-	10.30	2.35
Additional electricity needed, MW	-	3.17	1.71
CO ₂ production from the coal-fired power plant , kg/s	-	0.72	0.29
Heat rate of coal burned for electricity needed, MW	-	7.55	4.07
Energy in H ₂ stream, MW	112.63	112.63	112.63
Combustion fuel heat rate, MW	16.41	16.41	16.41
Feed to SMR heat rate, MW	174.06	174.06	174.06
Energy in steam, MW	34.33	34.33	7.82
Efficiency, %	77.15	56.88	57.89

As for the case with CO₂ capture, the steam produced for electricity generation is greater for the membrane capture plant than the MEA capture plant since most of the steam produced by the MEA based capture plant is for the reboiler of the stripper. However, the

membrane capture plant requires greater electricity requirement than the MEA capture plant. Major part of the electricity used for the membrane capture plant is for the vacuum pumps required to keep the permeate side pressure of the membrane to 1.01×10^5 N/m² and in compressing the product CO₂ for sequestration purposes. For the MEA capture plant, the electricity is mainly used to compress CO₂ for sequestration purposes. The table also shows better process outcomes in terms of additional electricity needed for the MEA based capture plant for this particular operating condition. The efficiency for MEA based capture plant is higher due to the lower additional electricity requirement. For the H₂ plant with either CO₂ capture process, the steam available for export is used for power generation instead.

The above statement where MEA is better in terms of additional electricity needed is not generally true for all operating conditions. It is worth mentioning that the H₂ plant with membrane capture process produces higher quality of steam for power generation compared to the H₂ plant with MEA capture process where most of the steam produced is used for the reboiler of the stripper. Because of this, the results found in this particular operating condition may not hold true at other operating conditions.

4.2.2 Sensitivity Analysis of H₂ Plant Operating Parameters

The sensitivity of variation in operating variables to H₂, steam and CO₂ production and the amount of external combustion fuel is determined. Four operating variables are considered (steam to carbon ratio (S/C), inlet temperature of the SMR (T_{SMRin}) and inlet temperature of the HTS and LTS (T_{HTSin} and T_{LTSin} , respectively)). In all simulations, the methane feed gas

and reformer heat duty are kept constant. Table 4.3 presents the four operating variables considered with their respective process bounds.

Table 4.3: Operating variables used in the simulation

Process Variable	Lower Bound	Upper Bound
S/C ratio	2.2	3.7
T_{SMRin} , K	725	900
T_{HTSin} , K	570	730
T_{LTSin} , K	450	530

The lower bound on S/C ratio is based on the acceptable level where carbon formation is avoided. However, it has been reported that a ratio of 1.6 has been used without carbon deposition on the catalyst [Akers et al, 1955]. An S/C ratio of 2.2 is used to accommodate the heat exchange operation within the plant. The upper bound is decided also based on the heat exchange operation in the H₂ plant. Using S/C ratios higher than 3.7 causes the inability of the H₂ plant to produce process steam since the higher S/C ratio, the higher is the heat needed for heating up at a desired process steam temperature. The lower bound for T_{SMRin} is used to prevent gum formation on the catalyst of the reformer while the upper bound is based on the maximum heat that can be obtained from the heat of the flue gas generated from the furnace of the SMR. Limitations on T_{HTSin} and T_{LTSin} are based on the operating ranges of the units used.

Eighty-one combinations of the four operating variables are tested and simulated in Aspen Plus for each case at different capture processes used. These combinations are created using the lower, middle and upper bounds of the four operating variables. Since the base

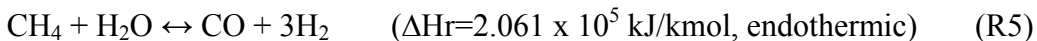
case for the H₂ plant without capture is the same as the H₂ production part of the H₂ plant with membrane, the output flue gas for each simulation is delivered to a separate flow sheet (i.e. membrane capture plant). This totals to 243 simulations and from these, the behaviour of the H₂ plant with CO₂ capture is determined.

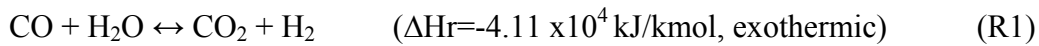
Table 4.4 shows the results of the sensitivity of the four operating variables to H₂ production, steam production, CO₂ production and combustion fuel (only the trends are indicated in this table).

Table 4.4: Sensitivity of operating parameters

Sensitivity of operating parameters to	Increase in S/C	Increase in T_{SMRin}	Increase in T_{HTSin}	Increase in T_{LTSin}
H ₂ Production	Increases	Increases	Decreases	Decreases
Steam Production	Decreases	Increases	Decreases	Decreases
CO ₂ Production	Increases	Increases	Decreases	Decreases
External Combustion Fuel	Increases	Increases	Decreases	Decreases

Some of the trends of the H₂ plant as shown in Table 4.4 are best explained by considering the reactions occurring inside the SMR and the WGS converters. SMR reactions are (R5), (R1) and (R6) while the WGS reaction is (R1).





Higher S/C ratio leads to an increase in H₂ product due to the presence of more molecules of H₂O. This also results in higher CO₂ production and less CO produced. The reduction in the steam production is due to the lower CO outlet from the SMR which leads to a reduction of exothermic reaction in WGS reactors. The lower CO production from the exit of the SMR at higher S/C is due to the higher impact of reaction (R6) over reaction (R5) leading to a more favourable CO₂ production. Since more CH₄ is converted at higher S/C ratio, less unreacted CH₄ in the recycle stream is available as fuel. Therefore, more external combustion fuel is needed.

An increase in T_{SMRin} leads to an increase in H₂, steam and CO₂ production and external combustion fuel. The SMR reaction is endothermic which gives higher CH₄ conversion at higher inlet temperature. This implies higher H₂ and CO₂ production. The cause of the increase in combustion fuel at higher T_{SMRin} is due to less CH₄ available in the off-gas. The increase in the steam production is due to the higher outlet temperature of the process gas exiting the SMR.

The effect of T_{HTSin} and T_{LTSin} are similar. Increasing T_{HTSin} and T_{LTSin} generally decreases H₂ production, which is due to the exothermic attribute of the WGS reaction (R1). This explains lower H₂ product and thus, lower CO₂ production at higher inlet temperatures for both HTS and LTS. The reduction in steam production is explained by lower CO

conversion to H₂ leading to lower production of heat which is attributed to the exothermic property of WGS reaction (R1). Some of these results are validated using results from Rajesh et al. (2001).

4.2.3 Energy Penalty Analysis

This study determines the best values of four operating variables to minimize the energy penalty taking into account an integrated CO₂ capture process. The energy penalty is the additional electrical requirement; it is assumed that any additional energy is generated from coal-fired power plant.

From Section 4.2.2, the behaviour of the H₂ plant with CO₂ capture is determined. In each of the simulation performed, corresponding H₂, steam and CO₂ production, external combustion fuel and electricity requirement are recorded. The steam produced is converted into electricity and is used to supply the power need of the plant. As previously mentioned, 30% efficiency [Rao et al, 2002] is used in converting steam into electricity. Additional electricity is supplied by burning coal (Highvale) and its equivalent CO₂ emission is calculated based on its HHV. The conversion efficiency of coal to electricity is 42% [Zanganeh et al, 2004]. The best operating condition is found where there is higher H₂ and steam production and lower CO₂ production. Higher steam production signifies lower additional electricity requirement.

Figure 4.1 shows the sensitivity of electricity requirement in capturing 80% of the amount of CO₂ produced by the H₂ plant. As seen in Figure 4.1, as expected, the relationship is linear. It can also be inferred that the H₂ plant with membrane separation technology requires about three times more electricity than the plant with MEA capture.

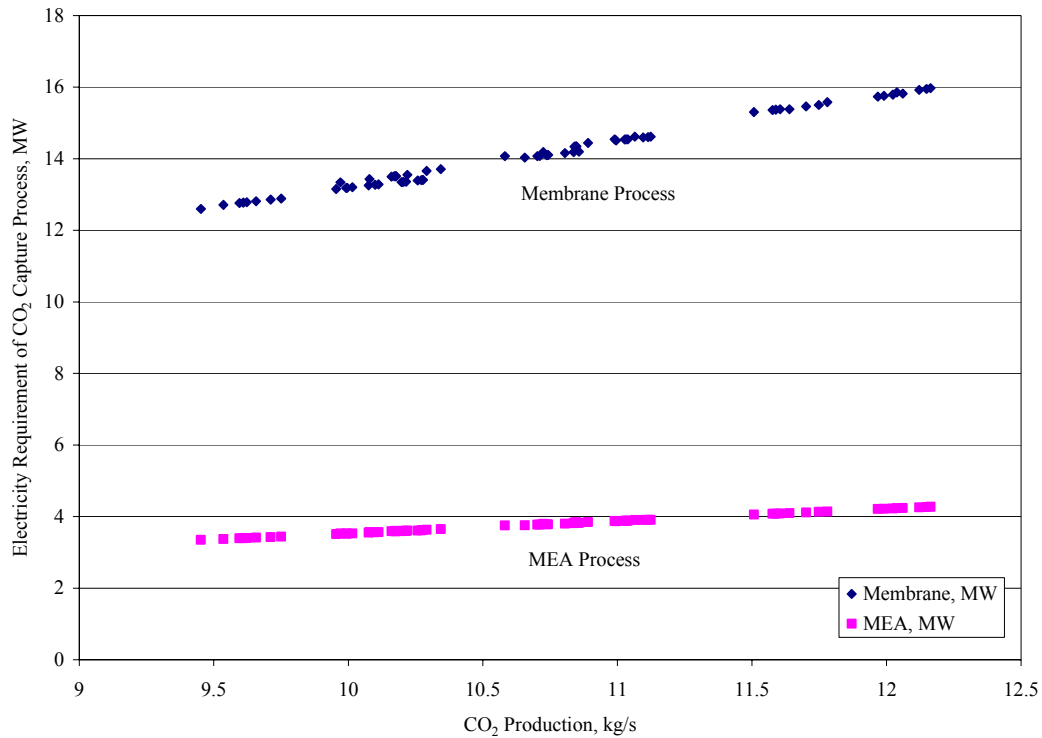


Figure 4.1: Sensitivity of electricity requirement of CO₂ capture process to CO₂ production (case of 80% CO₂ capture from the furnace of the SMR)

Figures 4.2 and 4.3 show the sensitivity of the electrical energy penalty and CO₂ productions for the MEA and the membrane processes, respectively. These figures show that both MEA and membrane processes always require additional electricity when capturing 80% of the

CO₂ produced from the H₂ plant. Figure 4.2 shows that for a given CH₄ feed rate, it is best to operate at a higher SMR inlet temperature and lower S/C ratio. This can be seen when comparing the results obtained at 900 K and S/C ratio of 2.2 to that at 800 K and S/C ratio of 3.7. The CO₂ production is comparable for both cases; however, there is higher H₂ production and lower additional electricity penalty at 900 K and S/C ratio of 2.2. At S/C = 3.7, reaction (R6) dominates over reaction (R5) which leads to more CO₂ and less CO. Since the WGS reaction (R1) is an exothermic reaction, it generates less heat when there is less CO available for the reaction which leads to lower steam production. Also, operating at lower inlet temperatures for WGS converters at the same T_{SMRin} and S/C ratio gives higher H₂ and CO₂ production as well as increase in electricity requirement. The result also shows that the steam production increases; the increased steam production, however, is mostly used in the stripper of the reboiler and does not result in the decrease in the electrical energy penalty. Although, there is higher CO₂ production resulting from operating at lower inlet temperatures of the WGS, the CO₂ production is dominant when operating at higher S/C ratio.

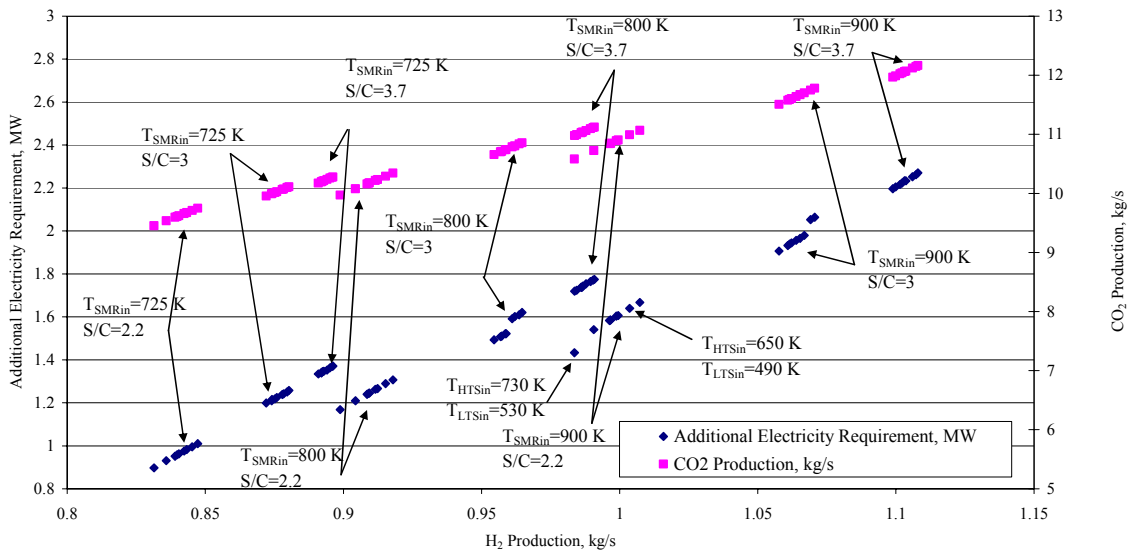


Figure 4.2: Sensitivity of additional electricity requirement and CO₂ production to H₂ production (MEA)

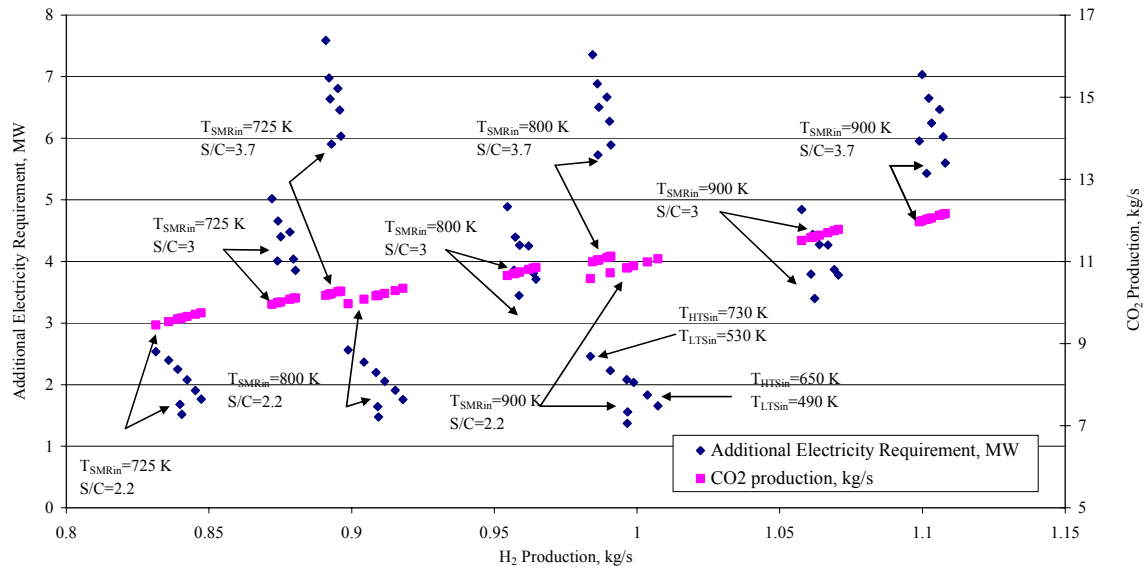


Figure 4.3: Sensitivity of additional electricity requirement and CO₂ production to H₂ production (Membrane)

Figure 4.3 shows the results for an H₂ plant using a membrane process; as in the MEA absorption process for a given CH₄ feed rate, it is best to operate at a higher SMR inlet temperature and lower S/C ratio. This is clearly viewed when comparing S/C = 3.7 and T_{SMRin} = 800 K to that at S/C = 2.2 and T_{SMRin} = 900 K. The effect of operating at lower T_{H₂TSin} and T_{L₂TSin} is significant for the case of the membrane. This is because all of the steam generated is converted into electricity to supply the membrane process and hence less additional electricity is required at lower T_{H₂TSin} and T_{L₂TSin}. Therefore, it can be inferred that it is best to operate the H₂ plant at higher inlet temperature of the SMR, lower S/C ratio and lower WGS inlet temperatures. At these operating conditions, the process requires more

external combustion fuel but it also yields more H₂ and steam production and lower CO₂ production. Thus, this is the best operating point in terms of energy penalty.

As previously noted, the additional electricity is assumed to be generated by a coal-fired power plant and its CO₂ equivalent emission is calculated. Figure 4.4 shows the amount of CO₂ emitted to the atmosphere per kg of H₂ produced at $T_{SMRin} = 900$ K, $T_{HTSin} = 570$ K, $T_{LTSin} = 490$ K and at various S/C ratios. At these operating conditions the minimum energy penalty occurs at the lowest S/C ratio of 2.2. The dotted portion of the blocks in the figure corresponds to the amount of CO₂ emitted to the atmosphere from the H₂ plant with CO₂ capture. This value is approximately equal to 2.2 kg CO₂/kg H₂ produced for all S/C ratios tested. The remaining portion of the blocks corresponds to the additional CO₂ emitted from the coal-fired power plant. This amount is approximately 0.4 kg CO₂/kg H₂ produced for the MEA absorption process and increases with S/C for the membrane process from 0.4 at S/C = 2.2 to 1.15 at S/C of 3.7.

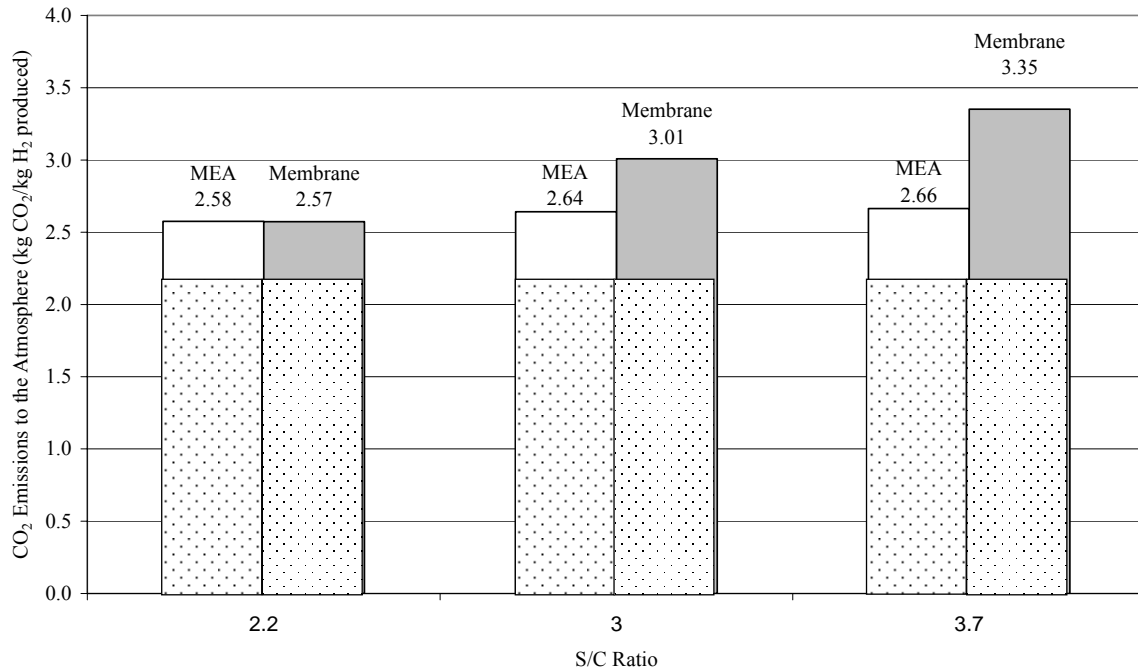


Figure 4.4: Comparison of CO₂ emissions to the atmosphere: $T_{SMRin} = 900$ K, $T_{HTSin} = 570$ K $T_{LTsin} = 490$ K

4.3 Comparison of the H₂ plant with CO₂ Capture

The comparison between the two capture processes considered is done in terms of energy penalty. The membrane based capture plant requires more electricity requirement than the MEA based capture plant as shown in Figure 4.1. However, the membrane based capture plant shows comparable energy penalty when operated at the best operating condition. As shown in Figure 4.5, at $T_{SMRin} = 900$ K and S/C ratio of 2.2, there is comparable additional

electricity requirement per kg of CO₂ production. This point is highlighted in Figure 4.5 enclosed by a square.

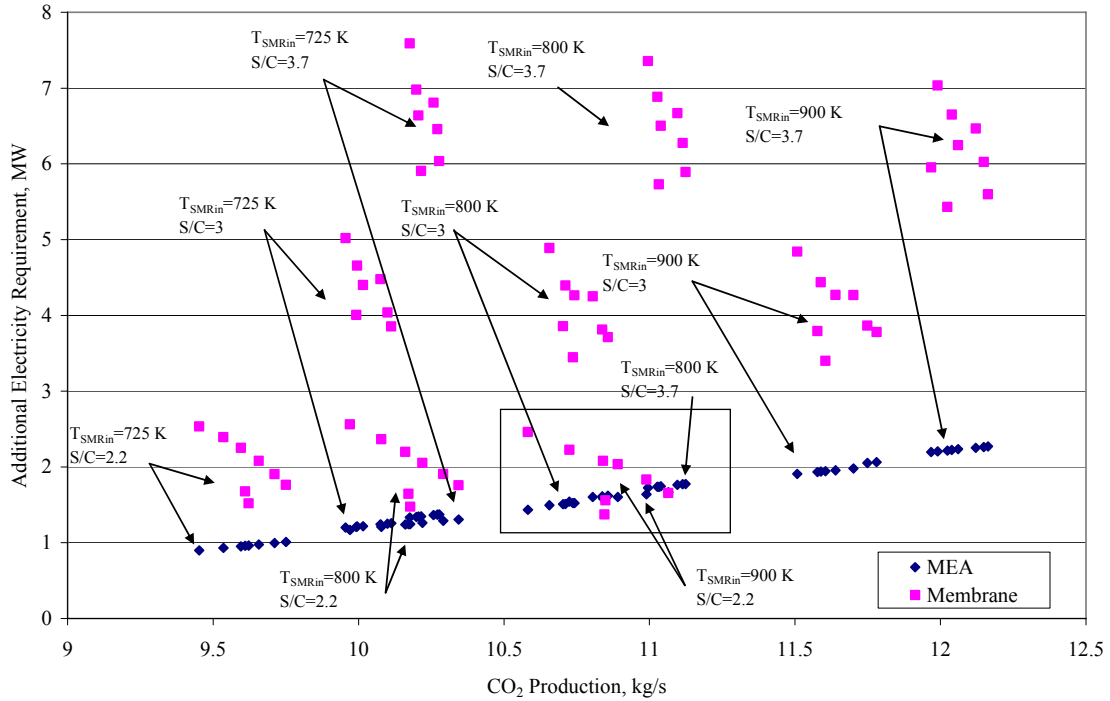


Figure 4.5: Sensitivity of additional electricity requirement of CO₂ capture process to CO₂ production

The percent of overall CO₂ avoided, which takes into account the amount of CO₂ emitted from the coal plant, is calculated in reference to the CO₂ production of the base case as shown in Table 4.5. MEA provides higher percent of overall CO₂ avoided at S/C ratios of 3 and 3.7 while membrane shows comparable amount at S/C ratio of 2.2.

Table 4.5 Comparison of CO₂ avoided

S/C Ratio	MEA, %	Membrane, %
2.2	77.52	77.54
3	76.94	73.74
3.7	76.74	70.74

4.4 Sensitivity of Energy Penalty to CO₂ Recovery

In an effort to determine if the H₂ plant with CO₂ capture can be self sufficient in terms of energy penalty, a study is conducted on the energy penalty as a function of the CO₂ recovery. Two additional cases are tested, i.e. 70% and 75% recovery at conditions of S/C = 2.2, T_{SMRin} = 900 K and at various T_{HTSin} and T_{LTSin}.

Figures 4.6 and 4.7 present the sensitivity of the energy penalty to the CO₂ recovery at 70%, 75% and 80%. At 70% CO₂ recovery, the MEA based capture plant does not require any additional electricity as can be seen in Figure 4.6. It can also be seen that between 70 to 75% recovery would correspond to a perfect match between the amount of energy generated (in form of steam) by the reforming plant and the energy required (in the form of steam and electricity) for the CO₂ capture process. This is the break-even point in the process where just enough energy is produced. The reduction in the energy penalty at lower CO₂ recovery is due to increased steam available for power generation.

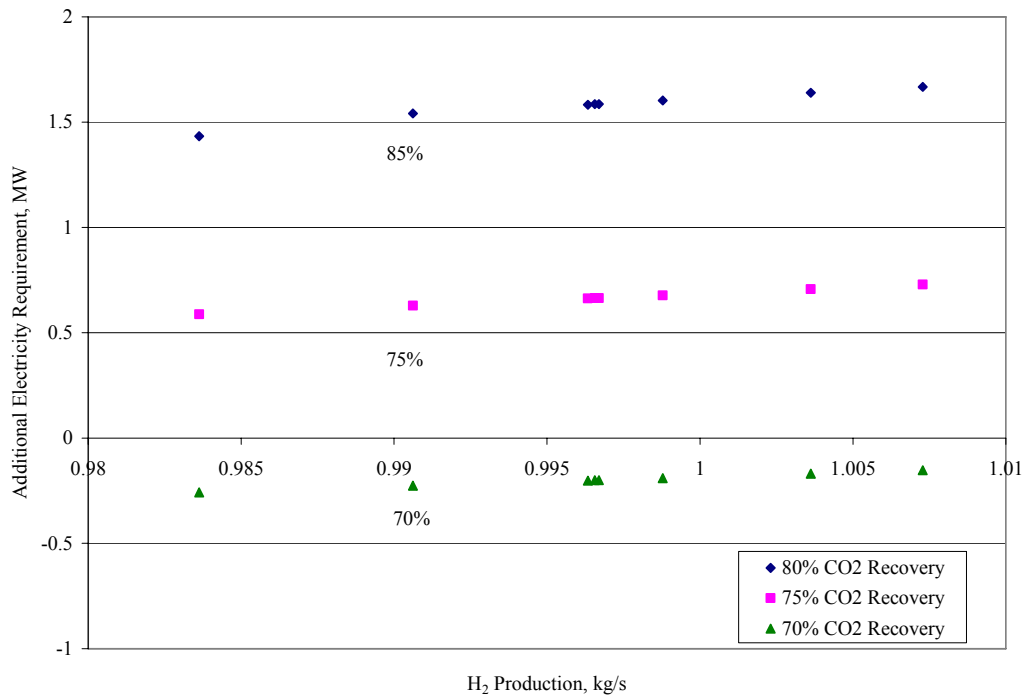


Figure 4.6: Sensitivity of additional electricity requirement to percent CO₂ recovery (MEA)

For the membrane based capture plant as seen in Figure 4.7, additional electricity is required at 70% and 75% recovery. Finding the break-even point that corresponds to no additional electricity requirement can be performed. However, the H₂ plant must be modified and the location of the CO₂ capture must also be changed. Because this represents a significant deviation from the base case, it was not pursued. However, based on the relatively constant slope of the curves in Figure 4.7, it is estimated that the break-even point occurs between 55 to 60% CO₂ recovery.

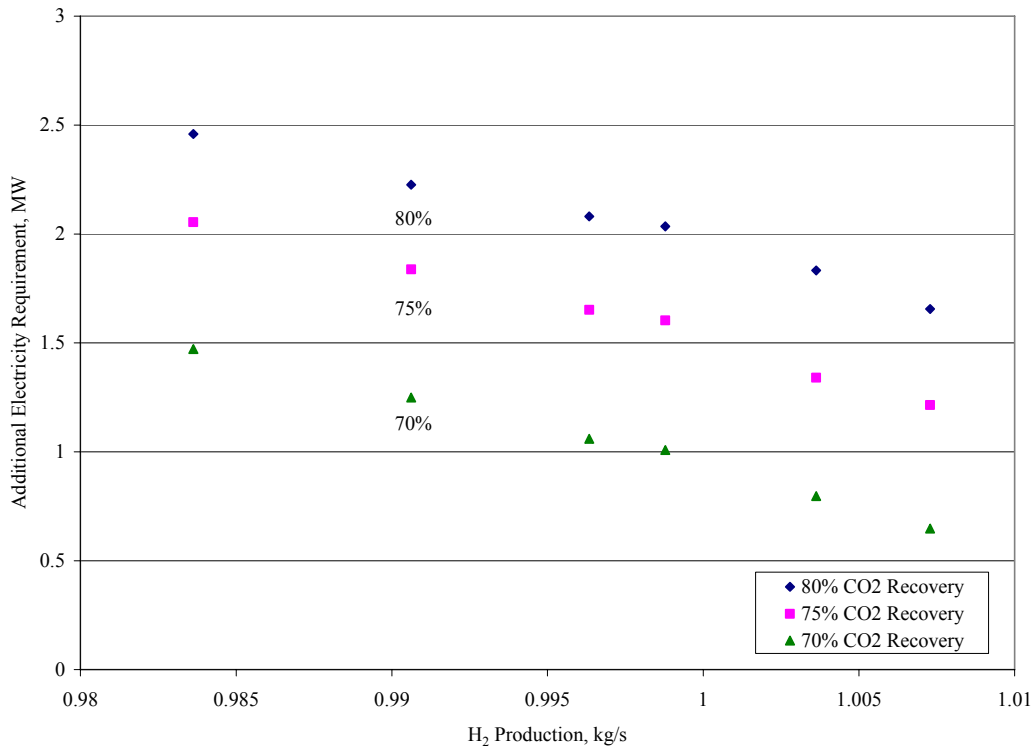


Figure 4.7: Sensitivity of additional electricity requirement to percent CO₂ recovery (Membrane)

Comparison of overall CO₂ avoided at various percent of CO₂ recovery is evaluated at the best operating condition (i.e. S/C ratio = 2.2, T_{SMRin} = 900 K, T_{HTSin} = 570 K, T_{LTSin} = 490 K). The result is shown in Figure 4.8. In this figure, the dotted portion presents the CO₂ emitted to the atmosphere and remaining portion stands for the CO₂ emitted from coal burned for additional electricity generation. These values are expressed as per kg of H₂ produced. As expected, the lower the percent CO₂ recovery, the higher is the CO₂ emitted to the atmosphere from the H₂ plant. It also follows that at this condition, there is lower CO₂

emitted from the coal due to lower additional electricity requirement that resulted from higher steam production for power generation. This is seen from the decreasing value of the remaining portion of the blocks.

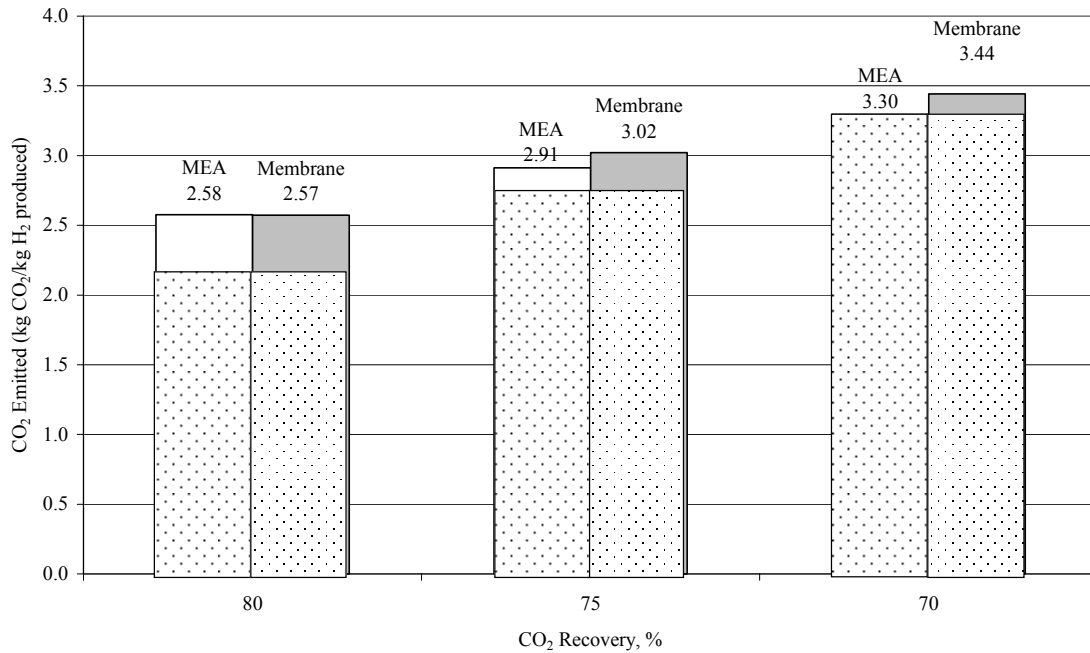


Figure 4.8: Comparison of CO₂ emissions to the atmosphere at various CO₂ recoveries

As shown in the figure and as previously noted, the membrane shows comparable results at 80% CO₂ recovery. The MEA provides better results at lower CO₂ recoveries (i.e. 75% and 70% CO₂ recoveries) as indicated by the lower CO₂ emission from the coal burned for additional electricity requirement. In addition to this, the MEA provides better capture

technology at 70% CO₂ recovery since no additional electricity is required and thus less CO₂ emissions.

Chapter 5

Conclusions

Based from the results of the study, the following conclusions can be drawn.

1. H₂ plants need to be modified for CO₂ capture. It is necessary to reduce CO₂ emissions resulting from the projected expansion of oil sands operation that require huge amounts of H₂.
2. To minimise the energy penalty H₂ plants should be operated at:
 - highest inlet SMR temperatures
 - lowest S/C ratios and
 - lowest WGS inlet temperatures.

From the operating conditions tested, the specific values are:

- $T_{SMRin} = 900 \text{ K}$
 - $S/C = 2.2$ and
 - $T_{HTSin} = 570 \text{ K}$, $T_{LTSin} = 490 \text{ K}$
3. Both capture processes require huge amounts of energy. Considering 80% CO₂ recovery, the results show that the use of MEA capture process requires less additional electricity for most of the operating conditions tested. However, it gives

comparable results in terms of energy penalty when run at higher inlet temperature of SMR, lower S/C ratio and lower WGS inlet temperatures.

4. At CO₂ recoveries less than 80% the MEA process has a lower energy penalty than membrane separation process. At ~73% CO₂ recovery the MEA capture process has no energy penalty in that the energy produced by the H₂ plant is just enough to supply the demands of the CO₂ capture process. The break-even point for the membrane process occurs at ~57% CO₂ recovery.

5. The amount of CO₂ emitted at 80% CO₂ recovery is evaluated at the best operating conditions. For both cases, the CO₂ emissions from the H₂ plant excluding that from the coal burned for electricity generation is approximately 2.2 kg CO₂/kg H₂ produced. An additional 0.4 kg CO₂/kg of H₂ is emitted from burning coal to generate electricity needed for the MEA capture process and from 0.4 to 1.15 for the membrane process depending on the S/C ratio.

Chapter 6

Recommendations

The following suggestions are recommended for further study.

1. Optimise the heat exchange operation of the H₂ plant with CO₂ capture to minimise the energy penalty.
2. Incorporate the unit operations needed for MEA based capture. This can be done by using two absorbers – one for the outlet of the condenser before feed to the PSA and the other is for the outlet of the furnace of the SMR. The output of these two absorbers are then mixed and sent to a single stripper. The advantage of this scheme is the smaller circulation of fluid in the absorber columns.
3. Modify and evaluate the membrane based capture process flow scheme by installing the membrane units on the LTS and SMR outlets, separately. The energy requirements for this suggested modification comes from two different locations – one is from the energy required to pressurize the treated syngas prior to entering PSA (when integrating membrane at the outlet of the LTS); second is from the vacuum pump used prior to each membrane stage (when integrating membrane at the outlet of the SMR). The energy requirement for the current PFD comes from the vacuum pump used by the membrane process integrated at the

outlet of the SMR furnace. A good comparison of the energy requirements can be made between the current PFD and the suggested PFD.

4. Perform and compare economic evaluation of the two capture processes tested and the modified PFDs as suggested in number 2 and 3. This can be accomplished using the Icarus costing software package interfaced with Aspen.

Nomenclature

Variables

A = pre-exponential factor, $(\text{kmol} \cdot \text{N}/\text{m}^2)/(\text{kgcat} \cdot \text{s})$

$\alpha_{i/j}$ = Selectivity ratio of component i to j

β = exponent 2 (driving force expression box in Aspen)

C = component concentration

D = diffusion coefficient, cm^2/s

E = activation energy, J/kmol

$F_{H_2, \text{out}}$ = flow rate of H_2 at PSA outlet, kmol/s

$F_{PSA, \text{in}}$ = total flow rate of PSA inlet, kmol/s

k_1 = driving term constants of term1 in Aspen

k_2 = driving term constants of term 2 in Aspen

k = rate constant

K = equilibrium constant

K_{ad} = adsorption constant ($i = \text{CO}, \text{H}_2, \text{CH}_4, \text{H}_2\text{O}$), m^2/N

η = H_2 efficiency, %

P = permeation rate, cm^3 (STP) $\text{cm}/(\text{cm}^2 \text{ s cmHg})$

p_i = partial pressure of component, N/m^2 ($i = \text{CH}_4, \text{H}_2\text{O}, \text{CO}, \text{CO}_2, \text{N}_2$)

r = rate of reaction, $\text{kmol}/(\text{s} \cdot \text{kgcat})$

R = gas law constant, $\text{J}/(\text{mol} \cdot \text{K})$

S = sorption coefficient, cm^3 (STP)/(cm^3 cmHg)

T_0 = reference temperature, K

T = absolute operating temperature, K

ψ = activity factor

x_i = mole fraction of component i at PSA inlet, ($i = \text{CH}_4, \text{H}_2\text{O}, \text{CO}, \text{CO}_2, \text{N}_2$)

$x_{\text{H}_2, \text{in}}$ = mole fraction of H_2 at PSA inlet

γ_i = mole fraction of component i at PSA outlet, ($i = \text{CH}_4, \text{H}_2\text{O}, \text{CO}, \text{CO}_2, \text{N}_2$)

Superscript

n = temperature exponent

m = adsorption term exponent

α = exponent 1 (driving force expression box)

nu = term exponent for each component

N = number of components

M = number of terms in adsorption expression

Acronyms and Abbreviations

GHG = Greenhouse gas

HTS = High-temperature shift

HX = Heat exchanger

LTS = Low temperature shift

MEA = Monoethanolamine

PSA = Pressure swing adsorber

SAGD = Steam assisted gravity drainage

SCO = Synthetic crude oil

SMR = Steam methane reformer

THAI = Toe-to-heel air injection

VAPEX = Vapour extraction process

WGS = Water gas shift

References

1. Adris, A. M., & Pruden, B. B. (1996). On the reported attempts to radically improve the performance of the steam methane reforming reactor. *The Canadian Journal of Chemical Engineering*, 74, 177-186.
2. Akers, W. W., & Camp D. P. (1955). Kinetics of the Methane-Steam Reaction. *American Institute of Chemical Engineers*, 1, 471-475.
3. Alie C, Backham L, Croiset E, Douglas P. (2005). Simulation of CO₂ Capture using MEA scrubbing: A flowsheet decomposition method. *Energy Conversion and Management*, 46, 475-487.
4. Alentiev A, Drioli E, Gokzhaev M, Golemme G, Ilinich O, Lapkin A, Volkov V, Yampolskii, Yu. (1998). Gas permeation properties of phenylene oxide polymers. *Journal of Membrane Science*, 138, 99-107.
5. Aspen Plus Technology, Inc., Cambridge, MA, USA. *Aspen Plus Version 12.1*, 2003.
6. Barba, J. J.; Hemmings, J., Bailey, T. C., Horne, N. (1998). Advances in hydrogen production technology: the options available. *Hydrocarbon Engineering*, 41, 48-54.
7. Bridger, G. W. (1970). *Catalyst Handbook*. Springer-Verlag, New York Inc., New York.
8. Buch, C., Grinna, S., & Kruse B. (2002). *Hydrogen*, Belona Foundation.
9. Canadian Institute of Mining, Metallurgy and Petroleum, *Oil Sands Discovery Centre*. Retrieved July, 2003 from <http://www.oilsandsdiscovery.com>.
10. Chlendi M, Tondeur D, Rolland F. (1995). A method to obtain a compact representation of process performances from a numerical simulator: example of pressure swing adsorption for pure hydrogen production. *Gas Separation and Purification*, 9,125-135.

11. Chowdhury M, Douglas P, Feng X, Croiset E. (2005). A new numerical approach for a detailed multicomponent gas separation membrane and Aspen Plus simulation. *Chem. Eng. Technol.*, 28(7), 773-782.
12. Chowdhury M, Douglas P, Feng X, Croiset E. (2004 September). *Design and simulation of membrane based gas separation processes in Aspen Plus™ for capturing CO₂ from flue gases*. In: Proceedings of the 7th International Conference on Greenhouse Gas Control Technologies, Vancouver, Canada.
13. Du, J. (2005). Poly (N, N-dimethylaminoethyl methacrylate)/polysulfone composite membrane for CO₂ separation. PhD comprehensive examination report. University of Waterloo.
14. Dybkjaer, Ib., Madsen W. S. (1997/1998). Advanced reforming technologies for hydrogen production. *Hydrocarbon Engineering*, 56.
15. Elnashaie S.S.E.H., Elshishini S.S. (1993). *Modelling, simulation and optimization of industrial fixed bed catalytic reactors. Topics in Chemical Engineering-Vol. 7*, Amsterdam: Gordon and Breach Science Publishers.
16. Freguia, S., Rochelle, G. T. (2003). Modeling of CO₂ Capture by Aqueous Monoethanolamine. *American Institute of Chemical Engineers*, 49(7), 1676.
17. Freund, P., Thambimuthu, K. (1999 May). *Options for decarbonising fossil energy supplies*. Paper presented at Combustion Canada '99, Telus Convention Centre, Calgary, Alberta, Canada.
18. Grover, S. S. (1970). Optimize hydrogen production by model. *Hydrocarbon Processing*, 49, 109-111.

19. Hyman, M. H. (1968). Simulate methane reformer reactions. *Hydrocarbon Processing*, 47, 131-137.
20. IEA Greenhouse Gas R&D Program. (2003 July). *International Test Network for CO₂ Capture: Report on 5th Workshop*. Pittsburg, PA, USA.
21. Johnson Matthey Catalysts (2003). *The steam reforming process*. Retrieved June, 2003 from www.syntex.com/hydrogen/steam_reforming_process.htm.
22. Karasiuk, C. J. (1985). *Simulate and control of a methane steam reformer*. MS Thesis, Department of Chemical Engineering, University of Waterloo.
23. Kazama S, Morimoto S, Tanaka S, Mano H, Yashima T, Yamada K, Haraya K. (2004 September). *Cardo polyimide membranes for CO₂ capture from flue gases*. In: Proceedings of the 7th International Conference on Greenhouse Gas Control Technologies, Vancouver, Canada.
24. Koros, W. J. (1985). Gas separation membranes: Needs for combined materials science and processing approaches. *Macromolecular symposia*, 188, 13-22.
25. Kohl, A., Riesenfeld, F. (1985). *Gas Purification*. Gulf Publishing Company, Houston, United States.
26. National Energy Board. (2004 May). *Canada's Oil Sands Opportunities and Challenges to 2015* (ISBN 0-662-36880-0). Calgary, Alberta: The Publications Office National Energy Board.
27. Newman, S. A. (1985). *Acid and Sour Gas Treating Processes*. Gulf Publishing Company, Houston, United States.
28. Schlumberger. *Oilfield Glossary*. Schlumberger Limited, 2006. Retrieved June 2006, from <http://www.glossary.oilfield.slb.com>.

29. Ordorica-Garcia, G. (2004). Development of H₂ economy for Alberta in a CO₂ constrained world. PhD comprehensive examination report. University of Waterloo.
30. Palm T., C. Buch, B. Kruse (1999). Green heat and Power: The Kvaener Carbon Black and Hydrogen Process. Retrieved June 2003 from www.bellona.no/en/energy/report_3-1999/11196.html.
31. Pan, C. Y. (1986). Gas separation by high-flux, asymmetric hollow-fiber membrane. *AIChE Journal*, 32, 2020-2027.
32. Phillipson, J. J., 1970. *Catalyst Handbook*. Springer-Verlag, New York Inc., New York
33. Rajesh, J. K., Gupta, S. K., Rangaiah, G. P., Ray, A. K. (2001). Multiobjective optimization of industrial hydrogen plants. *Chemical Engineering Science*, 56, 999-1010.
34. Rajesh, J. K.; Gupta, S. K.; Rangaiah, G. P.; & Ray, A. K. (2000). Multiobjective optimization of steam reformer performance using genetic algorithm. *Industrial and Engineering Chemistry Research*, 39, 706-717.
35. Rao B, Rubin S., 2002. A technical, economic, and environmental assessment of amine-based CO₂ capture technology for power plant greenhouse gas control. *Environ. Sci. Technol.*, 36, 4467-4475.
36. Rase, H. F. (1977). *Chemical Reactors Design for Process Plants, vol II Case Studies and Design Data*. John Wiley & Sons, New York.
37. Rase, H. F. (1977). *Chemical Reactors Design for Process Plants, vol I Case Studies and Design Data*. John Wiley & Sons, New York.
38. Rostrup-Nielsen, J. R. (1984). Catalytic steam reforming. In *Catalysis – Science and Technology*, A. R. Anderson & M. Boudart, (Eds.). Springer: Berlin, 5.

39. Shafeen, A., Croiset, E., Douglas, P. L. (2004). CO₂ sequestration in Ontario, Canada. Part 1. Storage evaluation of potential reservoirs. *Energy Conversion & Management*, 45, 2645-2659.
40. Singh D, Croiset E, Douglas P., Douglas M. (2003). Techno-Economic Study of CO₂ Capture from an Existing Coal-Fired Power Plant: MEA Scrubbing vs O₂/CO₂ Combustion. *Energy Conversion and Management*, 44 (19), 3073-3091.
41. Syncrude Canada, Ltd. (2006). The Oil Sands. Retrieved July, 2006 from <http://www.syncrude.ca/users/folder.asp?FolderID=5724>
42. Thumbimuthu, K. (2004). Personal communication.
43. Van Hook, J. P. (1980). Methane steam reforming. *Catal. Rev. Sci. Eng.*, 21, 1-51.
44. Van Weenan, W. F. (1983). Optimizing Hydrogen Plant Design. *AIChE*, 37.
45. Xu, J.; & Froment, G. F. (1989). Methane steam reforming, methanation and water-gas shift: I. Intrinsic kinetics. *AIChE Journal*, 35, 88.
46. Yurum, Y. (1995). Hydrogen Production Methods. *Hydrogen Energy System*, 15-30.
47. Zanganeh K, Shafeen A, Thambimuthu K. (2004 September). *A comparative study of refinery fuel gas oxy-fuel combustion options for CO₂ capture using simulated process data*. In: Proceedings of the 7th International Conference on Greenhouse Gas Control Technologies, Vancouver, Canada.

Appendix A: Kinetic Parameters for SMR (Xu and Froment, 1989)

1.1 Rate of reaction

$$r_{(R5)} = \left(\frac{k_{R5}}{P_{H_2}^{2.5}} (P_{CH_4} P_{H_2O} - \frac{P_{H_2}^3 P_{CO_2}}{K_{R5}}) \right) / (DEN)^2 \quad (A.1)$$

$$r_{(R6)} = \left(\frac{k_{R6}}{P_{H_2}^{3.5}} (P_{CH_4} P_{H_2O}^2 - \frac{P_{H_2}^4 P_{CO_2}}{K_6}) \right) / (DEN)^2 \quad (A.2)$$

$$r_{(R1)} = \left(\frac{k_{R1}}{P_{H_2}} (P_{CO} P_{H_2O} - \frac{P_{H_2} P_{CO_2}}{K_{R1}}) \right) / (DEN)^2 \quad (A.3)$$

$$DEN = 1 + K_{adCO} P_{CO} + K_{adH_2} P_{H_2} + K_{adCH_4} P_{CH_4} + (K_{adH_2O} P_{H_2O}) / P_{H_2} \quad (A.4)$$

1.2 Rate constants and adsorption constants

The rate coefficient and adsorption constants are computed using the following derived equations.

$$k_i = k_{i,T} \exp\left[-\frac{E_i}{R} \left(\frac{1}{T} - \frac{1}{T_r}\right)\right] \quad i = R5, R6, R1 \quad (A-5)$$

$$K_{adj} = K_{adj,T_r} \exp\left[-\frac{\Delta H_j}{R} \left(\frac{1}{T} - \frac{1}{T_r}\right)\right] \quad j = \text{CO, H}_2, \text{CH}_4, \text{H}_2\text{O} \quad (\text{A-6})$$

$$T_r = 648 \text{ K for } k_i, K_{adCO}, K_{adH2}$$

$$T_r = 823 \text{ K for } K_{adCH4}, K_{adH2O}$$

The preexponential factors $A(k_i)$ and $A(K_{adj})$ can be calculated using Arrhenius and Van't Hoff equations:

$$A(k_i) = k_i T \exp\left(\frac{E_i}{RT}\right) \quad i = R5, R6, R1 \quad (\text{A-7})$$

$$A(K_{adj}) = K_{adj,T} \exp\left(\frac{\Delta H_j}{RT}\right) \quad j = \text{CO, H}_2, \text{CH}_4, \text{H}_2\text{O} \quad (\text{A-8})$$

Appendix B: Kinetic Parameters for WGS (Rase, 1977)

The units for the following equations are available from the reference.

2.1 Rate of reaction

$$(-r_{CO}) = \frac{\psi k (y_{CO} y_{H_2O} - \frac{y_{CO_2} y_{H_2}}{K})}{379 \rho_b} \quad (B1)$$

2.2 Rate constants and equilibrium constants

$$k = \exp\left(15.95 - \frac{8820}{T}\right); \text{ for iron catalyst} \quad (B2)$$

$$= \exp\left(12.88 - \frac{3340}{T}\right); \text{ for copper zinc oxide} \quad (B3)$$

$$K = \exp\left(-4.72 + \frac{8640}{T}\right); \text{ for } 760 \leq T \leq 1060 \quad (B4)$$

$$= \exp\left(-4.33 + \frac{8240}{T}\right); \text{ for } 1060 \leq T \leq 1360 \quad (B5)$$

$$\text{Iron Catalyst } \psi = 0.816 + 0.184 P_{tot}; \text{ for } P_{tot} \leq 11.8 \quad (B6)$$

$$= 1.53 + 0.123 P_{tot}; \text{ for } 11.8 < P_{tot} \leq 20.0 \quad (B7)$$

$$= 4.0 \text{ for } P_{tot} > 20.0 \quad (B8)$$

Copper-zinc catalyst

$$\psi = 0.86 + 0.14P_{tot}; \text{ for } P_{tot} \leq 24.8 \quad (\text{B9})$$

$$= 4.33 \text{ for } P_{tot} > 24.8 \quad (\text{B10})$$

Appendix C: Simulation Stream Results (H₂ Plant – Base Case)

	AIR	AIR-FEED	AIR-FUEL	AIR-H2	AIR-OG	BFW2-INA	BFW3-INA	BFW3-INB
Substream: MIXED								
Mole Flow kmol/sec								
CH4	0	0	0	0	0	0	5.81E-07	0
H2O	0	0	0	0	0	0.188	0.343	1.637
H2	0	0	0	0	0	0	8.10E-07	0
CO2	0	0	0	0	0	0	1.50E-05	0
N2	0.907	1.482	0.140	0.829	0.649	0	3.43E-09	0
CO	0	0	0	0	0	0	1.48E-09	0
O2	0.241	0.394	0.037	0.220	0.173	0	0	0
Mass Flow kg/sec								
CH4	0	0	0	0	0	0	9.32E-06	0
H2O	0	0	0	0	0	3.382	6.186	29.495
H2	0	0	0	0	0	0	1.63E-06	0
CO2	0	0	0	0	0	0	6.59E-04	0
N2	25.405	41.526	3.911	23.234	18.180	0	9.61E-08	0
CO	0	0	0	0	0	0	4.16E-08	0
O2	7.714	12.609	1.188	7.055	5.520	0	0	0
Total Flow kmol/sec	1.148	1.876	0.177	1.050	0.821	0.188	0.343	1.637
Total Flow kg/sec	33.119	54.135	5.099	30.289	23.700	3.382	6.186	29.495
Total Flow cum/sec	28.069	45.881	4.322	25.671	20.105	3.95E-03	6.55E-03	0.0296874
Temperature K	298.150	298.150	298.150	298.150	298.429	429.296	298.571	298.150
Pressure N/sqm	1.013E+05	1.013E+05	1.013E+05	1.013E+05	1.013E+05	2.45E+06	1.01E+05	1.01E+05

	BFW3- INC	BFW3- IND	BFW4- INA	BFW4-OT	BFWTOT	COND- IN1	FEED1	FEED2
Substream: MIXED								
Mole Flow kmol/sec								
CH4	5.81E-07	5.81E-07	0	0	0	0.073	0.197	0.197
H2O	1.981	1.981	0.485	0.591	1.376	0.344	0.000	0.000
H2	8.10E-07	8.10E-07	0	0	0	0.545	0.049	0
CO2	1.50E-05	1.50E-05	0	0	0	0.140	0.018	0.0179
N2	3.43E-09	3.43E-09	0	0	0	3.94E-03	3.94E-03	3.94E-03
CO	1.48E-09	1.48E-09	0	0	0	2.12E-03	2.37E-06	0
O2	0	0	0	0	0	0	0	0
Mass Flow kg/sec								
CH4	9.32E-06	9.32E-06	0	0	0	1.167	3.162	3.161
H2O	35.681	35.681	8.736	10.648	24.790	6.205	2.14E-05	0
H2	1.63E-06	1.63E-06	0	0	0	1.098	0.099	0
CO2	6.59E-04	6.59E-04	0	0	0	6.177	0.796	0.789
N2	9.61E-08	9.61E-08	0	0	0	0.111	0.111	0.110
CO	4.16E-08	4.16E-08	0	0	0	0.059	6.63E-05	0
O2	0	0	0	0	0	0	0	0
Total Flow kmol/sec	1.981	1.981	0.485	0.591	1.376	1.108	0.268	0.219
Total Flow kg/sec	35.681	35.681	8.736	10.648	24.790	14.816	4.168	4.060
Total Flow cum/sec	0.0359778	0.0359298	0.010	1.428	0.025	0.963	0.671	0.209
Temperature K	298.222	298.602	430.000	733.000	298.150	313.150	733.000	298.150
Pressure N/sqm	1.013E+05	2.452E+06	2.452E+06	2.452E+06	1.013E+05	2.087E+06	2.452E+06	2.452E+06

	FEEDTOT	FLU-GAS1	FLU-GAS2	FLU-GAS3	FLU-GAS4	FPREHT1	FPREHT2	FRNFEEDP
Substream: MIXED								
Mole Flow kmol/sec								
CH4	0.197	0	0	0	0	0.197	0.197	0
H2O	0.591	0.238	0.238	0	0	0	0	0.394
H2	0.049	0	0	0	0	0	0	0
CO2	0.018	0.231	0.231	0.231	0.231	0.018	0.018	0.215
N2	3.94E-03	0.911	0.911	0.911	0.911	0.004	0.004	1.486
CO	2.37E-06	2.12E-03	2.12E-03	2.12E-03	2.12E-03	0	0	0
O2	0	0.031	0.031	0.031	0.031	0	0	0
Mass Flow kg/sec								
CH4	3.162	0	0	0	0	3.161	3.161	0
H2O	10.648	4.286	4.286	0	0	0	0	7.099
H2	0.099	0	0	0	0	0	0	0
CO2	0.796	10.183	10.183	10.183	10.183	0.789	0.789	9.460
N2	0.111	25.515	25.515	25.515	25.515	0.110	0.110	41.636
CO	6.63E-05	0.059	0.059	0.059	0.059	0	0	0
O2	0	1.006	1.006	1.006	1.006	0	0	0
Total Flow kmol/sec	0.859	1.414	1.414	1.176	1.176	0.219	0.219	2.095
Total Flow kg/sec	14.816	41.050	41.050	36.763	36.763	4.060	4.060	58.195
Total Flow cum/sec	2.103	101.164	51.014	42.450	30.184	0.209	0.209	42.684
Temperature K	731.606	871.899	440.000	440.000	313.150	298.150	298.150	298.150
Pressure N/sqm	2.452E+06	1.013E+05	1.013E+05	1.013E+05	1.013E+05	2.45E+06	2.45E+06	1.01E+05

	FRNFUELP	FRNH2P	FRNOGP	FRPREHT2	FUEL1	FUEL2	FUEL3	FUELTOT
Substream: MIXED								
Mole Flow kmol/sec								
CH4	0	0	0	0.197	0.019	0.019	0.019	0.0912
H2O	0.037	0.441	0.201	1.188E-06	0	0	0	1.066E-03
H2	0	0	0	0.049	0	0	0	0.054
CO2	0.019	0.000	0.213	0.018	0	0	0	0.140
N2	0.140	0.829	0.653	3.945E-03	0	0	0	3.940E-03
CO	0	0	2.122E-03	2.365E-06	0	0	0	2.122E-03
O2	0	0	0	0	0	0	0	0
Mass Flow kg/sec								
CH4	0	0	0	3.162	0.298	0.298	0.298	1.463
H2O	0.669	7.944	3.618	2.141E-05	0	0	0	0.0192
H2	0	0	0	0.099	0	0	0	0.1098
CO2	0.817	0	9.366	0.796	0	0	0	6.1691
N2	3.911	23.234	18.290	0.111	0	0	0	0.1104
CO	0	0	0.059	6.626E-05	0	0	0	0.0594
O2	0	0	0	0	0	0	0	0
Total Flow kmol/sec	0.195	1.270	1.069	0.268	0.019	0.019	0.019	0.293
Total Flow kg/sec	5.397	31.178	31.333	4.168	0.298	0.298	0.298	7.931
Total Flow cum/sec	3.969	0.099	21.764	0.261	0.019	0.019	0.019	7.166
Temperature K	298.150	298.150	298.150	296.585	319.100	319.100	319.100	298.827
Pressure N/sqm	1.013E+05	1.013E+05	1.013E+05	2.452E+06	2.452E+06	2.452E+06	2.452E+06	1.013E+05

	H2-PROD	H2-PROD2	H2-RCY1	H2O	H2O-OUT	HEAT-IN	HEAT-OUT	HTS-IN
Substream: MIXED								
Mole Flow kmol/sec								
CH4	0.0001	0	8.099E-05	0	5.808E-07	0	0	0.073
H2O	1.188E-06	0	1.188E-06	0.238	0.343	0.238	0.238	0.413
H2	0.490	0.441	0.049	0	8.100E-07	0	0	0.476
CO2	1.563E-04	0	1.563E-04	0	1.498E-05	0.231	0.231	0.072
N2	4.393E-06	0	4.393E-06	0	3.429E-09	0.911	0.911	3.945E-03
CO	2.365E-06	0	2.365E-06	0	1.485E-09	2.122E-03	2.122E-03	0.071
O2	0	0	0	0	0	0.0314	0.0314	0
Mass Flow kg/sec								
CH4	1.299E-03	0	1.299E-03	0	9.317E-06	0	0	1.167
H2O	2.141E-05	0	2.141E-05	4.286	6.186	4.286	4.286	7.445
H2	0.988	0.889	0.099	0	1.633E-06	0	0	0.959
CO2	6.878E-03	0	6.878E-03	0	6.593E-04	10.183	10.183	3.148
N2	1.231E-04	0	1.231E-04	0	9.607E-08	25.515	25.515	0.111
CO	6.626E-05	0	6.626E-05	0	4.158E-08	0.059	0.059	1.987
O2	0	0	0	0	0	1.006	1.006	0
Total Flow kmol/sec	0.490	0.441	0.050	0.238	0.343	1.414	1.414	1.108
Total Flow kg/sec	0.997	0.889	0.108	4.286	6.186	41.050	41.050	14.816
Total Flow cum/sec	0.588	0.529	0.059	8.543	6.227E-03	218.191	140.076	2.745
Temperature K	298.150	298.150	298.150	440	298.15	1880.657	1207.275	623.000
Pressure N/sqm	2.087E+06	2.087E+06	2.087E+06	1.013E+05	2.087E+06	1.013E+05	1.013E+05	2.087E+06

	HTS-OUT1	LTS-IN	LTS-OUT	LTS-OUT2	OFFGAS-A	OFFGAS-C	OFFGASB	PSA-IN
Substream: MIXED								
Mole Flow kmol/sec								
CH4	0.073	0.073	0.073	0.073	0.073	0.073	0.073	0.073
H2O	0.359	0.359	0.344	0.344	1.066E-03	1.066E-03	1.066E-03	1.067E-03
H2	0.531	0.531	0.545	0.545	0.0545	0.0545	0.0545	0.5447
CO2	0.126	0.126	0.140	0.140	0.1402	0.1402	0.1402	0.1403
N2	3.945E-03	3.945E-03	3.945E-03	3.945E-03	3.9404E-03	3.9404E-03	3.9404E-03	3.9448E-03
CO	0.016	0.016	2.12E-03	2.12E-03	2.1216E-03	2.1216E-03	2.1216E-03	2.1240E-03
O2	0	0	0	0	0	0	0	0
Mass Flow kg/sec								
CH4	1.167	1.167	1.167	1.167	1.165	1.165	1.165	1.167
H2O	6.459	6.459	6.205	6.205	0.019	0.019	0.019	0.019
H2	1.070	1.070	1.098	1.098	0.110	0.110	0.110	1.098
CO2	5.557	5.557	6.177	6.177	6.169	6.169	6.169	6.176
N2	0.111	0.111	0.111	0.111	0.110	0.110	0.110	0.111
CO	0.454	0.454	0.059	0.059	0.059	0.059	0.059	0.059
O2	0	0	0	0	0	0	0	0
Total Flow kmol/sec	1.108	1.108	1.108	1.108	0.274	0.274	0.274	0.765
Total Flow kg/sec	14.816	14.816	14.816	14.816	7.633	7.633	7.633	8.630
Total Flow cum/sec	2.983	2.040	2.107	0.963	6.697	6.697	6.697	0.908
Temperature K	675.314	466.700	481.132	313.000	298.150	298.150	298.150	298.150
Pressure N/sqm	2.087E+06	2.087E+06	2.087E+06	2.087E+06	1.013E+05	1.013E+05	1.013E+05	2.087E+06

	STM-SMR1	STM-SMR2	STM2-OUT	STM3-OUT	STM4-OUT	STMTOT	SYNGAS1	SYNGAS2
Substream: MIXED								
Mole Flow kmol/sec								
CH4	0	0	0	5.808E-07	0	0	0.073	0.073
H2O	0.591	0.591	0.188	1.981	0.485	1.376	0.413	0.413
H2	0	0	0	8.100E-07	0	0	0.476	0.476
CO2	0	0	0	1.498E-05	0	0	0.072	0.072
N2	0	0	0	3.429E-09	0	0	3.945E-03	3.945E-03
CO	0	0	0	1.485E-09	0	0	0.071	0.071
O2	0	0	0	0	0	0	0	0
Mass Flow kg/sec								
CH4	0	0	0	9.317E-06	0	0	1.167	1.167
H2O	10.648	10.648	3.382	35.681	8.736	24.790	7.445	7.445
H2	0	0	0	1.633E-06	0	0	0.959	0.959
CO2	0	0	0	6.593E-04	0	0	3.148	3.148
N2	0	0	0	9.607E-08	0	0	0.111	0.111
CO	0	0	0	4.158E-08	0	0	1.987	1.987
O2	0	0	0	0	0	0	0	0
Total Flow kmol/sec	0.591	0.591	0.188	1.981	0.485	1.376	1.108	1.108
Total Flow kg/sec	10.648	10.648	3.382	35.681	8.736	24.790	14.816	14.816
Total Flow cum/sec	0.012	0.353	0.341	0.042	0.882	0.025	4.638	4.103
Temperature K	410.662	495.989	573.232	429.296	573.134	298.462	1047.511	926.909
Pressure N/sqm	2.452E+06	2.452E+06	2.452E+06	2.452E+06	2.452E+06	2.032E+06	2.087E+06	2.087E+06

Appendix D: Stream Results in Approximating Electricity Requirement for the Base Case Condition (MEA Capture Plant)

	CO2PRD2	CO2PRD3	CO2PRD4	CO2PRD5	FLU-GAS3	FLU-GAS4	FLU-GAS5	FLU-GAS6
Substream: MIXED								
Mole Flow kmol/sec								
CH4	0	0	0	0	0	0	0	0
H2O	0	3.778E-03	3.778E-03	3.778E-03	0.238	0.078	0.078	0.065
H2	0	0	0	0	0	0	0	0
CO2	0.185	0.185	0.185	0.185	0.231	0.231	0.231	0.231
N2	0	0	0	0	0.911	0.911	0.911	0.911
CO	0	0	0	0	2.122E-03	2.122E-03	2.122E-03	2.122E-03
O2	0	0	0	0	0.031	0.031	0.031	0.031
Mass Flow kg/sec								
CH4	0	0	0	0	0	0	0	0
H2O	0	0.068	0.068	0.068	4.286	1.405	1.405	1.176
H2	0	0	0	0	0	0	0	0
CO2	8.146	8.146	8.146	8.146	10.183	10.183	10.183	10.183
N2	0	0	0	0	25.516	25.516	25.516	25.516
CO	0	0	0	0	0.059	0.059	0.059	0.059
O2	0	0	0	0	1.006	1.006	1.006	1.006
Total Flow kmol/sec	0.185	0.189	0.189	0.189	1.414	1.254	1.254	1.241
Total Flow kg/sec	8.146	8.214	8.214	8.214	41.050	38.169	38.169	37.940
Total Flow cum/sec	3.993	2.298	2.329	0.011	42.8705	32.1725	28.84173	26.88588
Temperature K	313.150	298.041	301.150	313.000	370.000	313.150	332.435	313.150
Pressure N/sqm	1.200E+05	2.000E+05	2.000E+05	1.500E+07	1.013E+05	1.013E+05	1.200E+05	1.200E+05

	H2O	IMP
Substream: MIXED		
Mole Flow kmol/sec		
CH4	0	0
H2O	3.778E-03	0.065
H2	0	0
CO2	0	0.046
N2	0	0.911
CO	0	2.122E-03
O2	0	0.031
Mass Flow kg/sec		
CH4	0	0
H2O	0.068	1.176
H2	0	0
CO2	0	2.037
N2	0	25.516
CO	0	0.059
O2	0	1.006
Total Flow kmol/sec	3.78E-03	1.056
Total Flow kg/sec	0.0680531	29.794
Total Flow cum/sec	6.87E-05	22.666
Temperature K	301.150	313.150
Pressure N/sqm	2.000E+05	1.200E+05

Appendix E: Stream Results in Approximating Electricity Requirement for the Base Case Condition (Membrane Capture Plant)

	CMP1OUT	CMP2OUT	CMP3OUT	CO2MEM1	CO2MEM2	CO2MEM3	CO2MEM4	CO2PRODI
Substream: MIXED								
Mole Flow kmol/sec								
CO2	0.219	0.208	0.197	0.219	0.208	0.197	0.188	0.188
N2	0.225	0.046	0.007	0.225	0.046	7.463E-03	9.936E-04	9.936E-04
O2	0.022	0.013	0.007	0.022	0.013	7.443E-03	3.843E-03	3.843E-03
AR	5.198E-11	1.956E-11	6.133E-12	5.198E-11	1.956E-11	6.133E-12	1.657E-12	1.657E-12
H2O	8.318E-17	2.656E-23	0	8.318E-17	2.656E-23	0	4.426E-35	4.426E-35
H2	8.318E-17	2.656E-23	0	8.318E-17	2.656E-23	0	4.426E-35	4.426E-35
NO	8.318E-17	2.656E-23	0	8.318E-17	2.656E-23	0	4.426E-35	4.426E-35
CO	5.240E-04	1.068E-04	1.738E-05	5.240E-04	1.068E-04	1.738E-05	2.314E-06	2.314E-06
SO2	8.318E-17	2.656E-23	0	8.318E-17	2.656E-23	0	4.426E-35	4.426E-35
N2O	8.318E-17	2.656E-23	0	8.318E-17	2.656E-23	0	4.426E-35	4.426E-35

	CMP1OUT	CMP2OUT	CMP3OUT	CO2MEM1	CO2MEM2	CO2MEM3	CO2MEM4	CO2PROD1
Substream: MIXED								
Mass Flow kg/sec								
CO2	9.641	9.146	8.668	9.641	9.146	8.668	8.276	8.276
N2	6.302	1.285	0.209	6.302	1.285	0.209	0.028	0.028
O2	0.693	0.430	0.238	0.693	0.430	0.238	0.123	0.123
AR	2.077E-09	7.816E-10	2.450E-10	2.077E-09	7.816E-10	2.450E-10	6.621E-11	6.621E-11
H2O	1.499E-15	4.785E-22	0	1.499E-15	4.785E-22	0	7.974E-35	7.974E-35
H2	1.677E-16	5.354E-23	0	1.677E-16	5.354E-23	0	8.923E-35	8.923E-35
NO	2.496E-15	7.970E-22	0	2.496E-15	7.970E-22	0	1.328E-34	1.328E-34
CO	1.468E-02	2.992E-03	4.869E-04	0.015	2.992E-03	4.87E-04	6.483E-05	6.483E-05
SO2	5.329E-15	1.702E-21	0	5.329E-15	1.702E-21	0	2.836E-34	2.836E-34
N2O	3.661E-15	1.169E-21	0	3.661E-15	1.169E-21	0	1.948E-34	1.948E-34
Total Flow kmol/sec	0.466	0.267	0.212	0.466	0.267	0.212	0.193	0.193
Total Flow kg/sec	16.651	10.864	9.115	16.651	10.864	9.115	8.427	8.427
Total Flow cum/sec	12.013	6.885	5.459	121.328	69.542	55.137	50.199	4.970
Temperature K	313.000	313.000	313.000	313.000	313.000	313.000	313.000	313.000
Pressure N/sqm	1.010E+05	1.010E+05	1.010E+05	10000.000	10000.000	10000.000	10000.000	1.010E+05

	CO2PROD2	FLUGAS	RETENT1	RETENT2	RETENT3	RETETN4
Substream: MIXED						
Mole Flow kmol/sec						
CO2	0.188	0.231	0.012	0.011	0.011	8.890E-03
N2	9.936E-04	0.911	0.686	0.179	0.038	6.469E-03
O2	3.843E-03	0.031	9.779E-03	8.227E-03	5.995E-03	3.601E-03
AR	1.657E-12	1.18E-10	6.559E-11	3.242E-11	1.343E-11	4.475E-12
H2O	4.426E-35	1.18E-10	1.176E-10	8.318E-17	2.656E-23	0
H2	4.426E-35	1.18E-10	1.176E-10	8.318E-17	2.656E-23	0
NO	4.426E-35	1.18E-10	1.176E-10	8.318E-17	2.656E-23	0
CO	2.314E-06	2.12E-03	1.598E-03	4.172E-04	8.945E-05	1.507E-05
SO2	4.426E-35	1.18E-10	1.176E-10	8.318E-17	2.656E-23	0
N2O	4.426E-35	1.18E-10	1.176E-10	8.318E-17	2.656E-23	0
Mass Flow kg/sec						
CO2	8.276	10.183	0.541	0.495	0.478	0.391
N2	0.028	25.515	19.213	5.017	1.076	0.181
O2	0.123	1.006	0.313	0.263	0.192	0.115
AR	6.621E-11	4.697E-09	2.620E-09	1.295E-09	5.366E-10	1.79E-10
H2O	7.974E-35	2.118E-09	2.118E-09	1.499E-15	4.785E-22	0
H2	8.923E-35	2.370E-10	2.370E-10	1.677E-16	5.354E-23	0
NO	1.328E-34	3.528E-09	3.528E-09	2.496E-15	7.970E-22	0
CO	6.483E-05	0.059	0.045	0.012	2.505E-03	4.221E-04
SO2	2.836E-34	7.532E-09	7.532E-09	5.329E-15	1.702E-21	0
N2O	1.948E-34	5.175E-09	5.175E-09	3.661E-15	1.169E-21	0
Total Flow kmol/sec	0.193	1.176	0.710	0.199	0.055	0.019
Total Flow kg/sec	8.427	36.764	20.113	5.787	1.748	0.688
Total Flow cum/sec	0.033	30.198	18.224	5.127	1.426	0.489
Temperature K	313.000	313.000	313.000	313.000	313.000	313.000
Pressure N/sqm	1.500E+07	1.013E+05	1.013E+05	1.010E+05	1.010E+05	1.010E+05